JOINT INSTITUTE FOR AERONAUTICS AND ACOUSTICS

STANFORD UNIVERSITY

AMES RESEARCH CENTER

JIAA TR - 4

EFFECTS OF FRICTION AND HEAT CONDUCTION ON SOUND PROPAGATION IN DUCTS

Patrick Huerre and K. Karamcheti

STANFORD UNIVERSITY
Department of Aeronautics and Astronautics
Stanford, California 94305

August 1976

EFFECTS OF FRICTION AND HEAT CONDUCTION ON SOUND PROPAGATION IN DUCTS

PATRICK HUERRE AND K. KARAMCHETI

AUGUST 1976

The work here presented has been supported by the National Aeronautics and Space Administration under Contract NASA NGL 05-020-275, NASA 05-020-526 and NASA NSG 2007

ACKNOWLEDGEMENTS

We wish to express our gratitude to the members of the Stanford Aeroacoustics Group for helpful suggestions and discussions throughout the entire program. We are especially indebted to Professors Milton Van Dyke and I-Dee Chang who read the manuscript and to Professor Sotiris Koutsoyannis who made many interesting comments.

The typing of the manuscript was ably handled by Miss Patricia Ortiz and by Mrs. Kay Sprung. Special thanks to them for their patience and skill.

We wish to express our appreciation to Cambridge University Press for their kind permission to reproduce some material from the Journal of Fluid Mechanics.

This research was carried out as part of the aeroacoustics program of the Joint Institute for Aeronautics and Acoustics, Department of Aeronautics and Astronautics, at Stanford University and was sponsored by NASA Ames Research Center under Contracts NASA NGL 05-020-275, NASA 05-020-526 and NASA NSG 2007.

TABLE OF CONTENTS

TABLE OF CONTENTS (Continued)

LIST OF ILLUSTRATIONS

LIST OF TABLES

I. INTRODUCTION

1.1 Motivation.

The purpose of this study is to examine the theory of sound propagation in a viscous, heat-conducting fluid, initially at rest and in a uniform state, and contained in a rigid, impermeable duct with isothermal walls.

In the past ten years, research in duct acoustics has been largely motivated by the necessity of reducing the noise level associated with the commercial operations of modern jet aircrafts. A large portion of this noise is internally generated in the jet engine itself, and is primarily due to the rotating turbomachinery blades and the combustion process. This noise then propagates in the form of acoustic modes through the inlet and exhaust pipes. Even though, there has been a great deal of effort devoted to the understanding of basic aerodynamic noise generation mechanisms, one of the most efficient ways of minimizing the radiated sound still consists of absorbing as much of the acoustic energy as possible along the propagation path inside the inlet or exhaust pipe. This is essentially achieved by treating the duct walls with a suitable sound absorbing material. However, the viscous and heat-conducting properties of the medium itself also contribute to the attenuation of the radiated sound. Most aeronautical applications fall in the high-frequency wide-tube range, i.e., the frequencies of interest and the cross-sectional dimensions of the duct are such that dissipation due to friction and heat conduction is restricted to a thin acoustic boundary layer close to the duct walls, and only constitutes a small part of the total attenuation. It is therefore not surprising

that most of the current studies in duct acoustics of jet engines assume the medium to be inviscid. Nevertheless, acoustic boundary layer attenuation has to be taken into account in any systematic evaluation of the total attenuation rate.

These effects also play a primary role in the propagation of blood pressure pulses in human arteries and in the performance of fluid transmission lines. The medium is then a liquid and heat conductivity is usually found to be negligible. The dimensions of the tube and the characteristics of the fluid are such that, in contrast to the previous instance, viscous forces are dominant throughout the cross-section, and viscous dissipation is large. This is the so-called low-frequency-narrow-tube range and the medium may then no longer be considered inviscid.

From a theoretical point of view, this problem may be viewed as one of the few instances where the basic equations pertaining to the unsteady motion of a viscous, heat-conducting, and compressible fluid are amenable to analytical treatment. Even though these equations are linearized, one expects the solution to retain most of the essential features of more complicated flow situations. The fundamental concern of this study is to develop a systematic methodology that would be of use in analyzing complex aerodynamic noise problems.

1.2 Review of the Literature.

In 1868, Kirchhoff published his famous study, "On the Influence of Heat Conduction on Sound Propagation in Gases." At about the same time, Regnault (1868) made the first measurements of sound attenuation in the sewers of Paris. A detailed account of Kirchhoff's theory is given in Lord Rayleigh's Theory of Sound (1877). Kirchhoff considered both vis-

cosity and heat conduction, and derived a general dispersion relation pertaining to axisymmetric waves in cylindrical tubes. This relation was then solved for plane waves in the high-frequency and low-frequency approximations. Many papers on this same subject have been written since, and it would be tedious to discuss them here in any detail. One may, however, within the extensive literature available, distinguish a few main trends.

A large number of investigators have sought to extend Kirchhoff's plane mode results to the entire frequency domain. Weston (1953a), in particular, computed additional terms in the first-order expansions given by Kirchhoff, in both the high- and low-frequency cases, and revealed the existence of an additional very-high-frequency range. Iberall (1950), Brown (1962), and Rott (1969), neglecting radial pressure gradients in the governing equations, derived a solution for the plane mode valid in the low and high frequency domains. Finally, Shields et al. (1965), and very recently Tijdeman (1969, 1975) made a comparison of the previous results with a numerical solution of the dispersion relation. It is worth mentioning at this point that another group of research workers, Sexl (1930), Womersley (1954), Lance (1955), and Uchida (1956), concerned more specifically with the propagation of sound in non-heat-conducting liquids, studied oscillating flows in tubes filled with an incompressible viscous fluid. Even though there is no wave propagation in this case, the axial velocity profile bears a close resemblance to the corresponding compressible flow result. In particular, in the high-frequency limit, the amplitude of the axial velocity presents a maximum close to the duct wall. This phenomenon, experimentally discovered by Richardson and Tyler (1929), is usually referred to as the

Richardson Annular Effect. All theoretical results pertaining to the plane or fundamental mode were abundantly checked experimentally by Fay (1940), Kemp and Nolle (1953), Meyer and Güth (1953), and Weston (1953b).

From inviscid acoustics, however, one would expect the existence at high frequencies, of higher-order propagating modes. A few studies have, indeed, been devoted to the determination of their attenuation characteristics. The first attempt seems to have been made by Hartig and Lambert (1950), whose theoretical formulation later proved to be unsatisfactory. Cremer (1948) suggested simulating viscous and thermal effects close to a rigid wall by an equivalent impedance, and Beatty (1950a,b) and Morse and Ingard (1968) then used the well-known soft-walled-duct model to compute the attenuation rate of higher order modes. Shaw (1950, 1953) directly perturbed Kirchhoff's dispersion relation to recover essentially the same results. Correpsonding expressions were also derived for a purely viscous fluid by Bogert (1950), Elco and Hughes (1962), and Cohen and Tu (1962). Nayfeh (1973) recently extended Cremer's equivalent impedance concept to situations where the medium is inhomogeneous and non-uniformly moving. Paradoxically, the full problem has not yet been solved numerically, although the case of waves in a viscous fluid contained in a cylindrical tube was treated by Gerlach and Parker (1967) and very recently by Scarton and Rouleau (1973). Scarton and Rouleau, in particular, used the method of eigen-valleys to show the existence of a previously unknown family of vorticity-dominated modes. Their work seems so far to be the most comprehensive study of the viscous effects on sound propagation in ducts.

Even though wave propagation in tubes is the ultimate concern of the present investigation, it is a particular case of the more general

theory of the small unsteady motions of a viscous, heat-conducting and compressible fluid, and a significant portion of this work has been devoted to a new mathematical formulation of such a class of problems. It is therefore appropriate to review here some of the studies made in this wider context. Lagerstrom et al. (1949) examined the fundamental principles underlying the linearized system of equations governing the flow of a viscous compressible fluid. They showed the existence of two types of waves, namely, longitudinal or pressure waves, and transversal or vorticity waves. In particular, a proof was given for the statement that any linearized flow may be split into a longitudinal and a transversal component. Wu (1956) generalized their results to the case of a viscous and heat-conducting fluid. Chu and Kovasznay (1958) were primarily interested in the measurement of fluctuating quantities in supersonic turbulent flows, and introduced the concept of three main modes of fluctuations, namely, sound, vorticity, and entropy modes. This idea was recently expanded in the wider context of aerodynamic noise theory by Doak (1973). Finally, two basic papers of general interest and dealing mainly with sound propagation in an unbounded medium are worth mentioning here. Truesdell (1953) conducted an exhaustive review and critique of Kirchhoff's theory of free space sound absorption, for fluids with different heat-conducting properties, and for different frequency regimes. Lighthill's survey (1956) on finite-amplitude sound waves shed further light on the physical mechanisms responsible for sound absorption. Both studies have interesting discussions on the controversial issue of bulk viscosity.

A century has passed since Kirchhoff's investigation and it is apparent from this brief review of the literature that a complete treat-

ment of the problem is yet unavailable. In the next section, we proceed to a general discussion of the scope and goals of the present work.

1.3 Scope of This Study.

This study is essentially concerned with the theory of small perturbations of a viscous, heat-conducting, and compressible fluid. As such, the second chapter is devoted to an alternative mathematical formulation of the problem, suggested by Doak (1973) in the general framework of aerodynamic noise theory. In this approach, the fluctuating velocity field is considered as the superposition of acoustic (related to pressure), thermal (related to entropy), and viscous (related to vorticity) parts. Such a decomposition reduces the linearized Navier-Stokes equations to a system of three partial differential equations for three basic unknown functions: an acoustic scalar potential; a thermal scalar potential; and, a viscous vector potential. No restrictive assumptions are made regarding the nature of the fluid or the magnitude of the Prandtl number. The physical implications of this formulation are discussed in detail, as well as particular cases where significant simplifications may be achieved.

The previous methodology is applied in the third chapter to a study of small-amplitude fluctuating motions in a duct of constant width with rigid and isothermal walls. The governing system of equations is properly non-dimensionalized in terms of five non-dimensional parameters which are functions of the cross-sectional dimension of the tube, the frequency of the perturbation and the characteristic properties of the fluid. The remainder of the investigation further assumes the duct to be two-dimensional, in order to minimize analytical complications. It

is then shown that each frequency may be associated with four distinct types of wave motion, namely, antiplane or inplane waves of symmetric or antisymmetric shapes with respect to the duct axis. Each family is characterized by a specific dispersion relation between a given circular frequency and the corresponding complex wave numbers. The relations pertaining to antiplane waves may readily be solved for arbitrary values of the parameters whereas the relations characterizing inplane motions are transcendental in nature and require the implementation either of a numerical scheme or of some approximation procedure. It is found that perturbation methods give relatively simple mathematical expressions in terms of the characteristic parameters of the problem, and, at the same time provide a convenient framework for the interpretation of the main physical phenomena occurring during the wave motion.

Consequently, Chapter IV is concerned with a perturbation study of the inplane dispersion relations in three ranges of frequencies or equivalently three ranges of duct widths: the low-frequency-narrow-tube range; the high-frequency-wide-tube range; and, the very-high-frequency-very-wide-tube range. It is shown that, in addition to the usual pressure-dominated modes encountered in inviscid propagation problems, two other families of entropy- and vorticity-dominated modes have to be considered. Expansions for the attenuation rates, phase velocities, and mode shapes are then obtained for each family in each frequency regime. The physical implications of the results are then discussed and a qualitative comparison is made with the numerical solution of Scarton and Rouleau (1973), in the limit of zero heat-conduction.

In the concluding remarks, we summarize the essential contributions of the research and suggest opportunities for further study based on the experience gained in the present undertaking.

II. THEORETICAL FORMULATION OF THE SMALL AMPLITUDE FLUCTUATING MOTIONS OF A VISCOUS, HEAT-CONDUCTING AND COMPRESSIBLE FLUID

2.1 Introduction.

In problems concerned with the acoustic motions of an inviscid fluid initially at rest and in a uniform state, it is customary to derive from the basic linearized equations of Fluid Mechanics a single wave equation for a perturbation velocity potential $\Phi(\vec{r},t)$:

$$\Box^2 \Phi = 0 \tag{2.1}$$

where

$$\Box^2 = \nabla^2 - \frac{1}{a_0^2} \frac{\partial^2}{\partial t^2} \tag{2.2}$$

is the wave operator and a_0 is the isentropic speed of sound. The other dependent variables such as the velocity perturbation $\vec{V}'$, and the pressure perturbation p' , are then directly related to the potential Φ through the classical expressions:

$$\vec{V}' = \text{grad}\, \Phi \tag{2.3}$$

$$p' = - \rho_0 \frac{\partial \Phi}{\partial t} \tag{2.4}$$

where ρ_0 is the density of the medium.

This procedure presents the important advantage of reducing a wide variety of acoustic problems to the determination of one scalar field $\Phi(\vec{r},t)$ obeying the wave equation (2.1) with appropriate initial and boundary conditions.

In this chapter, we wish to generalize this formulation to

situations where the medium is viscous and heat-conducting. We will be led to introduce, in addition to the acoustic potential defined above, two other fields, namely, a thermal scalar potential and a viscous vector potential. Governing equations for these "auxiliary" variables will be derived, and the physical implications will be discussed in light of the mathematical formulation.

2.2 Linearized Navier-Stokes Equations and Underlying Assumptions.

Let us consider the small amplitude motions of a simple thermodynamic fluid initially at rest and in a uniform state. Each dependent variable such as pressure, density, velocity, ... may be written in the form:

$$Q(\vec{r},t) = Q_0 + Q'(\vec{r},t) \tag{2.5}$$

where Q_0 is independent of $\vec{r}$ and t and characterizes the initial state of the fluid, and $Q'(\vec{r},t)$ designates a fluctuating quantity. In particular, since $\vec{V}_0 = 0$

$$\vec{V}(\vec{r},t) = \vec{V}'(\vec{r},t) \tag{2.6}$$

Such a decomposition is then substituted for each dependent variable into the equations of mass, motion, entropy, and the equations of state, pertaining to a Newtonian fluid obeying Fourier's law of heat conduction. When all non-linear terms in the perturbation variables are neglected, the following linearized equations result:

Equation of Mass $$\frac{\partial \rho'}{\partial t} + \rho_0 \operatorname{div} \vec{V}' = 0 \tag{2.7}$$

Equation of Motion $$\rho_0 \frac{\partial \vec{V}'}{\partial t} = -\operatorname{grad} p' - \mu_0 \operatorname{curl} \vec{\Omega}' + \eta_0 \operatorname{grad} \operatorname{div} \vec{V}' \tag{2.8}$$

Equation of Entropy $$\rho_0 T_0 \frac{\partial S'}{\partial t} = k_0 \nabla^2 T' \tag{2.9}$$

Equations of State $$p' = a_0^2 \rho' + \left[\frac{\partial p}{\partial S}_\rho\right]\Bigg|_{\rho_0, S_0} S' \tag{2.10}$$

$$T' = \left[\frac{\partial T}{\partial \rho}_S\right]\Bigg|_{\rho_0, S_0} \rho' + \left[\frac{\partial T}{\partial S}_\rho\right]\Bigg|_{\rho_0, S_0} S' \tag{2.11}$$

In the above relations, μ_0 is the coefficient of shear viscosity, k_0 the coefficient of heat conduction, a_0 the isentropic speed of sound, and η_0 is the dilatational viscosity given by

$$\eta_0 = K_0 + \frac{4}{3}\mu_0 \tag{2.12}$$

K_0 being the coefficient of bulk viscosity. All other symbols have their usual significance.

The system (2.7)-(2.11) constitutes the starting point of this investigation and we discuss below the main assumptions which have been introduced in the process of its derivation:

(a) Continuum Hypothesis: The characteristic length scales of the particular problem at hand are assumed to be much larger than the mean-free-path, so that the fluid may be treated as a continuum. In the case of propagation in ducts, the wavelength and duct diameter must both be large in comparison with the mean-free-path.

(b) Homogeneous Medium at Rest: The steady flow variables are independent of position and time and the velocity of the medium is identically zero.

(c) The fluid is assumed to satisfy the Navier-Stokes relation between stress and rate of strain as well as Fourier's law of heat conduction.

(d) Small Amplitude Motion: In other words, fluctuating and steady quantities satisfy the following relations:

$$\left|\frac{\vec{V}'}{a_0}\right| \ll 1 \; ; \quad \left|\frac{\rho'}{\rho_0}\right| \ll 1 \; ; \quad \left|\frac{S'}{S_0}\right| \ll 1 \tag{2.13}$$

This assumption justifies the linearization of the governing equations and drastically simplifies the mathematical formulation of acoustic problems.

(e) Laminar Motion. The presence of turbulent motion would at once invalidate the linearization of the basic equations since turbulence is characterized by strong non-linear interactions. Unfortunately, very few studies on the transition of unsteady laminar flows have been made. However, in the case of oscillatory flow in circular ducts, Sergeev (1966) and Nerem et al. (1972) determined experimentally a criterion for transition of the form

$$\hat{Re}_c = \text{const.}\sqrt{kR_\nu} \qquad \text{when } \sqrt{kR_\nu} > 4 \tag{2.14}$$

In the above relation, $\hat{Re}_c$ is the critical value of the Reynolds number based on the peak velocity $\hat{U}$, and k and R_ν are non-dimensionalized parameters which will be introduced in Chapter 3. They are defined as follows:

$$\hat{Re} = \frac{\hat{U}d}{\nu_0} \; ; \quad k = \frac{\omega d}{a_0} \; ; \quad R_\nu = \frac{a_0 d}{\nu_0} \tag{2.15}$$

where d is the duct diameter, ω the circular frequency of the laminar flow oscillations, and ν_0 the kinematic viscosity.

It will be shown in Chapter IV, that for values of $\sqrt{kR_\nu}$ larger than four, the flow is characterized by a thin acoustic boundary layer

close to the duct wall of thickness

$$\delta \sim \frac{d}{\sqrt{kR_\nu}} \tag{2.16}$$

A crude justification of relation (2.14) may then be given by applying the critical Reynolds number criterion for a steady flat plate boundary layer to the unsteady boundary layer of thickness, δ , i.e.,

$$\left(\frac{\hat{U}\delta}{\nu_0}\right)_c \sim 1000 \tag{2.17}$$

Upon combining this relation with the estimate of δ given by (2.16), the dependence of the critical Reynolds number on $\sqrt{kR_\nu}$ may be shown to be expressed by (2.14).

In this study, it is assumed that the peak Reynolds number is lower than the critical Reynolds number given by (2.14) so that the unsteady flow is laminar.

(f) Simple Thermodynamic Fluid: Nonequilibrium effects such as vibrational relaxation are assumed to be negligible and the fluid is in local thermodynamic equilibrium. The thermodynamic state of the fluid at any position and time is completely described by two state variables only, for instance, density and entropy. All other state variables such as pressure and temperature may then be expressed in terms of density and entropy, as in the two linearized equations of state (2.10) and (2.11). The partial derivatives in these equations may conveniently be expressed in terms of five characteristic properties of the medium, namely, the isentropic speed of sound a_0 , the temperature T_0 , the density ρ_0 , the specific heat at constant pressure c_{P_0} , and the ratio of specific heats γ_0 . Equations (2.10) and (2.11) may then be

written in the following manner:

$$p' = a_0^2 \rho' + \rho_0 a_0 \sqrt{\frac{(\gamma_0 - 1)T_0}{c_{p_0}}}\, S' \qquad (2.10)'$$

$$T' = \frac{a_0}{\rho_0}\sqrt{\frac{(\gamma_0 - 1)T_0}{c_{p_0}}}\, \rho' + \frac{\gamma_0 T_0}{c_{p_0}} S' \qquad (2.11)'$$

The form of the coefficients in the above relations is derived in Appendix A, by making use of the first and second law of thermodynamics. No additional assumption regarding the nature of the fluid needs to be introduced. In the case of a perfect gas, for instance, a_0 could be replaced by its expression as a function of T_0, but this restriction does not have to be made in order to derive (2.10)' and (2.11)'.

The linearized equations (2.7) - (2.9) and (2.10)', (2.11)' constitute a system of five linear partial differential equations for five unknown functions p', ρ', S', T', and $\vec{V}'$. We now proceed to the definition of the acoustic, thermal, and viscous potentials, and to the derivation of a corresponding system of three partial differential equations for these three potentials.

2.3 Acoustic, Thermal, and Viscous Potentials. Governing Equations:

According to Helmoltz' theorem, the velocity field $\vec{V}'$ can always be written as the sum of an irrotational part $\text{grad}\,\Phi$, and a solenoidal part $\text{curl}\,\vec{A}$ so that

$$\vec{V}' = \text{grad}\,\Phi + \text{curl}\,\vec{A} \qquad (2.18)$$

We will further assume that the so-called viscous vector potential $\vec{A}$ satisfies the additional condition

$$\text{div}\,\vec{A} = 0 \tag{2.19}$$

From (2.10)', the density ρ' may be expressed as a function of p' and S'. When (2.18) and the resulting equation for ρ' are substituted into the equation of mass (2.7), one obtains

$$\frac{1}{a_0^2}\frac{\partial p'}{\partial t} - \frac{\rho_0}{a_0}\sqrt{\frac{(\gamma_0-1)T_0}{c_{p_0}}}\,\frac{\partial S'}{\partial t} = -\rho_0\nabla^2\Phi \tag{2.20}$$

In order to satisfy (2.20) identically, Doak (1973) suggested in his, "Momentum Potential Description of Unsteady Fluid Flows," to further decompose the scalar potential Φ into two parts: an acoustic potential Φ_a giving rise to pressure fluctuations through the relation:

$$\frac{\partial p'}{\partial t} = -\rho_0 a_0^2\nabla^2\Phi_a \tag{2.21}$$

and a thermal potential Φ_{th} giving rise to entropy fluctuations through the relation:

$$\frac{\partial S'}{\partial t} = a_0\sqrt{\frac{c_{p_o}}{(\gamma_0-1)T_0}}\,\nabla^2\Phi_{th} \tag{2.22}$$

The velocity field $\vec{V}'$ is now the sum of three distinct acoustic, thermal, and vortical components, and is of the form:

$$\vec{V}' = \text{grad}\,\Phi_a + \text{grad}\,\Phi_{th} + \text{curl}\,\vec{A} \tag{2.23}$$

From (2.10)' and (2.11)', the other dependent variables may immediately be related to Φ_a, Φ_{th}, and $\vec{A}$ in the following manner:

$$\frac{\partial\rho'}{\partial t} = -\rho_0\nabla^2(\Phi_a+\Phi_{th}) \tag{2.24}$$

$$\frac{\partial T'}{\partial t} = a_0 \sqrt{\frac{T_0}{(\gamma_0 - 1) c_{p_0}}} \nabla^2 [\Phi_{th} - (\gamma_0 - 1)\Phi_a] \tag{2.25}$$

Equations (2.21) - (2.25) provide the necessary relations between the "auxiliary" dependent variables Φ_a , Φ_{th} , and $\vec{A}$, and the "physical" variables, pressure, entropy, velocity, density, and temperature. In the derivation of these relations, use has been made of the equation of continuity and the equation of state. We now seek to obtain the partial differential equations governing Φ_a , Φ_{th} , and $\vec{A}$, by requiring that the remaining equations of motion and entropy be satisfied. Substitution of (2.23) and (2.22) into (2.8) and (2.9) respectively, leads to the following system:

$$\text{(I)} \quad \begin{cases} \text{grad}\left[\frac{\partial}{\partial t}(\Phi_a + \Phi_{th}) - \frac{\eta_0}{\rho_0} \nabla^2 (\Phi_a + \Phi_{th}) + \frac{p'}{\rho_0}\right] & (2.26) \\ \qquad + \text{curl}\left[\frac{\partial \vec{A}}{\partial t} - \nu_0 \nabla^2 \vec{A}\right] = 0 & \\ \nabla^2 \left[\Phi_{th} - \frac{\nu_0}{a_0 P_r} \sqrt{\frac{(\gamma_0 - 1) c_{p_0}}{T_0}}\, T'\right] = 0 & (2.27) \end{cases}$$

where P_r is the Prandtl number of the medium:

$$P_r = \frac{c_{p_0} \mu_0}{k_0} \tag{2.28}$$

It is very tempting to replace System (I) by the following simpler system of three partial differential equations:

$$\text{(II)} \quad \begin{cases} \frac{\partial}{\partial t}(\Phi_a + \Phi_{th}) - \frac{\eta_0}{\rho_0} \nabla^2 (\Phi_a + \Phi_{th}) + \frac{p'}{\rho_0} = 0 & (2.29) \\ \frac{\partial \vec{A}}{\partial t} - \nu_0 \nabla^2 \vec{A} = 0 & (2.30) \\ \Phi_{th} - \frac{\nu_0}{a_0 P_r} \sqrt{\frac{(\gamma_0 - 1) c_{p_0}}{T_0}}\, T' = 0 & (2.31) \end{cases}$$

Each solution of (II) is obviously a solution of (I). But there are solutions of System (I) which are not solutions of System (II). In Appendix B, we prove that, to each solution $\{\Phi_a^*, \Phi_{th}^*, \vec{A}^*\}$ of (I), one may associate a solution $\{\Phi_a, \Phi_{th}, \vec{A}\}$ of (II), which will give the same values for the physical variables $\vec{V}'$, p', and S'. It may be concluded that Systems (I) and (II) yield the same number of possible physical states.

Equations (2.29) and (2.31) may immediately be expressed solely in terms of Φ_a and Φ_{th} by differentiating them once with respect to time and making use of relations (2.21) and (2.25). The final results of this section are then formulated in the following "Splitting Theorem."

Splitting Theorem: If $\{\vec{V}', p', S', \rho', T'\}$ satisfy the linearized equations of Fluid Mechanics (2.7)-(2.9) and (2.10)' - (2.11)', then there exists an acoustic potential Φ_a, a thermal potential Φ_{th}, and a viscous vector potential $\vec{A}$ such that the physical variables are represented by:

$$\vec{V}' = \text{grad}\,\Phi_a + \text{grad}\,\Phi_{th} + \text{curl}\,\vec{A} \tag{2.32}$$

$$\frac{\partial p'}{\partial t} = -\rho_0 a_0^2 \nabla^2 \Phi_a \tag{2.33}$$

$$\frac{\partial S'}{\partial t} = a_0 \sqrt{\frac{c_{p_0}}{(\gamma_0 - 1)T_0}}\ \nabla^2 \Phi_{th} \tag{2.34}$$

$$\frac{\partial \rho'}{\partial t} = -\rho_0 \nabla^2 (\Phi_a + \Phi_{th}) \tag{2.35}$$

$$\frac{\partial T'}{\partial t} = a_0 \sqrt{\frac{T_0}{(\gamma_0 - 1)c_{p_0}}} \left[\nabla^2 \Phi_{th} - (\gamma_0 - 1)\nabla^2 \Phi_a\right] = P_r \frac{a_0}{\nu_0} \sqrt{\frac{T_0}{(\gamma_0 - 1)c_{p_0}}}\ \frac{\partial \Phi_{th}}{\partial t} \tag{2.36}$$

with $$\text{div}\,\vec{A} = 0 \tag{2.37}$$

and where $\Phi_a(\vec{r},t)$, $\Phi_{th}(\vec{r},t)$ and $\vec{A}(\vec{r},t)$ satisfy the following system:

$$\Box_S^2 \Phi_a = \frac{1}{a_0^2} \frac{\partial}{\partial t} \left[\frac{\partial \Phi_{th}}{\partial t} - \frac{\eta_0}{\rho_0} \nabla^2 \Phi_{th} \right] \tag{2.38}$$

$$\frac{\partial \Phi_{th}}{\partial t} - \frac{\nu_0}{P_r} \nabla^2 \Phi_{th} = -(\gamma_0 - 1) \frac{\nu_0}{P_r} \nabla^2 \Phi_a \tag{2.39}$$

$$\frac{\partial \vec{A}}{\partial t} - \nu_0 \nabla^2 \vec{A} = 0 \tag{2.40}$$

In equation (2.36), equation (2.39) was used to derive an alternative expression for $\frac{\partial T'}{\partial t}$ in terms of Φ_{th} only. $\Box_S^2$ in equation (2.38) is the modified wave operator.

$$\Box_S^2 = \nabla^2 - \frac{1}{a_0^2} \frac{\partial^2}{\partial t^2} + \frac{\eta_0}{\rho_0 a_0^2} \nabla^2 \frac{\partial}{\partial t} \tag{2.41}$$

The traditional wave operator as defined in (2.2), is immediately recognized in the first two terms of (2.41). The last third-order term represents attenuation brought about by the dilatational viscosity η_0 . The subscript S has been added to notify that the operator pertains to the isentropic speed of sound a_0 .

Furthermore, cross differentiation of (2.38) and (2.39) leads to the additional fourth order partial differential equations:

$$\frac{\partial}{\partial t} \Box_S^2 \{\Phi_a \text{ or } \Phi_{th}\} = \frac{\nu_0}{P_r} \nabla^2 \Box_T^2 \{\Phi_a \text{ or } \Phi_{th}\} \tag{2.42}$$

where

$$\Box_T^2 = \nabla^2 - \frac{\gamma_0}{a_0^2} \frac{\partial^2}{\partial t^2} + \frac{\gamma_0 \eta_0}{\rho_0 a_0^2} \nabla^2 \frac{\partial}{\partial t} \tag{2.43}$$

The above operator is a modified wave operator similar to $\Box_S^2$ defined in (2.41), but pertaining to the isothermal speed of sound $a_0/\sqrt{\gamma_0}$.

Discussion: Upon examination of the previous theorem, it may be noted that the propagation problem has been reduced, as expected, to the determination of an acoustic scalar potential Φ_a, a thermal scalar potential Φ_{th}, and a viscous vector potential $\vec{A}$.

The acoustic component gives rise to pressure, density, and velocity perturbations. It is inherently coupled to the thermal component, as seen from (2.38) and (2.39), and therefore is bound to generate entropy fluctuations. The thermal component gives rise to entropy fluctuations and, as a result of coupling will generate the acoustic component. Both components satisfy equation (2.42) independently. However, coupling is still achieved through the lower-order relations (2.38) and (2.39). Finally, the velocity fluctuations associated with Φ_a and Φ_{th} are irrotational so that investigators have often considered these two components as one single longitudinal part. The uncoupling of the vortical component represented by $\vec{A}$ is the most significant feature of the splitting theorem. The vector potential is governed by a diffusion equation and only gives rise to rotational velocity fluctuations. However, in the presence of solid surfaces, one expects the vortical component to generate the other two through the no-slip boundary conditions.

We wish to emphasize that the decomposition presented here is not the only possible one, and several alternative schemes have indeed been proposed. In particular, Wu (1956) distinguished a longitudinal and a transversal component, without any further splitting of the longitudinal part. Chu and Kovasznay (1958) defined three modes, namely, pressure, entropy, and vorticity modes, but the first two modes do not coincide with the acoustic and thermal components considered in this study. In both of these investigations, the governing equations were expressed in

terms of the physical variables. We can see from the results of the splitting theorem that significant simplification results from the use of three "auxiliary" variables Φ_a , Φ_{th} , and $\vec{A}$, since each component is, in the end, associated with one variable only. Finally, in previous works, the fluid is assumed to be a perfect gas with a Prandtl number equal to 3/4 , whereas, no such restrictions are imposed here. We now briefly examine a few cases where simpler versions of the equations for Φ_a , Φ_{th} , and $\vec{A}$ may be obtained.

2.4. Some Particular Cases.

2.4.1. Prandtl Number = $\nu_0/(\eta_0/\rho_0)$: When the bulk viscosity is zero, this coincides with situations where the Prandtl number is equal to 3/4 . Air, which has a Prandtl number equal to .72 , closely approaches this case, as long as its bulk viscosity may be neglected. The two diffusion operators on the right-hand side of (2.38) and the left-hand side of (2.39) are then identical so that equation (2.39) may be used to eliminate Φ_{th} in Eq. (2.38). The governing equations reduce to:

$$\nabla^2\Phi_a - \frac{1}{a_0^2}\frac{\partial^2\Phi_a}{\partial t^2} + \frac{\gamma_0\eta_0}{\rho_0 a_0^2}\nabla^2\frac{\partial\Phi_a}{\partial t} = 0 \qquad (2.44)$$

$$\frac{\partial\Phi_{th}}{\partial t} - \frac{\eta_0}{\rho_0}\nabla^2\Phi_{th} = -\frac{\eta_0}{\rho_0}(\gamma_0-1)\nabla^2\Phi_a \qquad (2.45)$$

$$\frac{\partial\vec{A}}{\partial t} - \nu_0\nabla^2\vec{A} = 0 \qquad (2.46)$$

The acoustic potential satisfies the modified wave equation (2.44) with an "effective" dilatational viscosity $\gamma_0\eta_0/\rho_0$. The decoupling is incomplete, however, since (2.45) still relates Φ_a and Φ_{th} . As mentioned above, this is the situation considered by Wu (1956) and Chu and

Kovasznay (1958).

2.4.2. Non-Heat-Conducting Viscous Fluid: The Prandtl number of the fluid is then equal to infinity. The entropy is constant and the thermal component is identically zero. The governing equations, therefore reduce to:

$$\Box_S^2 \Phi = 0 \tag{2.47}$$

$$\frac{\partial \vec{A}}{\partial t} - \nu_0 \nabla^2 \vec{A} = 0 \tag{2.48}$$

This case was extensively studied by Lagerstrom et al. (1949) and equations identical to (2.47) and (2.48) were derived by several authors, in particular, Cohen and Tu (1962), Gerlach and Parker (1967), and Scarton and Rouleau (1973).

It is interesting to note that wave phenomena in elastic solids are governed by equations which are analogous to (2.47) and (2.48). The displacement vector

$$\vec{u} = \text{grad}\,\Phi + \text{curl}\,\vec{A} \tag{2.49}$$

is then shown to satisfy the displacement equations of motion provided that the Lamé potentials, $\Phi(\vec{r},t)$ and $\vec{A}(\vec{r},t)$, are solutions of two wave equations with different characteristic velocities, c_L and c_T :

$$\nabla^2 \Phi - \frac{1}{c_L^2} \frac{\partial^2 \Phi}{\partial t^2} = 0 \tag{2.50}$$

$$\nabla^2 \vec{A} - \frac{1}{c_T^2} \frac{\partial^2 \vec{A}}{\partial t^2} = 0 \tag{2.51}$$

The absence of any diffusion operator or attenuation term in the above system is a consequence of the elasticity of the medium which does not

allow for dissipative phenomena. A detailed account of elastodynamic theory is given by Achenbach (1973).

2.4.3. Viscous and Perfectly Heat-Conducting Fluid: The Prandtl number of the fluid is assumed to be zero so that there are no temperature fluctuations. In such a situation, any wave motion is isothermal. Equations (2.38)-(2.40) become:

$$\Box_T^2 \Phi_a = 0 \tag{2.52}$$

$$\Phi_{th} = (\gamma_0 - 1)\Phi_a \tag{2.53}$$

$$\frac{\partial \vec{A}}{\partial t} - \nu_0 \nabla^2 \vec{A} = 0 \tag{2.54}$$

where $\Box_T^2$ is the isothermal wave operator defined in (2.43). As seen from (2.52) and (2.53), plane longitudinal waves, which, in an inviscid, non-heat-conducting medium propagate isentropically with Laplace's velocity a_0, propagate isothermally in a perfect conductor, with Newton's velocity, $a_0/\sqrt{\gamma_0}$.

2.4.4. Barotropic Fluid: A fluid is said to be barotropic when the ratio of its specific heats γ_0 is equal to unity.* As mentioned by Truesdell (1953), many liquids such as pure water may be assumed to be barotropic with a reasonably good approximation. The linearized equations of state (2.10)' and (2.11)' now become

$$p' = a_0^2 \rho' \tag{2.55}$$

$$T' = \frac{T_0}{c_{p_0}} S' \tag{2.56}$$

*More commonly, a fluid is said to be barotropic when its density is a function only of pressure. From the expression for $(\partial p/\partial S)_\rho$ given in equation (2.10)', one can immediately establish that these two definitions are strictly equivalent.

and there is no need to define a thermal potential Φ_{th} as before since the equation of mass and the equation of motion will not contain S'. The thermal potential is therefore identically set equal to zero in (2.32-2.40), and the entropy fluctuation S' is chosen to characterize the thermal component. The governing equations then reduce to:

$$\vec{V}' = \text{grad } \Phi_a + \text{curl } \vec{A} \tag{2.57}$$

$$\frac{\partial p'}{\partial t} = a_0^2 \frac{\partial \rho'}{\partial t} = -\rho_0 a_0^2 \nabla^2 \Phi_a \tag{2.58}$$

$$T' = \frac{T_0}{c_{P_0}} S' \tag{2.59}$$

$$\text{div } \vec{A} = 0 \tag{2.60}$$

$$\Box_S^2 \Phi_a = 0 \tag{2.61}$$

$$\frac{\partial S'}{\partial t} - \frac{\nu_0}{P_r} \nabla^2 S' = 0 \tag{2.62}$$

$$\frac{\partial \vec{A}}{\partial t} - \nu_0 \nabla^2 \vec{A} = 0 \tag{2.63}$$

Equation (2.62) was obtained by substituting (2.56) into the equation of entropy (2.9).

As discussed previously, the acoustic component is associated with pressure, density and longitudinal velocity fluctuations. But in a contrast with the general case, it does not give rise to temperature fluctuations. The acoustic potential Φ_a is now governed by the modified wave equation (2.61), as in paragraph 2.4.2.

The thermal component is characterized by entropy and temperature perturbations only, and does not give rise to velocity fluctuations. It is governed by the classical diffusion equation (2.62). Moreover, as shown in (2.61) and (2.62), acoustic and thermal components are completely uncoupled, so that an acoustic wave will not generate entropy

fluctuations and conversely. This feature persists even in the presence of solid surfaces, since it is preserved in the boundary conditions on velocity and temperature as seen from (2.57) and (2.59). The analytical relationships between thermal and acoustic components are therefore considerably simplified.

2.4.5. Inviscid, Non-Heat-Conducting Fluid: In this case it may immediately be verified that we recover the basic results mentioned in the introduction to this chapter. The acoustic potential is now identical to the usual velocity potential Φ, and the thermal and viscous components are identically zero. Moreover, the state of the fluid is governed by the classical wave equation (2.1).

In the next chapter, we proceed to apply the results of Section 2.3 to the propagation of small perturbations in cylindrical tubes.

III. SOUND PROPAGATION IN A TWO-DIMENSIONAL DUCT

3.1 Introduction.

The results of the preceding chapter provide a theoretical framework for the study of the small-amplitude motions of a fluid in a cylindrical duct. In this part of the investigation, we first derive the basic equations governing sound propagation through a duct of constant cross-section and then investigate in detail the particular case of a two-dimensional duct.

3.2 Formulation: Parameters of the Problem.

Consider a harmonic wave of circular frequency ω propagating in an infinite tube of constant cross-section S and typical cross-sectional diameter d (see Figure 1). The fluid is assumed to obey restrictions (a)-(f) discussed in Section 2.2, and in addition, the walls of the duct are assumed to be rigid, impermeable, and isothermal.

The independent variables are non-dimensionalized as follows:

$$x' = \frac{x}{d} \quad ; \quad y' = \frac{y}{d} \quad ; \quad z' = \frac{z}{d} \quad ; \quad t' = \omega t \tag{3.1}$$

and three non-dimensional parameters are introduced:

$$k = \frac{\omega d}{a_0} \qquad \text{the reduced frequency} \tag{3.2}$$

$$R_\nu = \frac{a_0 d}{\nu_0} \qquad \text{the "Reynolds number" based on the speed of sound and the shear viscosity } \mu_0 \text{ .} \tag{3.3}$$

$$R_\eta = \frac{a_0 d}{\eta_0/\rho_0} \qquad \text{the "Reynolds number" based on the speed of sound and the dilatational viscosity } \eta_0 \text{ .} \tag{3.4}$$

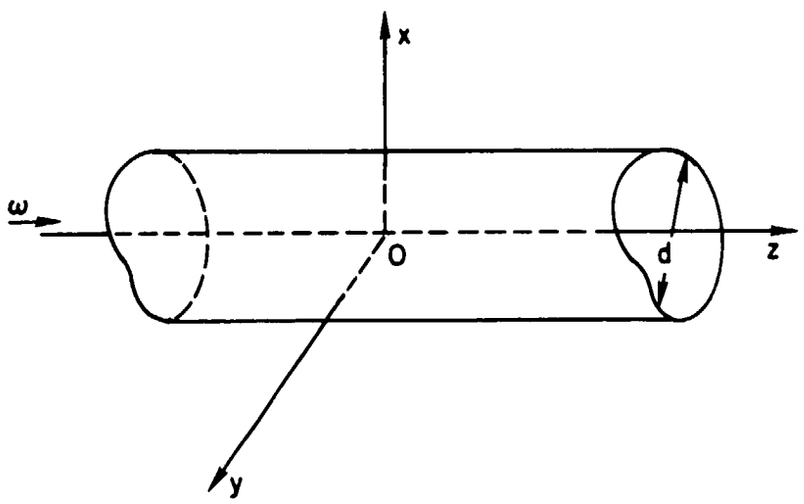

Figure 1. Duct Configuration.

The problem therefore depends on the values of five parameters: γ_0 ; P_r ; R_ν ; R_η ; and k , which are functions of the state of the medium, the dimensions of the tube, and the characteristic frequency of the fluctuations. The dependent variables are kept in dimensional form. The basic equations of Section 2.3 then take the following form:

$$\vec{V}' = \frac{1}{d}[\text{grad}\,\Phi_a + \text{grad}\,\Phi_{th} + \text{curl}\,\vec{A}] \tag{3.5}$$

$$\frac{\partial p'}{\partial t} = -\frac{\rho_0 a_0}{kd}\nabla^2\Phi_a \tag{3.6}$$

$$\frac{\partial S'}{\partial t} = \frac{1}{kd}\sqrt{\frac{c_{p_0}}{(\gamma_0-1)T_0}}\nabla^2\Phi_{th} \tag{3.7}$$

$$\frac{\partial \rho'}{\partial t} = -\frac{\rho_0}{ka_0 d}\nabla^2(\Phi_a+\Phi_{th}) \tag{3.8}$$

$$\frac{\partial T'}{\partial t} = \frac{P_r R_\nu}{d}\sqrt{\frac{T_0}{(\gamma_0-1)c_{p_0}}}\frac{\partial \Phi_{th}}{\partial t} \tag{3.9}$$

with $$\text{div}\,\vec{A} = 0 \tag{3.10}$$

and where Φ_a , Φ_{th} , and $\vec{A}$ obey the following system:

$$\Box_S^2\,\Phi_a = k^2\frac{\partial}{\partial t}\left[\frac{\partial \Phi_{th}}{\partial t} - \frac{1}{kR_\eta}\nabla^2\Phi_{th}\right] \tag{3.11}$$

$$\frac{\partial \Phi_{th}}{\partial t} - \frac{1}{kP_r R_\nu}\nabla^2\Phi_{th} = -\frac{\gamma_0-1}{kP_r R_\nu}\nabla^2\Phi_a \tag{3.12}$$

$$\frac{\partial \vec{A}}{\partial t} - \frac{1}{kR_\nu}\nabla^2\vec{A} = 0 \tag{3.13}$$

$$\frac{\partial}{\partial t}\Box_S^2\{\Phi_a \text{ or } \Phi_{th}\} = \frac{1}{kP_r R_\nu}\nabla^2\Box_T^2\{\Phi_a \text{ or } \Phi_{th}\} \tag{3.14}$$

where

$$\Box_S^2 = \nabla^2 - k^2 \frac{\partial^2}{\partial t^2} + \frac{k}{R_\eta} \nabla^2 \frac{\partial}{\partial t} \tag{3.15}$$

$$\Box_T^2 = \nabla^2 - \gamma_0 k^2 \frac{\partial^2}{\partial t^2} + \frac{\gamma_0 k}{R_\eta} \nabla^2 \frac{\partial}{\partial t} \tag{3.16}$$

In the above relations, the primes on x' , y' , z' , t' , have been omitted for convenience. The system (3.10)-(3.14) is to be supplemented with the following boundary conditions at the walls:

$$\begin{cases} \vec{V}' = 0 \\ \\ T' = 0 \end{cases} \qquad \text{on duct boundary walls.} \tag{3.17}$$

We wish to determine the potentials $\Phi_a(\vec{r},t)$, $\Phi_{th}(\vec{r},t)$, and $\vec{A}(\vec{r},t)$ which satisfy (3.10)-(3.14) and the associated boundary conditions (3.17).

The previous considerations define an eigenvalue problem which is more easily handled if $\Phi_a(\vec{r},t)$, $\Phi_{th}(\vec{r},t)$, and $\vec{A}(\vec{r},t)$ are assumed to be travelling waves of the form

$$\Phi_a(\vec{r},t) = \varphi_a(x,y) e^{i(t-\beta_z z)} \tag{3.18}$$

$$\Phi_{th}(\vec{r},t) = \varphi_{th}(x,y) e^{i(t-\beta_z z)} \tag{3.19}$$

$$\vec{A}(\vec{r},t) = \vec{G}(x,y) e^{i(t-\beta_z z)} \tag{3.20}$$

Note that in these relations, both z and t are non-dimensionalized. The circular frequency ω is embedded in the non-dimensional time t , and the complex wave number β_z is non-dimensionalized with respect to the duct width. Equations (3.18)-(3.20) physically correspond to standing waves in the cross-section of the tube and travelling waves along the duct axis z. The real part of β_z denotes the actual propagation

wave number, while the imaginary part represents the attenuation rate. The complex quantity β_z , and the functions $\varphi_a(x,y)$, $\varphi_{th}(x,y)$, and $\vec{\Omega}(x,y)$ are to be determined as a function of the five previously defined parameters. We now proceed to derive the governing equations for φ_a , φ_{th} , and $\vec{\Omega}$.

Substitution of (3.18) or (3.19) into the fourth order partial differential equation (3.14) yields the following relation:

$$\nabla_1^4\{\varphi_a \text{ or } \varphi_{th}\} - [ikP_rR_\nu \frac{1+\frac{i\nu_0 k}{P_rR_\nu}+\frac{ik}{R_\eta}}{1+i\nu_0 k/R_\eta}$$

$$+ 2\beta_z^2]\nabla_1^2\{\varphi_a \text{ or } \varphi_{th}\} + [\beta_z^4 + ikP_rR_\nu \cdot \frac{1+i\nu_0 k/P_rR_\nu + ik/R_\eta}{1+i\nu_0 k/R_\eta}\beta_z^2 \quad (3.21)$$

$$- \frac{ik^3P_rR_\nu}{1+i\nu_0 k/R_\eta}]\{\varphi_a \text{ or } \varphi_{th}\} = 0$$

where

$$\nabla_1 = \vec{e}_x \frac{\partial}{\partial x} + \vec{e}_y \frac{\partial}{\partial y} \quad (3.22)$$

Solutions of (3.21) may be obtained in the form of a combination of solutions of the following Helmholtz equations:

$$\nabla_1^2\{\varphi_{ao} \text{ or } \varphi_{tho}\} + \alpha_o^2\{\varphi_{ao} \text{ or } \varphi_{tho}\} = 0 \quad (3.23)$$

$$\nabla_1^2\{\varphi_{a1} \text{ or } \varphi_{th1}\} + \alpha_1^2\{\varphi_{a1} \text{ or } \varphi_{th1}\} = 0 \quad (3.24)$$

where α_0^2 and α_1^2 are the roots of the algebraic equation in α^2 , obtained from (3.21) by changing ∇_1^2 and ∇_1^4 into $-\alpha^2$ and α^4 , respectively. The acoustic potential φ_a will therefore be the sum of φ_{ao} and φ_{a1} , solutions of (3.23) and (3.24). Similarly, φ_{th} will

be the sum of φ_{tho} and φ_{th1}.

It is a straight-forward procedure to derive expressions for α_o^2 and α_1^2 from (3.21). The results are as follows:

$$\alpha_o^2 = \beta_o^2 - \beta_z^2 \quad (3.25) \; ; \quad \alpha_1^2 = \beta_1^2 - \beta_z^2 \tag{3.26}$$

with

$$\beta_{o,1}^2 = \frac{-ikP_r R_\nu}{2(1+i\gamma_0 k/R_\eta)} \left[1 + i\frac{\gamma_0 k}{P_r R_\nu} + i\frac{k}{R_\eta}\right] \cdot$$

$$\cdot \left[1 \mp \sqrt{1 - \frac{4ik}{P_r R_\nu} \frac{1+i\gamma_0 k/R_\eta}{(1+i\gamma_0 k/P_r R_\nu + ik/R_\eta)^2}}\right] \tag{3.27}$$

where the o and 1 subscripts correspond to the - and + signs respectively.

In addition, the acoustic and thermal potentials φ_a and φ_{th} are coupled through (3.11) and (3.12). When (3.18) and (3.19) are substituted into (3.12) and use is made of (3.23) and (3.24), one easily arrives at the following relations:

$$\varphi_{ao}(x,y) = \frac{\beta_0^2 + ikP_r R_\nu}{(\gamma_0 - 1)\beta_0^2} \varphi_{tho}(x,y) \tag{3.28}$$

$$\varphi_{a1}(x,y) = \frac{\beta_1^2 + ikP_r R_\nu}{(\gamma_0 - 1)\beta_1^2} \varphi_{th1}(x,y) \tag{3.29}$$

One then may check that the second coupling relation, (3.11), is also satisfied.

In a similar fashion, when use is made of (3.20) in (3.13) and (3.10), one obtains the governing equation for the vector potential:

$$\nabla_1^2 \vec{G} + \alpha_2^2 \vec{G} = 0 \tag{3.30}$$

where

$$\alpha_2^2 = \beta_2^2 - \beta_z^2 \tag{3.31}$$

and

$$\beta_2^2 = -ikR_\nu \tag{3.32}$$

with the following restriction on the possible solutions

$$\nabla_1 \cdot \vec{G}_1 = i \beta_z G_z \tag{3.33}$$

In the above coupling relation, the vector potential $\vec{G}$ has been decomposed into an axial component $\vec{G}_z$ and a component in the cross-sectional plane $\vec{G}_1$. A similar notation will subsequently be used for the velocity vector $\vec{V}'$.

Finally, the boundary conditions (3.17) may be written in terms of the auxiliary variables as follows:

$$\begin{cases} d\vec{V}_1'(x,y) = \nabla_1(\varphi_a + \varphi_{th}) + \nabla_1 \times \vec{G}_z - i\beta_z \vec{e}_z \times \vec{G}_1 = 0 & (3.24) \\ d\vec{V}_z'(x,y) = -i\beta_z(\varphi_a + \varphi_{th})\vec{e}_z + \nabla_1 \times \vec{G}_1 = 0 \quad \text{on duct boundary walls.} & (3.35) \\ \frac{d}{P_r R_\nu} \sqrt{\frac{(\nu_0 - 1)c_{p_0}}{T_0}}\, T'(x,y) = \varphi_{th} = 0 & (3.36) \end{cases}$$

Discussion: For a cylindrical duct of arbitrary cross-section and given values of the parameters ν_0, P_r, R_ν, R_η, and k, the problem has been reduced to the determination of a complex wave number β_z and three unknown functions φ_a, φ_{th}, and $\vec{G}$. The general analytical form of the auxiliary functions is given by equations (3.23), (3.24), and (3.30)

which have to be supplemented with the coupling relations (3.28), (3.29), and (3.33). Enforcement of the boundary conditions (3.34) - (3.36) then determines the remaining unknown β_z . For arbitrary cross-sectional shapes, it is unfortunately impossible to find separable solutions of equations (3.23), (3.24), and (3.30), compatible with the boundary conditions at the walls, and leading to a dispersion relation for β_z expressible in terms of a finite number of transcendental functions. It was shown in Section 2.4.2 that the analytical formulation of wave propagation problems in elastic solids bore a close resemblance with the model presented in Chapter II. The same mathematical difficulties have indeed been encountered by researchers interested in the propagation of elastic fluctuations in solid wave guides. A review of this subject is given by Meeker and Meitzler (1964) and Achenbach (1973). However, in the case of a two-dimensional or a circular tube, one may arrive at an exact dispersion relation in terms of a finite number of tabulated functions.

We have chosen to treat here the propagation of waves between two parallel infinite plates, i.e., through a two-dimensional duct. Many similarities will be shown to exist between the families of modes in a two-dimensional duct and a circular tube, and identical methods may be used in both instances. Since we are mainly interested in bringing out the main physical features of the problem, and wish to minimize analytical complications, we devote the major part of this study to a detailed investigation of wave propagation in a two-dimensional duct.

3.3 Two-Dimensional Duct:

Let us consider a two-dimensional duct of width d as shown on Figure 2 and a harmonic wave of frequency ω propagating in the positive

z direction, under the same assumptions as in the previous section.

In analogy with equations (3.18) - (3.20), we further restrict the functional forms of Φ_a , Φ_{th} , and $\vec{A}$ to the following:

$$\Phi_a(\vec{r},t) = \varphi_a(x)e^{i(t-\beta_z z)} \tag{3.37}$$

$$\Phi_{th}(\vec{r},t) = \varphi_{th}(x)e^{i(t-\beta_z z)} \tag{3.38}$$

$$\vec{A}(\vec{r},t) = \vec{G}(x)e^{i(t-\beta_z z)} \tag{3.39}$$

Note that φ_a , φ_{th} , and $\vec{G}$ are assumed to be independent of the space coordinate y . In other words, the wave motion is the same in all planes normal to the y-axis. However, since we allow the vector potential to have x- and z-components, the motion is not restricted to the y-plane, and the velocity field may admit a non-zero component along the y-axis.

The governing equations (3.23), (3.24), and (3.30) simply become:

$$\frac{d^2}{dx^2}\{\varphi_{ao} \text{ or } \varphi_{tho}\} + \alpha_0^2\{\varphi_{ao} \text{ or } \varphi_{tho}\} = 0 \tag{3.40}$$

$$\frac{d^2}{dx^2}\{\varphi_{a1} \text{ or } \varphi_{th1}\} + \alpha_1^2\{\varphi_{a1} \text{ or } \varphi_{th1}\} = 0 \tag{3.41}$$

$$\frac{d^2\vec{G}}{dx^2} + \alpha_2^2\vec{G} = 0 \tag{3.42}$$

so that the general form of $\varphi_{th}(x)$ is:

$$\varphi_{th}(x) = A\cos\alpha_o x + B\sin\alpha_o x + C\cos\alpha_1 x + D\sin\alpha_1 x \tag{3.43}$$

and the corresponding form of $\varphi_a(x)$ derived from the coupling relations (3.28) and (3.29) is:

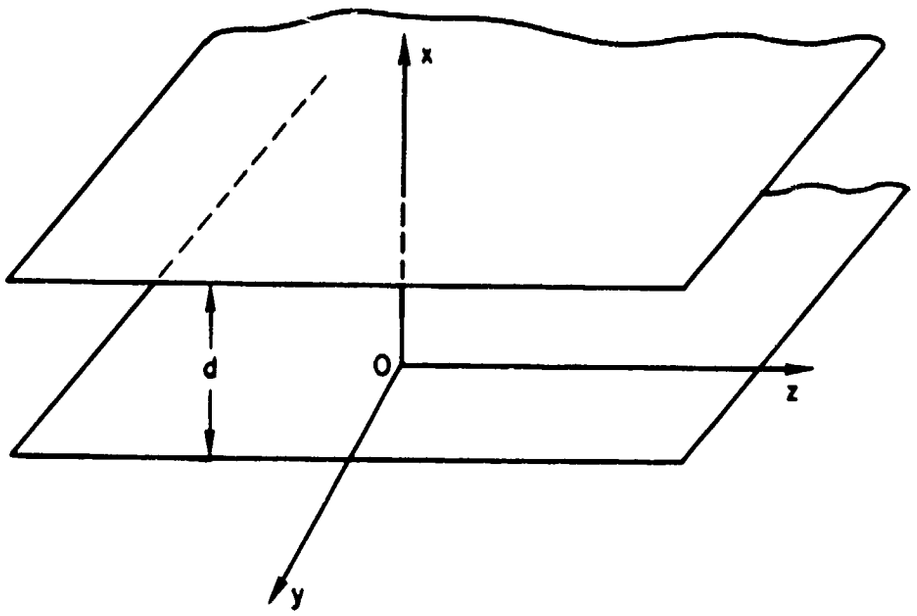

Figure 2. Two-dimensional duct.

$$\varphi_a(x) = \frac{\beta_0^2 + ikP_r R_\nu}{(\gamma_0 - 1)\beta_0^2}[A\cos\alpha_0 x + B\sin\alpha_0 x]$$

$$+ \frac{\beta_1^2 + ikP_r R_\nu}{(\gamma_0 - 1)\beta_1^2}[C\cos\alpha_1 x + D\sin\alpha_1 x] \qquad (3.44)$$

Similarly, use of (3.42) and the condition (3.33) yields the following expressions for the components of the viscous potential:

$$G_x(x) = E\cos\alpha_2 x + F\sin\alpha_2 x \qquad (3.45)$$

$$G_y(x) = G\cos\alpha_2 x + H\sin\alpha_2 x \qquad (3.46)$$

$$G_z(x) = \frac{i\alpha_2}{R_z}(-F\cos\alpha_2 x + E\sin\alpha_2 x) \qquad (3.47)$$

Finally, the boundary conditions (3.34) - (3.36) become:

$$V_x'(x) \propto \frac{d}{dx}(\varphi_a \text{ or } \varphi_{th}) + i\beta_z G_y = 0 \qquad (3.48)$$

$$V_y'(x) \propto -\frac{dG_z}{dx} - i\beta_z G_x = 0 \qquad (3.49)$$

at $x = \pm \frac{1}{2}$

$$V_z'(x) \propto -i\beta_z(\varphi_a + \varphi_{th}) + \frac{dG_y}{dx} = 0 \qquad (3.50)$$

$$T'(x) \propto \varphi_{th} = 0 \qquad (3.51)$$

and substitution of (3.43) - (3.47) into (3.48) - (3.51) yields the following set of eight homogeneous linear equations for the eight unknown constants: A, B, C, D, E, F, G, and H:

$$\alpha_0 \frac{\gamma_0\beta_0^2 + ikP_r R_\nu}{(\gamma_0 - 1)\beta_0^2}[-A\sin\frac{\alpha_0}{2} + B\cos\frac{\alpha_0}{2}] + \alpha_1 \frac{\gamma_0\beta_1^2 + ikP_r R_\nu}{(\gamma_0 - 1)\beta_1^2} \cdot$$

$$[-C\sin\frac{\alpha_1}{2} + D\cos\frac{\alpha_1}{2}] + i\beta_z[G\cos\frac{\alpha_2}{2} + H\sin\frac{\alpha_2}{2}] = 0 \qquad (3.52)$$

$$\alpha_0 \frac{\gamma_0\beta_0^2+ikP_rR_\nu}{(\gamma_0-1)\beta_0^2}\left[A\sin\frac{\alpha_0}{2}+B\cos\frac{\alpha_0}{2}\right]+\alpha_1\frac{\gamma_0\beta_1^2+ikP_rR_\nu}{(\gamma_0-1)\beta_1^2}\cdot$$

$$\left[C\sin\frac{\alpha_1}{2}+D\cos\frac{\alpha_1}{2}\right]+i\beta_z\left[G\cos\frac{\alpha_2}{2}-H\sin\frac{\alpha_2}{2}\right]=0 \qquad (3.53)$$

$$-i\beta_z\frac{\gamma_0\beta_0^2+ikP_rR_\nu}{(\gamma_0-1)\beta_0^2}\left[A\cos\frac{\alpha_0}{2}+B\sin\frac{\alpha_0}{2}\right]-i\beta_z\frac{\gamma_0\beta_1^2+ikP_rR_\nu}{(\gamma_0-1)\beta_1^2}\cdot$$

$$\left[C\cos\frac{\alpha_1}{2}+D\sin\frac{\alpha_1}{2}\right]+\alpha_2\left[-G\sin\frac{\alpha_2}{2}+H\cos\frac{\alpha_2}{2}\right]=0 \qquad (3.54)$$

$$-i\beta_z\frac{\gamma_0\beta_0^2+ikP_rR_\nu}{(\gamma_0-1)\beta_0^2}\left[A\cos\frac{\alpha_0}{2}-B\sin\frac{\alpha_0}{2}\right]-i\beta_z\frac{\gamma_0\beta_1^2+ikP_rR_\nu}{(\gamma_0-1)\beta_1^2}\cdot$$

$$\left[C\cos\frac{\alpha_1}{2}-D\sin\frac{\alpha_1}{2}\right]+\alpha_2\left[G\sin\frac{\alpha_2}{2}+H\cos\frac{\alpha_2}{2}\right]=0 \qquad (3.55)$$

$$A\cos\frac{\alpha_0}{2}+B\sin\frac{\alpha_0}{2}+C\cos\frac{\alpha_1}{2}+D\sin\frac{\alpha_1}{2}=0 \qquad (3.56)$$

$$A\cos\frac{\alpha_0}{2}-B\sin\frac{\alpha_0}{2}+C\cos\frac{\alpha_1}{2}-D\sin\frac{\alpha_1}{2}=0 \qquad (3.57)$$

$$E\cos\frac{\alpha_2}{2}+F\sin\frac{\alpha_2}{2}=0 \qquad (3.58)$$

$$E\cos\frac{\alpha_2}{2}-F\sin\frac{\alpha_2}{2}=0 \qquad (3.59)$$

By elementary manipulations such as addition or subtraction of consecutive equations the above system may be immediately expanded into the four following subsystems.

System I:

$$E\cos\frac{\alpha_2}{2}=0 \qquad (3.60)$$

System II:

$$F \sin \frac{\alpha_2}{2} = 0 \tag{3.61}$$

System III:

$$\alpha_0 \frac{\gamma_0 \beta_0^2 + ikP_r R \nu}{(\gamma_0 - 1)\beta_0^2} A \sin \frac{\alpha_0}{2} + \alpha_1 \frac{\gamma_0 \beta_1^2 + ikP_r R \nu}{(\gamma_0 - 1)\beta_1^2} C \sin \frac{\alpha_1}{2} - i\beta_z H \sin \frac{\alpha_2}{2} = 0 \tag{3.62}$$

$$-i\beta_z \frac{\gamma_0 \beta_0^2 + ikP_r R \nu}{(\gamma_0 - 1)\beta_0^2} A \cos \frac{\alpha_0}{2} - i\beta_z \frac{\gamma_0 \beta_1^2 + ikP_r R \nu}{(\gamma_0 - 1)\beta_1^2} C \cos \frac{\alpha_1}{2} + \alpha_2 H \cos \frac{\alpha_2}{2} = 0 \tag{3.63}$$

$$A \cos \frac{\alpha_0}{2} + C \cos \frac{\alpha_1}{2} = 0 \tag{3.64}$$

System IV:

$$\alpha_0 \frac{\gamma_0 \beta_0^2 + ikP_r R \nu}{(\gamma_0 - 1)\beta_0^2} B \cos \frac{\alpha_0}{2} + \alpha_1 \frac{\gamma_0 \beta_1^2 + ikP_r R \nu}{(\gamma_0 - 1)\beta_1^2} D \cos \frac{\alpha_1}{2} + i\beta_z G \cos \frac{\alpha_2}{2} = 0 \tag{3.65}$$

$$-i\beta_z \frac{\gamma_0 \beta_0^2 + ikP_r R \nu}{(\gamma_0 - 1)\beta_0^2} B \sin \frac{\alpha_0}{2} - i\beta_z \frac{\gamma_0 \beta_1^2 + ikP_r R \nu}{(\gamma_0 - 1)\beta_1^2} D \sin \frac{\alpha_1}{2} - \alpha_2 G \sin \frac{\alpha_2}{2} = 0 \tag{3.66}$$

$$B \sin \frac{\alpha_0}{2} + D \sin \frac{\alpha_1}{2} = 0 \tag{3.67}$$

In order for these subsystems to admit non-trivial solutions, the determinants formed with the coefficients of their respective variables must be set equal to zero. Those conditions yield four compatibility conditions or so-called dispersion relations which may be written as follows:

Dispersion Relation I:

$$\cos \frac{\alpha_2}{2} = 0 \tag{3.68}$$

Dispersion Relation II:

$$\sin \frac{\alpha_2}{2} = 0 \tag{3.69}$$

Dispersion Relation III:

$$k^2\left(\frac{1}{\beta_0^2} - \frac{1}{\beta_1^2}\right)\beta_z^2 \cos\frac{\alpha_0}{2}\cos\frac{\alpha_1}{2}\sin\frac{\alpha_2}{2} + \left(\frac{k^2}{\beta_0^2} - \frac{i\gamma_0 k}{P_r R_\nu}\right)\alpha_0\alpha_2$$

$$\sin\frac{\alpha_0}{2}\cos\frac{\alpha_1}{2}\cos\frac{\alpha_2}{2} - \left(\frac{k^2}{\beta_1^2} - \frac{i\gamma_0 k}{P_r R_\nu}\right)\alpha_1\alpha_2 \cos\frac{\alpha_0}{2}\sin\frac{\alpha_1}{2}\cos\frac{\alpha_2}{2} = 0 \tag{3.70}$$

Dispersion Relation IV:

$$k^2\left(\frac{1}{\beta_0^2} - \frac{1}{\beta_1^2}\right)\beta_z^2 \sin\frac{\alpha_0}{2}\sin\frac{\alpha_1}{2}\cos\frac{\alpha_2}{2} + \left(\frac{k^2}{\beta_0^2} - \frac{i\gamma_0 k}{P_r R_\nu}\right)\alpha_0\alpha_2$$

$$\cos\frac{\alpha_0}{2}\sin\frac{\alpha_1}{2}\sin\frac{\alpha_2}{2} - \left(\frac{k^2}{\beta_1^2} - \frac{i\gamma_0 k}{P_r R_\nu}\right)\alpha_1\alpha_2 \sin\frac{\alpha_0}{2}\cos\frac{\alpha_1}{2}\sin\frac{\alpha_2}{2} = 0 \tag{3.71}$$

Discussion: As seen from equations (3.60) - (3.67), each subsystem pertains to distinct groups of unknown constants. Consequently, if any one of the dispersion relations (I) to (IV) is satisfied, there exists a non-zero solution for the unknowns of the corresponding subsystem. At the same time, since the remaining determinants then take non-zero values, the only possible solution for the other subsystems is zero. Hence, each set (I) to (IV) and its dispersion relation may be investigated separately, the constants associated with the other sets being identically zero. Even though a detailed description of the four corresponding types of wave motion will be given in Section 3.4 and Chapter IV, we take advantage of this mathematical feature to briefly outline their main characteristics.

Let us first indroduce the following definitions: A wave motion will be called symmetric (respectively, antisymmetric) if its velocity is symmetric (respectively, antisymmetric) with respect to the median y-z plane. It will be referred to as inplane (respectively, antiplane) when its velocity vector lies in (respectively, is perpendicular to) the x-z plane. From the above discussion, and the form of equations (3.60)-(3.61), we infer that, in sets (I) and (II), all constants are zero with the exception of E or F. As seen from (3.43) - (3.47), the acoustic and thermal components are then identically zero, and the vector potential lies in the x-z plane. The velocity vector is therefore purely rotational and its only non-zero component is V_y given by (3.49). Furthermore, F is zero in System (I) so that V_y is then an even function of x. Likewise, E is zero in System (II), so that V_y is then an odd function of x. We may conclude that sets (I) and (II) describe the behavior of antiplane symmetric and antisymmetric velocity fluctuations. In a similar fashion, when one considers set (III) (respectively, (IV)), B, D, E, F, G, (respectively A, C, E, F, H) are zero. Upon examination of (3.43) - (3.50), it is clear that both sets describe inplane wave motions, and that (III) and (IV) are associated with symmetric and antisymmetric velocity fields respectively. However, in contrast with the antiplane motions, acoustic, thermal, and viscous components are now inherently coupled and lead to complicated wave configurations. The initial problem of wave propagation between two infinite parallel walls has thus been reduced to four simpler subproblems, namely, inplane or antiplane, symmetric or antisymmetric wave motions, each one being governed by one of the Systems (I) to (IV) and its corresponding dispersion relation.

In equations (3.68) - (3.71), the complex quantities α_0 , α_1 and α_2 may be expressed in terms of the complex wave number β_z through the use of (3.25), (3.26), and (3.31). Each one of the dispersion relations is then an equation for β_z , and its solutions are to be determined as a function of the given non-dimensional parameters γ_0 , P_r , R_ν , R_η and k . Each solution defines a mode of propagation, characterized by specific variations for $\varphi_a(x)$, $\varphi_{th}(x)$ and $\vec{\Omega}(x)$. Such characteristic variations constitute a mode shape, and they may be obtained exactly by solving the appropriate subsystem (I) - (IV) for the corresponding unknown constants. Equations (3.68) - (3.69) are trivial and the next section will examine their solutions and associated mode shapes. On the other hand, the dispersion relations (3.70) - (3.71) pertaining to the inplane modes, are transcendental equations for β_z , and cannot be solved exactly. In Chapter IV, we will propose a perturbation scheme, whereby approximate solutions may be obtained.

We have previously pointed out the analogy between wave propagation in viscous fluids and in elastic solids. It is indeed striking to note that wave motion in an elastic layer is governed by equations which are very similar to the subsystems developed here. Meeker and Meitzler (1964), in particular, assumed the Lamé potentials to have a form analogous to the expressions chosen in (3.37) - (3.39), and were thus led to classify the possible solutions in terms of four families of waves, namely, symmetric and antisymmetric SH (Shear-Horizontal) waves, and longitudinal and flexural plane strain waves. The dispersion relations describing the latter two families, or so-called Rayleigh-Lamb equations are found to present essentially the same basic features as relations (3.70) and (3.71) when heat flow is assumed to be zero. In such a case,

the last term in relations (III) and (IV) disappears. In the next section, we discuss the characteristics of the symmetric and antisymmetric antiplane wave motions.

3.4 Symmetric and Antisymmetric Antiplane Wave Motion.

The solutions of dispersion relation (I) are immediately given by:

$$\alpha_{2n}^{SA} = (2n+1)\pi \tag{3.72}$$

when n is a zero or positive integer. Hence, there exists an infinity of symmetric antiplane SA-modes. Their shape in any cross-sectional plane is characterized by a specific value of the coefficient α_2. The propagation wave number attached to each mode is obtained by substituting (3.72) into (3.31). In solving the resulting equation for β_z, we select the complex root which pertains to waves attenuating in the positive z-direction, i.e. of negative imaginary part, the other root being associated with waves attenuating in the negative z-direction.* Such a choice does not restrict the scope of the study, since the propagation characteristics are obviously independent of the direction along the z-axis. The wave number is then given by the following relation:

$$\beta_{zn}^{SA} = \frac{1}{\sqrt{2}}\left[\sqrt{\sqrt{((2n+1)\pi)^4+(kR_\nu)^2}-((2n+1)\pi)^2}\right.$$
$$\left.-i\sqrt{\sqrt{((2n+1)\pi)^4+(kR_\nu)^2}+((2n+1)\pi)^2}\right] \tag{3.73}$$

*We have avoided here using a radiation condition based on the sign of the phase velocity, i.e. the direction of propagation of the wavefronts, since, in Chapter IV, we will encounter backward-propagating waves which decay in the positive z-direction.

As discussed in the preceding section, E is the only non-zero constant, so that from (3.43) - (3.47), acoustic and thermal potentials are identically zero, and the viscous potential lies in the x-z plane with the following components:

$$\Omega_{xn}^{SA}(x) = E \cos((2n+1)\pi x) \tag{3.74}$$

$$\Omega_{yn}^{SA}(x) = 0 \tag{3.75}$$

$$\Omega_{zn}^{SA}(x) = \frac{(2n+1)\pi i}{\beta_{zn}^{SA}} E \sin((2n+1)\pi x) \tag{3.76}$$

the rotational velocity field is then such that:

$$\vec{V}_n'^{SA}(x) = -\frac{kR_\nu}{d\beta_{zn}^{SA}} E \cos((2n+1)\pi x)\vec{e}_y \tag{3.77}$$

All other physical variables are identically zero.

The velocity profile of each mode will be normalized by the following condition

$$V_{yn}'(0) = 1 \tag{3.78}$$

which determines the value of the arbitrary constant E . The final form of the mode shape is:

$$V_{yn}'^{SA}(x) = \cos(2n+1)\pi x \tag{3.79}$$

The characteristics of the symmetric antiplane mode have therefore been derived in a straight-forward manner due to the extreme simplicity of the associated dispersion relation. They are purely transversal rotational waves, the velocity fluctuations being perpendicular to the plane of propagation. An interesting interpretation of equation (3.79) follows

from the decomposition of the cosine function into complex exponentials. The velocity may then be written as follows:

$$V'^{SA}_{yn}(x,z,t) = \frac{1}{2} e^{\mathrm{Im}\beta^{SA}_{zn} z} \cdot e^{i[t + (2n+1)\pi x - \mathrm{Re}\,\beta^{SA}_{zn} z]}$$

$$+ \frac{1}{2} e^{\mathrm{Im}\,\beta^{SA}_{zn} z} \cdot e^{i[t - (2n+1)\pi x - \mathrm{Re}\,\beta^{SA}_{zn} z]} \qquad (3.80)$$

Each mode V'^{SA}_{yn} may thus be considered as the superposition of two plane transversal waves travelling in symmetric directions with respect to the median yz-plane and, which, upon multiple reflections at the boundaries, give rise to a standing wave pattern in the cross-sectional plane, and a propagating wave along the z-axis.

Analogous results may be obtained for the antisymmetric antiplane AA-modes. Their complex wave number is then given by:

$$\beta^{AA}_{zn} = \frac{1}{\sqrt{2}} \left[\sqrt{\sqrt{(2n\pi)^4 + (kR_\nu)^2} - (2n\pi)^2} \right.$$

$$\left. - i \sqrt{\sqrt{(2n\pi)^4 + (kR_\nu)^2} + (2n\pi)^2} \right] \qquad (3.81)$$

where n is a positive integer,* and the corresponding mode shape is:

$$V'^{AA}_{yn}(x) = \sin 2n\pi x \qquad (3.82)$$

The magnitude of the imaginary part of the complex wave number defines the non-dimensional attenuation rate per diameter along the duct

*The integer n cannot be zero, since such a value leads to a mode shape which is identically zero.

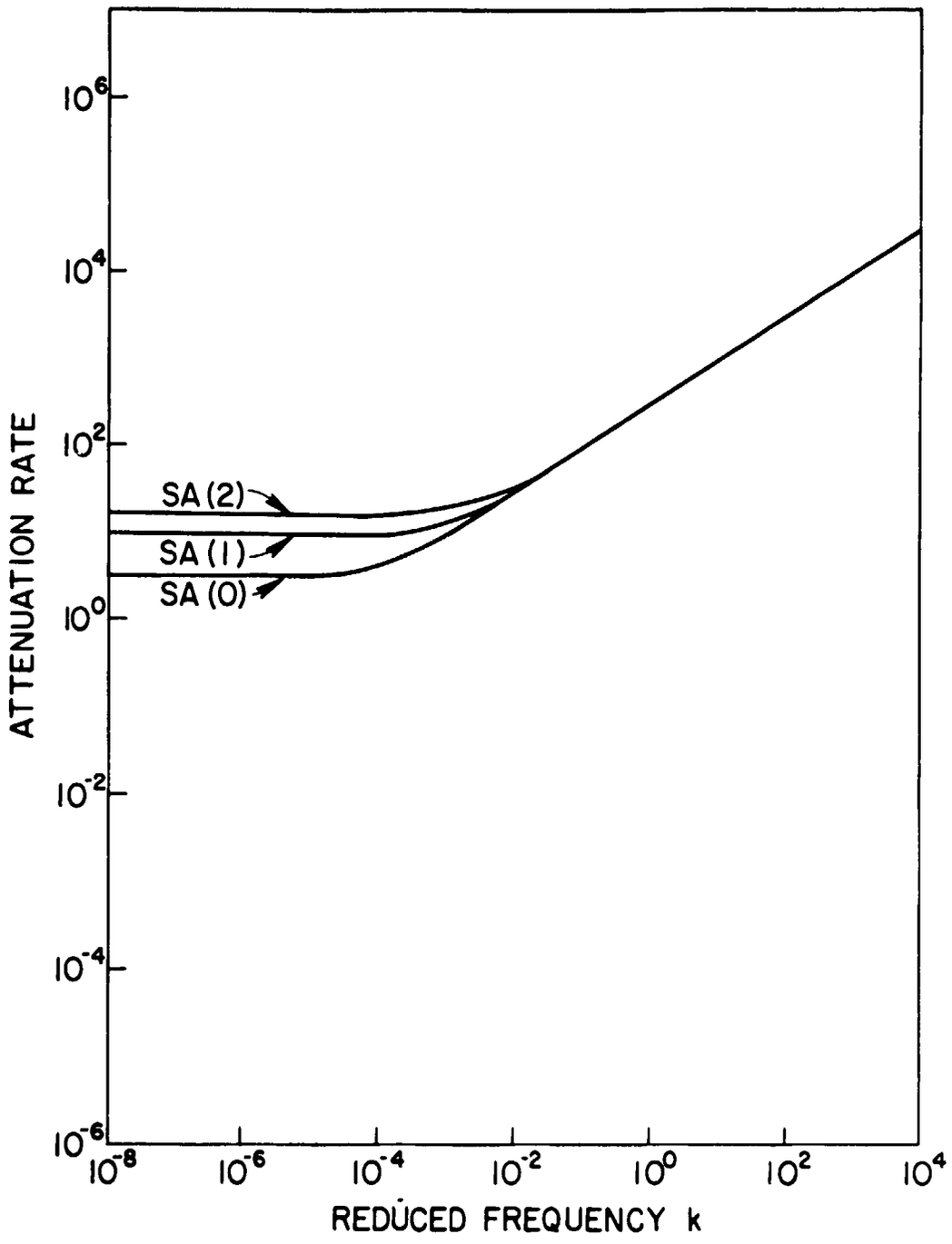

Figure 3. Symmetric Antiplane Modes. Attenuation rate versus reduced frequency for $R_\upsilon = 2.35 \times 10^5$, $d = 10^{-2}_{m}$, medium is air at 15°C, 1 atm.

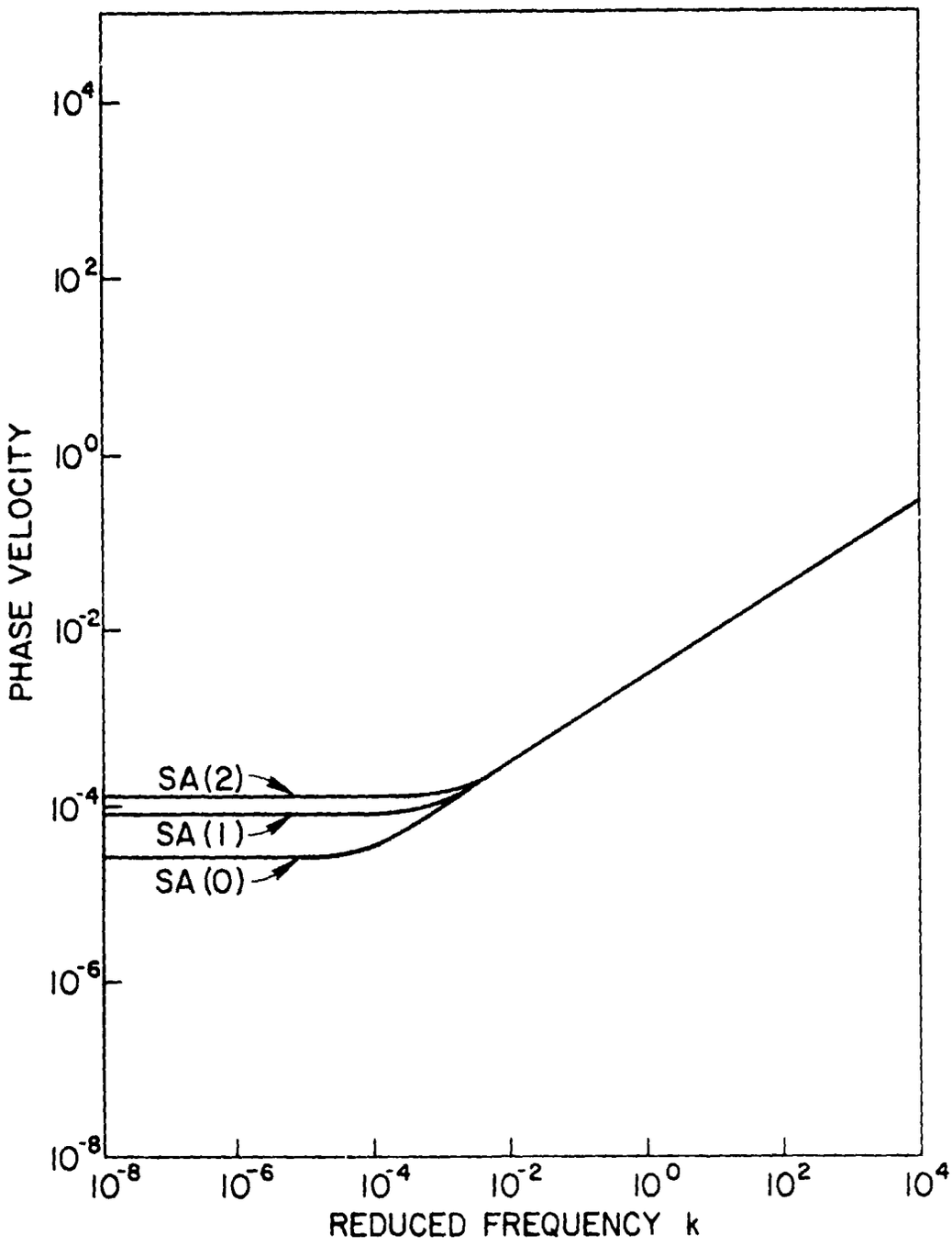

Figure 4. Symmetric Antiplane Modes. Phase velocity versus reduced frequency. Same values of the parameters as in Figure 3.

axis, whereas the real part is the actual propagation wave number. The phase velocity non-dimensionalized with respect to the speed of sound may be obtained by the formula:

$$V_{phn} = \frac{k}{Re\beta_{zn}} \tag{3.83}$$

On Figures 3 and 4, the attenuation rate and the phase velocity of the first three symmetric antiplane modes are represented as a function of the reduced frequency k, for a given set of values of the other four parameters. These curves describe the dispersive properties of the waves, and will be used extensively in the next chapter. As seen from these plots, one may distinguish two ranges of reduced frequencies: the low-frequency range where both attenuation rate and phase velocity are constant and independent of k, and the high-frequency range where they increase as the square root of k. These two regions are separated by a transition region. Further details on this question will be given in Chapter IV. At any rate, it is apparent from Figure 3, that antiplane modes are highly attenuated at all frequencies.

The antisymmetric antiplane modes have strictly similar characteristics, and since this study focuses on the symmetric modes, we do not need to elaborate on their properties. One may finally note that equations (3.73) and (3.81) may be merged into a single relation in terms of a new index N, equal to $2n+1$ for the symmetric modes and $2n$ for the antisymmetric modes. The eigenvalues of the antiplane modes are then given as follows:

$$\beta^{A}_{zN} = \frac{1}{\sqrt{2}}\left[\sqrt{\sqrt{(N\pi)^4+(kR_\nu)^2}-(N\pi)^2} - i\sqrt{\sqrt{(N\pi)^4+(kR_\nu)^2}+(N\pi)^2}\right] \tag{3.84}$$

where

$N = 1, 3, 5, \ldots$ for the SA modes

and

$N = 2, 4, 6, \ldots$ for the AA modes

3.5 Conclusion.

For the purpose of illustrating the basic method of solution, we have treated in detail the simple case of the antiplane modes. In this instance, exact solutions of the dispersion relation were immediately obtained throughout the entire reduced frequency domain. Unfortunately, dispersion relations (III) and (IV) are much more complicated, and require the use of some approximation scheme, if any analytical results are to be obtained. Chapter IV is, therefore, devoted to a perturbation study of the inplane wave motions, with particular emphasis on the symmetric inplane modes.

IV. PERTURBATION STUDY OF THE INPLANE MODES

4.1 Introduction.

In was shown in Section 3.3 that the eigenvalues associated with the symmetric (respectively, antisymmetric) inplane modes are solutions of dispersion relation (III) (respectively, (IV)), and that the corresponding eigenfunctions are given by (3.43) - (3.47) where the coefficients A, C, H (respectively, B, D, G) satisfy System (III) (respectively, (IV)), and E and F are zero.* This part of the investigation will be mainly concerned with the derivation of approximate solutions of the transcendental dispersion relations (III) and (IV). From these solutions, a detailed picture of the possible inplane wave motions will emerge.

Before undertaking such a study, we note that, when dispersion relation (III) is satisfied for a given eigenvalue β_z, System (III) admits an infinity of non-zero solutions which may be obtained by solving equations (3.62) and (3.64) for C and H. We have then the following relations:

$$C = - \frac{\cos \alpha_0/2}{\cos \alpha_1/2} A \tag{4.1}$$

$$H = - \frac{kP_r R_\nu}{\gamma_0 - 1}\left(\frac{1}{\beta_0^2} - \frac{1}{\beta_1^2}\right)\frac{\beta_z}{\alpha_2}\frac{\cos \alpha_0/2}{\cos \alpha_1/2} A \tag{4.2}$$

where A is still an arbitrary constant and will be determined later by imposing a suitable normalization condition. Substitution of the above

*The motion is therefore purely two-dimensional and the vector potential reduces to a stream function A_y. In an earlier report, Huerre and Karamcheti (1975) a priori considered such a stream function, and thus restricted their investigation to inplane motions. The slightly more general approach used in this study presents the advantage of also revealing the existence of antiplane wave motions.

values for C and H into (3.43), (3.44), and (3.46) leads to the expressions for $\varphi_a(x)$, $\varphi_{th}(x)$ and $G_y(x)$. The corresponding variations of the physical variables are then given by (3.5) - (3.9). The resulting symmetric inplane mode shapes are shown in Table I. We must emphasize that such mode shapes are functions of the specific wave number β_z and that they cannot be determined completely until the dispersion relation has been solved. However, when the eigenvalue is known, the associated mode shape will be obtained immediately by substitution into the relations of Table I. The same procedure may be used to determine the antisymmetric mode shapes given in Table II. We now proceed to an in-depth analysis of the inplane eigenvalues.

4.2 Methodology - Preliminary Assumptions.

In order to display the common features of the dispersion relations pertaining to the inplane wave motions, we divide (3.70) by $\alpha_2 \cos\alpha_o/2 \cdot \cos\alpha_1/2 \cos\alpha_2/2$ and (3.71) by $\alpha_2 \sin\alpha_o/2 \sin\alpha_1/2 \sin\alpha_2/2$, and recast them into the following single formula:

$$\left(\frac{k^2}{\beta_0^2} - \frac{k^2}{\beta_1^2}\right)\frac{\beta_z^2}{\alpha_2}\left\{\begin{matrix}\tan\\ \text{cotan}\end{matrix}\right\}\frac{\alpha_2}{2} + \left(\frac{k^2}{\beta_0^2} - \frac{i\gamma_0 k}{P_r R_\nu}\right)\alpha_0\left\{\begin{matrix}\tan\\ \text{cotan}\end{matrix}\right\}\frac{\alpha_0}{2}$$

$$- \left(\frac{k^2}{\beta_1^2} - \frac{i\gamma_0 k}{P_r R_\nu}\right)\alpha_1\left\{\begin{matrix}\tan\\ \text{cotan}\end{matrix}\right\}\frac{\alpha_1}{2} = 0 \qquad (4.3a,b)$$

where the upper and lower trigonometric functions refer to the symmetric (4.3a) and antisymmetric (4.3b) dispersion relations, respectively. In most instances, we will only need to consider the above expressions. However, the normalization which has just been performed may have restricted the number of possible solutions of the initial relations (III) and (IV), and in a few cases, we will find it more convenient to study the alternate

$\varphi_n(x) = A'\left[\left(\frac{k^2}{\beta_0^2} - \frac{ik}{P_r R_\nu}\right)\frac{\cos\alpha_0 x}{\cos\alpha_0/2} - \left(\frac{k^2}{\beta_1^2} - \frac{ik}{P_r R_\nu}\right)\frac{\cos\alpha_1 x}{\cos\alpha_1/2}\right]$
$\varphi_{th}(x) = -i\frac{(\gamma_0-1)k}{P_r R_\nu} A'\left[\frac{\cos\alpha_0 x}{\cos\alpha_0/2} - \frac{\cos\alpha_1 x}{\cos\alpha_1/2}\right]$
$\varphi_v(x) \quad iA'\left(\frac{k^2}{\beta_0^2} - \frac{k^2}{\beta_1^2}\right)\frac{\beta_z}{\alpha_2}\frac{\sin\alpha_2 x}{\cos\alpha_2/2}$
$p'(x) = -i\frac{\rho_0 a_0}{d} kA'\left[\left(1-\frac{i\beta_0^2}{kP_r R_\nu}\right)\frac{\cos\alpha_0 x}{\cos\alpha_0/2} - \left(1-\frac{i\beta_1^2}{kP_r R_\nu}\right)\frac{\cos\alpha_1 x}{\cos\alpha_1/2}\right]$
$S'(x) = \frac{1}{d}\sqrt{\frac{(\gamma_0-1)c_{p_0}}{T_0}}\frac{\beta_1^2}{P_r R_\nu} A'\left[\frac{\beta_0^2}{\beta_1^2}\frac{\cos\alpha_0 x}{\cos\alpha_0/2} - \frac{\cos\alpha_1 x}{\cos\alpha_1/2}\right]$
$\Omega_y'(x) = A'\frac{kR_\nu}{d^2}\left(\frac{k^2}{\beta_0^2} - \frac{k^2}{\beta_1^2}\right)\frac{\beta_z}{\alpha_2}\frac{\sin\alpha_2 x}{\cos\alpha_2/2}$
$T'(x) = -\frac{i}{d}\sqrt{\frac{(\gamma_0-1)T_0}{c_{p_0}}} kA'\left[\frac{\cos\alpha_0 x}{\cos\alpha_0/2} - \frac{\cos\alpha_1 x}{\cos\alpha_1/2}\right]$
$\rho'(x) = -\frac{i\rho_0}{a_0 d} kA'\left[\left(1-\frac{i\gamma_0\beta_0^2}{kP_r R_\nu}\right)\frac{\cos\alpha_0 x}{\cos\alpha_0/2} - \left(1-\frac{i\gamma_0\beta_1^2}{kP_r R_\nu}\right)\frac{\cos\alpha_1 x}{\cos\alpha_1/2}\right]$
$V_z'(x) = -\frac{iA'}{d}\beta_z\left[\left(\frac{k^2}{\beta_0^2} - \frac{i\gamma_0 k}{P_r R_\nu}\right)\frac{\cos\alpha_0 x}{\cos\alpha_0/2} - \left(\frac{k^2}{\beta_1^2} - \frac{i\gamma_0 k}{P_r R_\nu}\right)\frac{\cos\alpha_1 x}{\cos\alpha_1/2} - \left(\frac{k^2}{\beta_0^2} - \frac{k^2}{\beta_1^2}\right)\frac{\cos\alpha_2 x}{\cos\alpha_2/2}\right]$
$V_x'(x) = -\frac{A'}{d}\left[\left(\frac{k^2}{\beta_0^2} - \frac{i\gamma_0 k}{P_r R_\nu}\right)\alpha_0\frac{\sin\alpha_0 x}{\cos\alpha_0/2} - \left(\frac{k^2}{\beta_1^2} - \frac{i\gamma_0 k}{P_r R_\nu}\right)\alpha_1\frac{\sin\alpha_1 x}{\cos\alpha_1/2} + \left(\frac{k^2}{\beta_0^2} - \frac{k^2}{\beta_1^2}\right)\frac{\beta_z^2}{\alpha_2}\frac{\sin\alpha_2 x}{\cos\alpha_2/2}\right]$

TABLE 1. Symmetric Inplane Mode Shapes. For simplicity the constant A has been replaced by $A' = \frac{iP_r R_\nu}{(\gamma_0-1)k} A\cos\frac{\alpha_0}{2}$.

$$\varphi_a(x) = B' \left[\left(\frac{k^2}{\beta_0^2} - \frac{ik}{P_r R_\nu} \right) \frac{\sin\alpha_0 x}{\sin\alpha_0/2} - \left(\frac{k^2}{\beta_1^2} - \frac{ik}{P_r R_\nu} \right) \frac{\sin\alpha_1 x}{\sin\alpha_1/2} \right]$$

$$\varphi_{th}(x) = - \frac{i(\gamma_0 - 1)k}{P_r R_\nu} B' \left[\frac{\sin\alpha_0 x}{\sin\alpha_0/2} - \frac{\sin\alpha_1 x}{\sin\alpha_1/2} \right]$$

$$\Omega_y(x) = -iB' \left(\frac{k^2}{\beta_0^2} - \frac{k^2}{\beta_1^2} \right) \frac{\beta_z}{\alpha_2} \frac{\cos\alpha_2 x}{\sin\alpha_2/2}$$

$$p'(x) = - \frac{i\rho_0 a_0 k}{d} B' \left[\left(1 - \frac{i\beta_0^2}{kP_r R_\nu} \right) \frac{\sin\alpha_0 x}{\sin\alpha_0/2} - \left(1 - \frac{i\beta_1^2}{kP_r R_\nu} \right) \frac{\sin\alpha_1 x}{\sin\alpha_1/2} \right]$$

$$S'(x) = \frac{1}{d} \sqrt{\frac{(\gamma_0 - 1)c_{p_0}}{T_0}} \frac{\beta_1^2}{P_r R_\nu} B' \left[\frac{\beta_0^2}{\beta_1^2} \frac{\sin\alpha_0 x}{\sin\alpha_0/2} - \frac{\sin\alpha_1 x}{\sin\alpha_1/2} \right]$$

$$\Omega_y'(x) = -B' \frac{kR_\nu}{d^2} \left(\frac{k^2}{\beta_0^2} - \frac{k^2}{\beta_1^2} \right) \frac{\beta_z}{\alpha_2} \frac{\cos\alpha_2 x}{\sin\alpha_2/2}$$

$$T'(x) = - \frac{i}{d} \sqrt{\frac{(\gamma_0 - 1)T_0}{c_{p_0}}} k B' \left[\frac{\sin\alpha_0 x}{\sin\alpha_0/2} - \frac{\sin\alpha_1 x}{\sin\alpha_1/2} \right]$$

$$\rho'(x) = - \frac{i\rho_0}{a_0 d} k B' \left[\left(1 - \frac{i\gamma_0 \beta_0^2}{kP_r R_\nu} \right) \frac{\sin\alpha_0 x}{\sin\alpha_0/2} - \left(1 - \frac{i\gamma_0 \beta_1^2}{kP_r R_\nu} \right) \frac{\sin\alpha_1 x}{\sin\alpha_1/2} \right]$$

$$V_z'(x) = - \frac{iB'}{d} \beta_z \left[\left(\frac{k^2}{\beta_0^2} - \frac{i\gamma_0 k}{P_r R_\nu} \right) \frac{\sin\alpha_0 x}{\sin\alpha_0/2} - \left(\frac{k^2}{\beta_1^2} - \frac{i\gamma_0 k}{P_r R_\nu} \right) \frac{\sin\alpha_1 x}{\sin\alpha_1/2} - \left(\frac{k^2}{\beta_0^2} - \frac{k^2}{\beta_1^2} \right) \frac{\sin\alpha_2 x}{\sin\alpha_2/2} \right]$$

$$V_x'(x) = \frac{B'}{d} \left[\left(\frac{k^2}{\beta_0^2} - \frac{i\gamma_0 k}{P_r R_\nu} \right) \alpha_0 \frac{\cos\alpha_0 x}{\sin\alpha_0/2} - \left(\frac{k^2}{\beta_1^2} - \frac{i\gamma_0 k}{P_r R_\nu} \right) \alpha_1 \frac{\cos\alpha_1 x}{\sin\alpha_1/2} + \left(\frac{k^2}{\beta_0^2} - \frac{k^2}{\beta_1^2} \right) \frac{\beta_z^2}{\alpha_2} \frac{\cos\alpha_2 x}{\sin\alpha_2/2} \right]$$

TABLE II. Antisymmetric Inplane Mode Shapes. The constant B has been replaced by

$$B' = \frac{iP_r R_\nu}{(\gamma_0 - 1)k} B \sin\frac{\alpha_0}{2} .$$

set of relations:

$$\left(\frac{k^2}{\beta_0^2}-\frac{k^2}{\beta_1^2}\right)\frac{\beta_z^2}{\alpha_2}\left\{\begin{matrix}\text{cotan}\\ \tan\end{matrix}\right\}\frac{\alpha_0}{2}\left\{\begin{matrix}\text{cotan}\\ \tan\end{matrix}\right\}\frac{\alpha_1}{2}+\left(\frac{k^2}{\beta_0^2}-\frac{i\gamma_0 k}{P_r R_\nu}\right)\alpha_0 \cdot$$

$$\left\{\begin{matrix}\text{cotan}\\ \tan\end{matrix}\right\}\frac{\alpha_1}{2}\left\{\begin{matrix}\text{cotan}\\ \tan\end{matrix}\right\}\frac{\alpha_2}{2}-\left(\frac{k^2}{\beta_1^2}-\frac{i\gamma_0 k}{P_r R_\nu}\right)\alpha_1\left\{\begin{matrix}\text{cotan}\\ \tan\end{matrix}\right\}\frac{\alpha_0}{2}\left\{\begin{matrix}\text{cotan}\\ \tan\end{matrix}\right\}\frac{\alpha_2}{2}=0 \qquad (4.3c,d)$$

with the same conventions for the trigonometric functions as in (4.3a,b). This latter form of the dispersion relations results from the divisions of (3.70) by $\alpha_2 \sin\frac{\alpha_0}{2}\sin\frac{\alpha_1}{2}\sin\frac{\alpha_2}{2}$ and (3.71) by $\alpha_2 \cos\frac{\alpha_0}{2}\cos\frac{\alpha_1}{2}\cos\frac{\alpha_2}{2}$. Together with the first normalized set, it will ensure that all possible solutions of the original equations are examined.

Expression (4.3a) is strikingly similar to the dispersion relation first derived by Kirchhoff (1868), and describing the axisymmetric modes of a duct of circular cross-section. To obtain the latter, one simply replaces the trigonometric tangent in (4.3a) by the ratio of Bessel functions, J_1/J_0. We, therefore, expect the symmetric inplane modes to be closely related to the axisymmetric modes of the circular geometry.

As mentioned in Chapter III, both equations are transcendental and cannot be solved exactly. This constitutes the major obstacle of the present investigation. The problem may be approached from two basically different ways. A numerical scheme can be developed to isolate the solutions of the equations. Such a method was implemented by Shields et al. (1965) and Tijdeman (1975) to determine the characteristics of the fundamental zeroth-pressure mode, and by Scarton and Rouleau (1973) to study all the axisymmetric eigenfunctions in the case of zero heat-conduction. The analysis is then considerably simplified by the presence of only two terms in the dispersion relations. In a second approach sug-

gested by Kirchhoff (1868) and Rayleigh (1877), and adopted by a large number of investigators to be mentioned later in the course of this chapter, one attempts to obtain approximate solutions of the dispersion relations analytically. Applications of this type of procedure have traditionally been restricted to the determination of the characteristics of the pressure modes in the acoustic boundary layer approximation. The pressure modes, in the limit of zero boundary layer thickness, reduce to the familiar acoustic modes encountered in inviscid propagation problems, so that the first terms in the approximations are then readily available. In this study, we develop a methodology whereby perturbation expansions of the complex wave number may be extracted from the dispersion relation for all the eigenfunctions of the problem, in as many ranges of the parameters as possible. The main advantage of this approach over the purely numerical one is that it exhibits in a compact mathematical form the essential physical features of the inplane modes as well as their dependence on a few non-dimensional parameters. Before describing the details of the method, we draw the consequences of some of the assumptions made in Chapter II.

Preliminary Assumptions. Let us seek, in the particular case of a gaseous medium, an estimate of the non-dimensional quantities R_ν and k/R_ν, where k and R_ν are defined by equations (3.2) and (3.3). From elementary kinetic theory considerations, we know that the kinematic viscosity ν_0 is such that

$$\nu_0 \simeq a_0 \ell \tag{4.4}$$

where ℓ is the mean free path. This relation yields the following approximation for R_ν and k/R_ν :

$$R_\nu \simeq \frac{d}{\ell} \qquad (4.5); \qquad \frac{k}{R_\nu} \simeq \frac{\omega \ell}{a_0} \simeq \frac{\ell}{\lambda} \qquad (4.6)$$

where λ is the wavelength associated with the circular frequency ω. Hence, R_ν and k/R_ν are respectively a measure of the ratio of duct width to mean free path and mean free path to wavelength. In order to be able to write the basic equations of Fluid Mechanics, we assumed in Section 2.2 that the fluid was a continuum. Consequently, in the case of a gaseous medium, the width of the duct and the characteristic wavelength of the fluctuations λ are both assumed to be much larger than the mean free path, so that we have:

$$R_\nu \gg 1 \qquad ; \qquad \frac{k}{R_\nu} \ll 1 \qquad (4.7a,b)$$

Without any additional assumptions other that those stated in Chapter II, we may then consider (4.7a) and (4.7b) to be satisfied. Hence, the present investigation is restricted to values of the frequency parameter k such that

$$0 < k \ll R_\nu \qquad (4.8)$$

For air at normal pressure and temperature, the above inequalities imply the following limits on the duct diameter and frequency of the wave:

$$d \gg 5\times10^{-6}\text{cm} \quad (4.9) \; ; \quad f \ll 10^{9}\text{Hz} \qquad (4.10)$$

When we examine the corresponding limits for water under the same conditions,

$$d \gg 8\times10^{-8}\text{cm} \quad (4.11); \quad f \ll 3\times10^{11}\text{Hz} \qquad (4.12)$$

it is clear that, in all practical situations, $1/R_\nu$ and k/R_ν may be considered as very small quantities. The same conclusions may be drawn

for $1/R_\eta$ and k/R_η since the bulk viscosity is never much larger than the shear viscosity. Furthermore, R_ν and R_η are of the same order of magnitude.

As a result of this discussion, the complicated expression (3.27), which defines β_0^2 and β_1^2 can be considerably simplified by expansion in powers of k/R_ν to yield the following:

$$\beta_0^2 = k^2\left[1 - i\left(\frac{\gamma_0 - 1}{P_r} + \frac{R_\nu}{R_\eta}\right)\frac{k}{R_\nu}\right] \tag{4.13}$$

$$\beta_1^2 = -ikP_rR_\nu\left[1 + i(\gamma_0 - 1)\left(\frac{1}{P_r} - \frac{R_\nu}{R_\eta}\right)\frac{k}{R_\nu}\right] \tag{4.14}$$

When such expressions are substituted into relations (4.3a,d) we obtain:

$$\left[1 + i\left(\frac{\gamma_0 - 2}{P_r} + \frac{R_\nu}{R_\eta}\right)\frac{k}{R_\nu} - \frac{\gamma_0 - 1}{P_r}\left(\frac{1}{P_r} - \frac{R_\nu}{R_\eta}\right)\left(\frac{k}{R_\nu}\right)^2\right]\frac{\beta_z^2}{\alpha_2} \cdot$$

$$\left\{\begin{matrix}\tan\\ \text{cotan}\end{matrix}\right\}\frac{\alpha_2}{2} + \left[1 - i\left(\frac{1}{P_r} - \frac{R_\nu}{R_\eta}\right)\frac{k}{R_\nu}\right]\alpha_0\left\{\begin{matrix}\tan\\ \text{cotan}\end{matrix}\right\}\frac{\alpha_0}{2} +$$

$$i(\gamma_0 - 1)\frac{k}{P_rR_\nu}\left[1 + i\left(\frac{1}{P_r} - \frac{R_\nu}{R_\eta}\right)\frac{k}{R_\nu}\right]\alpha_1\left\{\begin{matrix}\tan\\ \text{cotan}\end{matrix}\right\}\frac{\alpha_1}{2} = 0 \tag{4.15a,b}$$

and

$$\left[1 + i\left(\frac{\gamma_0 - 2}{P_r} + \frac{R_\nu}{R_\eta}\right)\frac{k}{R_\nu} - \frac{\gamma_0 - 1}{P_r}\left(\frac{1}{P_r} - \frac{R_\nu}{R_\eta}\right)\left(\frac{k}{R_\nu}\right)^2\right]\frac{\beta_z^2}{\alpha_2} \cdot$$

$$\left\{\begin{matrix}\text{cotan}\\ \tan\end{matrix}\right\}\frac{\alpha_0}{2} \cdot \left\{\begin{matrix}\text{cotan}\\ \tan\end{matrix}\right\}\frac{\alpha_1}{2} + \left[1 - i\left(\frac{1}{P_r} - \frac{R_\nu}{R_\eta}\right)\frac{k}{R_\nu}\right]\alpha_0 \cdot$$

$$\left\{\begin{matrix}\text{cotan}\\ \tan\end{matrix}\right\}\frac{\alpha_1}{2}\left\{\begin{matrix}\text{cotan}\\ \tan\end{matrix}\right\}\frac{\alpha_2}{2} + i(\gamma_0 - 1)\frac{k}{P_rR_\nu}\left[1 + i\left(\frac{1}{P_r} - \frac{R_\nu}{R_\eta}\right)\frac{k}{R_\nu}\right] \cdot$$

$$\alpha_1\left\{\begin{matrix}\text{cotan}\\ \tan\end{matrix}\right\}\frac{\alpha_0}{2} \cdot \left\{\begin{matrix}\text{cotan}\\ \tan\end{matrix}\right\}\frac{\alpha_2}{2} = 0 \tag{4.15c,d}$$

where

$$\alpha_0^2 = k^2\left[1 - i\left(\frac{\gamma_0 - 1}{P_r} + \frac{R_\nu}{R_\eta}\right)\frac{k}{R_\nu}\right] - \beta_z^2 \tag{4.16}$$

$$\alpha_1^2 = -ikP_r R_\nu\left[1 + i(\gamma_0 - 1)\left(\frac{1}{P_r} - \frac{R_\nu}{R_\eta}\right)\frac{k}{R_\nu}\right] - \beta_z^2 \tag{4.17}$$

$$\alpha_2^2 = -ikR_\nu - \beta_z^2 \tag{4.18}$$

and the coefficients of each term in (4.15a,d) have been expanded to order $\left(\frac{k}{R_\nu}\right)^2$ included.

Methodology. Even though the previous comments have led to a substantial simplification of the dispersion relations, as shown in equations (4.15a,d), they do not provide a method of solution. An important indication as to how to approach this problem, may be seen in a short examination of the physics of wave phenomena in viscous, heat-conducting and compressible fluids. As mentioned briefly in Section 1.2, Chu and Kovasznay (1958) distinguish three main types of fluctuations in such a fluid: pressure fluctuations corresponding to the propagation of sound waves in an inviscid fluid, vorticity fluctuations related to the diffusion of vorticity perturbations in a viscous medium, and entropy fluctuations related to the diffusion of so-called "hot spots" in a heat-conducting medium. In this study, we therefore expect to encounter three families of pressure-, entropy-, and vorticity-dominated modes, and we are faced with the problem of finding a method which enables us to determine their respective characteristics. In inviscid wave propagation, the first and last terms in (4.15a,b) are identically zero, and the dispersion relation is immediately solved for α_0, to yield the pressure or acoustic modes. In the case of a viscous and heat-conducting medium, these terms are no longer negligible. They may be recast solely in terms

of α_0 through the use of (4.16), (4.17), and (4.18), and the resulting relation is still to be solved for α_0, to yield the pressure-dominated modes. Similarly, the characteristics of the entropy- (respectively, vorticity-) dominated modes will be found by recasting the dispersion relation in terms of α_1 (respectively, α_2) and solving for α_1 (respectively, α_2). The main advantages of such a procedure, as compared to a straightforward solution in terms of the complex wave number β_z, will become apparent in the next few sections.

We are still confronted with the task of expanding the dispersion relation, and the unknown; α_0, α_1, or α_2, in terms of a suitable small parameter. Three such parameters may be defined, and they correspond to three ranges of frequencies, or equivalently three ranges of duct widths:

The High-Frequency-Wide-Tube Range.

Where the reduced frequency k is such that:

$$\frac{1}{R_\nu} \ll k \ll R_\nu^{1/3} \tag{4.19}$$

and the small parameter is defined as:

$$\epsilon = \frac{1}{\sqrt{kR_\nu}} \tag{4.20}$$

This is the familiar acoustic boundary layer approximation.

The Low-Frequency-Narrow-Tube Range.

Where the reduced frequency k is such that:

$$k \ll \frac{1}{R_\nu} \tag{4.21}$$

and the small parameter is defined as

$$\epsilon = kR_\nu \tag{4.22}$$

The Very-High-Frequency-Very-Wide-Tube Range.

Where the reduced frequency k is such that

$$R_\nu^{1/3} \ll k \ll R_\nu \tag{4.23}$$

and the small parameter is defined as

$$\epsilon = \left(\frac{R_\nu}{k^3}\right)^{1/2} \tag{4.24}$$

These ranges were first suggested, in a somewhat different form, by Weston (1953a) in an analytical study of the zeroth-pressure mode. A full justification of such definitions will arise from the detailed analysis of the next three sections.

The methodology which has just been outlined is now applied to the determination of the characteristics of the pressure-, entropy-, and vorticity-dominated modes in the three ranges of parameters defined above.

4.3 High Frequency - Wide Tube Range.

We showed in the preceding section that, in all practical situations, $1/R_\nu$ is a very small parameter. It is, therefore, legitimate to seek a formal expansion of α_0 (respectively, α_1, α_2) in powers of $1/R_\nu$. The range of validity of such expansions will be examined a posteriori, by requiring that the ratio of two successive terms be smaller than unity.

4.3.1 Pressure-Dominated Modes. We assume the unknown α_0 to be of order $(1/R_\nu)^0$ or of higher order, and wish to expand the dispersion relation (4.15a,b) to order $1/R_\nu$, inclusively. From (4.16) - (4.18), the coefficients β_z^2, α_1, and α_2 may be approximated by the following expressions:

$$\beta_z^2 = (k^2-\alpha_0^2)\left[1 - \frac{ik^2}{k^2-\alpha_0^2}\left(\frac{\gamma_0-1}{P_r}+\frac{R_\nu}{R_\eta}\right)\frac{k}{R_\nu}\right] \tag{4.25}$$

$$\alpha_1 = (1-i)\sqrt{\frac{kP_r R_\nu}{2}}\left[1+i\,\frac{\alpha_0^2-k^2}{2kP_r R_\nu}+i\,\frac{\nu_0-1}{2}\left(\frac{1}{P_r}-\frac{R_\nu}{R_\eta}\right)\frac{k}{R_\nu}\right] \quad (4.26)$$

$$\alpha_2 = (1-i)\sqrt{\frac{kR_\nu}{2}}\left[1+i\,\frac{\alpha_0^2-k^2}{2kR_\nu}\right] \quad (4.27)$$

Note that in the last two relations the first terms are very large, of order $R_\nu^{\frac{1}{2}}$. Consequently, the trigonometric tangents in α_1 and α_2 may be written as

$$\tan\frac{\alpha_1}{2} = \tan\frac{\alpha_2}{2} = -i \quad (4.28)$$

where exponentially small terms have been neglected. When equations (4.25) - (4.28) are substituted into (4.15a,b), one obtains the following equations in α_0 :

$$\alpha_0\left\{\begin{matrix}\tan\\ \cot an\end{matrix}\right\}\frac{\alpha_0}{2} = \mp\,\frac{1-i}{\sqrt{2kR_\nu}}\,(k^{*2}-\alpha_0^2) \quad (4.29a,b)$$

where

$$k^{*2} = \left(1+\frac{\nu_0-1}{\sqrt{P_r}}\right)k^2 \quad (4.30)$$

Higher order terms on the right-hand side of (4.29a,b) are of magnitude $(1/R_\nu)^{3/2}$, and have therefore been omitted. As we let the parameter R_ν go to infinity, the above equations yield the solutions α_0 which pertain to the acoustic modes propagating in an inviscid medium. Hence, the zeroth order terms are given by:

$$\alpha_{0N}^P = N\pi \quad (4.31)$$

where the integer N is of the form

$$N = 2n \qquad n = 0\ ,\ 1\ ,\ 2\ ,\ \ldots$$

for the symmetric mode of order n , described by (4.29a), and

$$N = 2n+1 \qquad n = 0 , 1 , 2 , \ldots$$

for the antisymmetric mode of order n , described by (4.29b). It is then a straightforward procedure to derive a more accurate representation of α_0 by assuming that it may be expanded as:

$$\alpha_{0N}^{P} = N\pi\left[1 + \frac{a}{\sqrt{R_\nu}} + \frac{b}{R_\nu}\right] \tag{4.32}$$

when N is different from zero, and,

$$\alpha_{00}^{P} = \frac{a}{R_\nu^{1/2}} + \frac{b}{R_\nu^{3/4}} \tag{4.33}$$

when N is zero. The unknown constants a and b associated with even (respectively, odd) values of N , are determined by substituting (4.32) and (4.33) into equation (4.29a), (respectively, (4.29b)). The resulting expressions are expanded to order $1/R_\nu$, and the coefficient of each higher-order term is set equal to zero. The final solutions are then given by:

$$\alpha_{00}^{P} = i\sqrt{2}\, e^{-\frac{i\pi}{8}} k^{*} \left(\frac{1}{kR_\nu}\right)^{1/2}\left[1 + (1-i)\left(1 + \frac{k^{*2}}{12}\right)\frac{1}{\sqrt{2kR_\nu}}\right] \tag{4.34}$$

$$\alpha_{0N}^{P} = N\pi\left[1 - \frac{1-i}{(N\pi)^2}\left(k^{*2} - (N\pi)^2\right)\sqrt{\frac{2}{kR_\nu}} + 4i\,\frac{k^{*4} - (N\pi)^4}{(N\pi)^4}\,\frac{1}{kR_\nu}\right] \tag{4.35}$$

Substitution of the previous results into equations (4.25) - (4.27) yields the corresponding expressions for α_1 , α_2 , and β_z :

$$\alpha_{1N}^{P} = (1-i)\sqrt{\frac{kP_r R_\nu}{2}}\left[1 - \frac{i}{2}\left\{\frac{k^2 - (N\pi)^2}{P_r} + (\nu_0 - 1)\cdot\left(\frac{R_\nu}{R_\eta} - \frac{1}{P_r}\right)k^2\right\}\frac{1}{kR_\nu}\right] \tag{4.36}$$

$$\alpha^P_{2N} = (1-i)\sqrt{\frac{kR_\nu}{2}}\left[1-\frac{i}{2}\cdot\frac{k^2-(N\pi)^2}{kR_\nu}\right] \tag{4.37}$$

$$\beta^P_{z0} = k\Big[1+(1-i)\Big(1+\frac{\gamma_0-1}{\sqrt{P_r}}\Big)\frac{1}{\sqrt{2kR_\nu}} - 2i\Big(1+\frac{\gamma_0-1}{\sqrt{P_r}}\Big)\cdot$$

$$\Big(1+\frac{k^{*2}}{12}-\frac{1}{4}\Big(1+\frac{\gamma_0-1}{\sqrt{P_r}}\Big)\Big)\frac{1}{kR_\nu} - \frac{i}{2}\Big(\frac{\gamma_0-1}{P_r}+\frac{R_\nu}{R_\eta}\Big)\frac{k}{R_\nu}\Big] \tag{4.38}$$

$$\beta^P_{zN} = \Big[k^2-(N\pi)^2+2(1-i)(k^{*2}-(N\pi)^2)\sqrt{\frac{2}{kR_\nu}} - \frac{4i}{(N\pi)^2}\cdot$$

$$(k^{*2}-(N\pi)^2)(k^{*2}+3(N\pi)^2)\frac{1}{kR_\nu} - ik^4\Big(\frac{\gamma_0-1}{P_r}+\frac{R_\nu}{R_\eta}\Big)\frac{1}{kR_\nu}\Big]^{\frac{1}{2}} \tag{4.39}$$

The index N may be set equal to zero in (4.36) and (4.37) but not in (4.39). When N is an even integer:

$$N = 2n \qquad n = 0, 1, 2, \ldots$$

the above results describe the symmetric pressure-dominated mode of order n, $SP(n)$, and the associated mode shape is given in Table I. When N is an odd integer:

$$N = 2n+1 \qquad n = 0, 1, 2, \ldots$$

they describe the antisymmetric pressure-dominated mode of order n, $AP(n)$, and the associated mode shape is given in Table II.

As already explained in Section 3.4, we select in (4.39) the complex root which pertains to waves attenuating in the positive z-direction, i.e. of negative imaginary part. In the course of the previous derivation we tacitly assumed the right-hand side of (4.29a,b) to be much smaller than

unity. Furthermore, in order for the above expansions to be valid each term has to be smaller than the preceding one. Enforcement of these conditions results in the following restrictions on the possible values of the frequency parameter k :

$$\frac{1}{R_\nu} \ll k \ll R_\nu^{1/3} \tag{4.40}$$

This double inequality may be written in two other equivalent ways as:

$$\frac{\nu_0}{d^2} \ll \omega \ll \left(\frac{a_0^4}{\nu_0 d^2}\right)^{1/3} \tag{4.41}$$

or

$$\left(\frac{\nu_0}{\omega}\right)^{1/2} \ll d \ll \frac{a_0^2}{(\omega^3 \nu_0)^{1/2}} \tag{4.42}$$

which is immediately interpreted as an a posteriori justification of the name given to the present approximation. Whereas α_0 is of order unity (except for SP(0)), α_1 and α_2 are complex numbers of very large modulus. Consequently, if we examine the mode shapes of Table I, terms such as $\frac{\cos \alpha_1 x}{\cos \alpha_1/2}$ or $\frac{\cos \alpha_2 x}{\cos \alpha_2/2}$ may be written in the following manner:

$$\frac{\cos \alpha_1 x}{\cos \alpha_1/2} = e^{-\frac{1+i}{\sqrt{2}} |\alpha_1| \left(x - \frac{1}{2}\right)} + e^{-\frac{1+i}{\sqrt{2}} |\alpha_1| \left(x + \frac{1}{2}\right)} \tag{4.43}$$

where $|\alpha_1|$ is very large, of the order of $(k R_\nu)^{1/2}$. Hence, they will be of significant magnitude in only a thin layer close to the duct walls at $x = -1/2$ and $x = 1/2$. In the center of the tube, they will be exponentially small.* As will be clear when we discuss the mode shapes in

*Identical conclusions may be reached with the corresponding expressions in Table II.

Section 4.6, such a behavior is linked with the diffusion of entropy and vorticity in thermal and viscous boundary layers attached to the walls of the tube. If the boundary layer thickness is defined as the distance from the duct walls where the magnitude of these terms is e^{-1} of its maximum value, the non-dimensional viscous and thermal boundary layer thicknesses are respectively:

$$\delta_{VN} = \frac{\sqrt{2}}{|\alpha_{2N}|} = \sqrt{\frac{2}{kR_\nu}}\left[1 + \frac{(N\pi)^2 - k^2}{2kR_\nu}\right] \tag{4.44}$$

$$\delta_{thN} = \frac{\sqrt{2}}{|\alpha_{1N}|} = \sqrt{\frac{2}{kP_r R_\nu}}\left[1 + \left\{\frac{(N\pi)^2 - k^2}{P_r} - (\gamma_0 - 1)\cdot\right.\right.$$

$$\left.\left.\left(\frac{R_\nu}{R_\eta} - \frac{1}{P_r}\right)k^2\right\}\frac{1}{2kR_\nu}\right] \tag{4.45}$$

The lower bound imposed on k in equation (4.40) implies that viscous and thermal effects are important only in layers of approximate non-dimensional thicknesses $\sqrt{\frac{2}{kR_\nu}}$ and $\sqrt{\frac{2}{kP_r R_\nu}}$, respectively. By invoking elementary notions of kinetic theory as used in Section 4.2, this may be translated as follows:

$$\delta_{VN} \simeq \delta_{thN} \simeq \frac{\sqrt{\lambda \ell}}{d} \ll 1 \tag{4.46}$$

i.e., the dimensional boundary layer thickness is approximately equal to the geometric mean of the wavelength and mean free path, and it is much smaller than the duct width. The high-frequency-wide-tube regime might just as well have been called the acoustic boundary layer approximation.

To the author's knowledge, all investigations to date with the exception of Scarton and Rouleau's have only been concerned with the deter-

mination of the complex wave number of pressure-dominated modes, and most of them have considered the acoustic boundary layer approximation. It is therefore interesting to compare our results with those available in the literature.

Expression (4.38) relative to the zeroth "plane" pressure mode is composed of:

- an inviscid term
- a second term of order $(1/R_\nu)^{\frac{1}{2}}$, proportional to the square root of the reduced frequency, representing attenuation and dispersion effects brought about by the acoustic boundary layers, and first calculated by Kirchhoff (1868) in the case of a circular tube.
- a third term of order $1/R_\nu$, representing higher-order acoustic boundary layer attenuation.
- a fourth term of the same order of magnitude as the preceding one, proportional to the square of the reduced frequency, and associated with the dilatational attenuation of longitudinal waves in the bulk of the fluid. This last part of the complex wave number was also derived by Kirchhoff in a study of the propagation of plane waves in an unbounded medium.

Weston (1953a), in an analytical treatment of the characteristics of the plane mode in a circular duct, subdivides the wide-tube range into two subranges or transition regions. In the wide-narrow tube subrange, k is assumed to be smaller than unity and "closer" to $1/R_\nu$, so that terms of the form k/R_ν in the brackets of (4.38) can be neglected. In the wide-very-wide-tube subrange, k is assumed to be larger than unity and "closer" to $R_\nu^{1/3}$, so that terms of the form

$1/\sqrt{kR_\nu}$ or $1/kR_\nu$ can be omitted. The simplified expressions resulting from the manipulation of (4.38) in the above prescribed manner are then very analogous to those obtained by Weston in these subranges.

In order to give the corresponding interpretation of the results pertaining to the higher-order P modes, it is convenient to get rid of the square root in (4.39) by expansion in powers of $1/R_\nu$. Since the dominant term in the square root may be positive or negative, one must distinguish several ranges of frequencies which are discussed below:

When $k > N\pi$, the complex wave number is given by

$$\beta_{zN}^{P} = \sqrt{k^2-(N\pi)^2}\ \left[1 + (1-i)\ \frac{k^{*2}-(N\pi)^2}{k^2-(N\pi)^2}\ \sqrt{\frac{2}{kR_\nu}} - \frac{4i}{(N\pi)^2}\cdot\right.$$

$$\frac{k^{*2}-(N\pi)^2}{k^2-(N\pi)^2}\cdot\left(k^{*2}+(N\pi)^2-\frac{k^2}{2}\cdot\frac{k^{*2}-(N\pi)^2}{k^2-(N\pi)^2}\right)\frac{1}{kR_\nu} - \frac{ik^4}{2}\cdot$$

$$\left.\frac{(\gamma_0-1)/P_r+R_\nu/R_\eta}{k^2-(N\pi)^2}\ \frac{1}{kR_\nu}\right] \qquad (4.47)$$

Shaw (1953) studied wave propagation between a pair of infinite parallel walls and obtained identical results to order $(1/R_\nu)^{\frac{1}{2}}$. In the present expression, the expansion has been carried out to higher order. This enables us to analyze the different terms in the same manner as in (4.38). In particular, the first term is the well-known inviscid higher-mode wave number. The total attenuation rate is of order $(1/R_\nu)^{\frac{1}{2}}$ and dilatational dissipation is smaller than acoustic boundary layer dissipation as can be seen by comparing the second and last term of (4.47). In the vicinity of the reduced frequency $N\pi$, the denominators of the perturbation terms in (4.47) tend to zero, so that the above ex-

pansion becomes invalid. One then evaluates the wave number directly from (4.39).

When the reduced frequency k is equal to the inviscid cut-off frequency $N\pi$, the wave number is:

$$\beta_{zN}^{P} = 2e^{-\frac{i\pi}{8}\left(\frac{\gamma_0-1}{\sqrt{P_r}}\right)}\sqrt{N\pi}\left(\frac{1}{N\pi R_\nu}\right)^{\frac{1}{4}}\left[1+\frac{1-i}{2}\left(\frac{\gamma_0-1}{\sqrt{P_r}}+4\right)\cdot\right.$$

$$\left.\frac{1}{\sqrt{2N\pi R_\nu}}+\frac{1-i}{8}\frac{\sqrt{P_r}}{\gamma_0-1}\left(\frac{\gamma_0-1}{P_r}+\frac{R_\nu}{R_\eta}\right)\frac{(N\pi)^2}{\sqrt{2N\pi R_\nu}}\right] \qquad (4.48)$$

In contrast with duct propagation in an inviscid medium, it is not zero. Furthermore, its real part is finite, so that a wave still propagates along the duct axis. Even though the attenuation rate is now larger, of order $(1/R_\nu)^{\frac{1}{4}}$ instead of $(1/R_\nu)^{\frac{1}{2}}$, $N\pi$ is not the cut-off frequency of the higher-order modes.

When $\dfrac{N\pi}{\left(1+\dfrac{\gamma_0-1}{\sqrt{P_r}}\right)^{\frac{1}{2}}} < k < N\pi$, equation (4.47) is changed into:

$$\beta_{zN}^{P} = -i\sqrt{(N\pi)^2-k^2}\left[1-(1-i)\frac{k^{*2}-(N\pi)^2}{(N\pi)^2-k^2}\sqrt{\frac{2}{kR_\nu}}+\right.$$

$$\frac{4i}{(N\pi)^2}\cdot\frac{k^{*2}-(N\pi)^2}{(N\pi)^2-k^2}\left(k^{*2}+(N\pi)^2+\frac{k^2}{2}\,\frac{k^{*2}-(N\pi)^2}{(N\pi)^2-k^2}\right)\frac{1}{kR_\nu}$$

$$\left.+\frac{ik^4}{2}\,\frac{(\gamma_0-1)/P_r+R_\nu/R_\eta}{(N\pi)^2-k^2}\,\frac{1}{kR_\nu}\right] \qquad (4.49)$$

It is important to note that the sudden increase of the attenuation rate shown in the above relation is not due to enhanced viscous dissipation,

but rather to the storage of the acoustic energy in a smaller region of space. The physical mechanism is the same as in inviscid wave motion. However, the real part of the wave number remains finite and leads to a positive phase velocity.

When $k^* = N\pi$ or $k = \dfrac{N\pi}{[1+(\gamma_0 - 1/\sqrt{P_r})]^{\frac{1}{2}}}$ the real part of the complex wave number is almost zero, of order $1/R_\nu$ as seen from (4.49)*. Hence, the true cut-off frequency is given by:

$$k_N^{co} = \frac{N\pi}{\left(1+\dfrac{\gamma_0 - 1}{\sqrt{P_r}}\right)^{\frac{1}{2}}} < N\pi \qquad (4.50)$$

This downward shift in cut-off is solely attributable to thermal effects, and disappears when the Prandtl number goes to infinity. The practical significance of such a phenomenon is limited, since the attenuation rate is already very high at the inviscid cut-off.

Below Cut-off, the real part of (4.49) leads to a negative phase velocity. Wave fronts propagate in the negative z-direction, whereas the amplitude is attenuated in the opposite direction. It is shown in Appendix C that, in this instance, the acoustic intensity is indeed positive, and acoustic energy is moving against the wavefronts. These so-called backward-propagating waves were also encountered by Meitzler (1965) in the equivalent elastic plate problem, and by Scarton and Rouleau (1973) in a numerical study of the axisymmetric modes in a viscous fluid.

This completes our discussion of the pressure-dominated solutions

*In order for the real part of β_z to be identically zero to order $1/R_\nu$ included, one would have to slightly perturb k^* around the value $N\pi$. This has not been done here for simplicity.

of the dispersion relations (4.15a,b) in the high-frequency-wide-tube approximation.

4.3.2 Entropy-Dominated Modes. Following the methodology described in Section 4.2, we assume the unknown α_1 to be of order $(1/R_\nu)^0$ of higher order. In this situation, it is preferable to attack the problem from the normalized dispersion relations (4.15c,d) instead of (4.15a,b). These equations are to be solved for α_1 to order $(1/R_\nu)^{3/2}$ included. Relations (4.16) - (4.18) enable us to approximate β_z^2, α_0, and α_2 by the following expressions:

$$\beta_z^2 = -ikP_rR_\nu\left[1 - \frac{i\alpha_1^2}{kP_rR_\nu} + i(\gamma_0-1)\left(\frac{1}{P_r} - \frac{R_\nu}{R_\eta}\right)\frac{k}{R_\nu}\right] \tag{4.51}$$

$$\alpha_0 = (1+i)\sqrt{\frac{kP_rR_\nu}{2}}\left[1 - \frac{i}{2}\frac{\alpha_1^2+k^2}{kP_rR_\nu} + i\frac{\gamma_0-1}{2}\left(\frac{1}{P_r} - \frac{R_\nu}{R_\eta}\right)\frac{k}{R_\nu}\right] \tag{4.52}$$

$$\alpha_2 = (1-i)\sqrt{\frac{k(1-P_r)R_\nu}{2}}\left[1 + \frac{i\alpha_1^2}{2(1-P_r)kR_\nu} - i\frac{\gamma_0-1}{2}\cdot\right.$$

$$\left.\cdot\frac{P_r}{1-P_r}\left(\frac{1}{P_r} - \frac{R_\nu}{R_\eta}\right)\frac{k}{R_\nu}\right] \tag{4.53}$$

Since α_0 and α_2 are complex numbers of very large amplitude, their trigonometric tangents can be written as:

$$\tan\frac{\alpha_0}{2} = -\tan\frac{\alpha_2}{2} = i \tag{4.54}$$

When these relations are substituted into the dispersion relations (4.15c,d), two equations in α_1 follow:

$$\left\{\begin{matrix}\text{cotan}\\ \tan\end{matrix}\right\}\frac{\alpha_1}{2} = \mp\frac{1-i}{\sqrt{2}}\,\frac{(\gamma_0-1)k^2}{1+i\sqrt{\frac{P_r}{1-P_r}}}\,\frac{1}{(kP_rR_\nu)^{3/2}}\,\alpha_1 \qquad (4.55a,b)$$

the upper (respectively, lower) expression pertaining to the symmetric (respectively, antisymmetric) entropy-dominated modes. The solutions of the above equations are obtained in exactly the same manner as the P-modes of the preceding subsection. The final results are given as follows:

$$\alpha_{1N}^{S} = N\pi\left[1+(1-i)\sqrt{2}\;\frac{(\gamma_0-1)k^2}{1+i\sqrt{\frac{P_r}{1-P_r}}}\,\frac{1}{(kP_rR_\nu)^{3/2}}\right] \qquad (4.56)$$

where the integer N is an odd number of the form

$$N = 2n+1 \qquad n = 0\ ,\ 1\ ,\ 2\ ,\ \ldots$$

for the symmetric mode of order n, $SS(n)$, and an even number of the form

$$N = 2n \qquad n = 1\ ,\ 2\ ,\ 3\ ,\ \ldots$$

for the antisymmetric mode of order n, $AS(n)$. Corresponding expressions for α_0, α_1, and β_z are given by:

$$\alpha_{0N}^{S} = (1+i)\sqrt{\frac{kP_rR_\nu}{2}}\left[1-\frac{i}{2}\,\frac{k^2+(N\pi)^2}{kP_rR_\nu}+i\,\frac{\gamma_0-1}{2}\left(\frac{1}{P_r}-\frac{R_\nu}{R_\eta}\right)\frac{k}{R_\nu}\right] \qquad (4.57)$$

$$\alpha_{2N}^{S} = (1-i)\sqrt{\frac{k(1-P_r)R_\nu}{2}}\left[1+i\,\frac{(N\pi)^2}{2k(1-P_r)R_\nu}\right.$$

$$\left.-i\,\frac{\gamma_0-1}{2}\,\frac{P_r}{1-P_r}\left(\frac{1}{P_r}-\frac{R_\nu}{R_\eta}\right)\frac{k}{R_\nu}\right] \qquad (4.58)$$

$$\beta_{zN}^{S} = (1-i)\sqrt{\frac{kP_r R_\nu}{2}}\left[1 - \frac{i(N\pi)^2}{2kP_r R_\nu} + i\,\frac{\gamma_0 - 1}{2}\left(\frac{1}{P_r} - \frac{R_\nu}{R_\eta}\right)\frac{k}{R_\nu}\right] \qquad (4.59)$$

At first sight, $\alpha_1 = 0$ appears to be an exact solution of the antisymmetric dispersion relation (3.71) throughout the entire reduced frequency domain. However, it is easily checked that the only possible mode shape that can be associated with such a solution is identically zero. Hence, $\alpha_1 = 0$ is not a relevant antisymmetric eigenvalue, and as prescribed above, the index n characterizing the antisymmetric S-modes takes positive values only.

The same reasoning as in Subsection 4.3.1 leads to the following restrictions on values of the reduced frequency k :

$$\frac{1}{R_\nu} \ll k \ll R_\nu \qquad (4.60)$$

where the upper bound is a consequence of the preliminary assumptions made in Section 4.2. Consequently, upon comparison of (4.60) with (4.40), it is clear that the range of validity of the S-mode expansions is wider than the range of validity of the corresponding P-mode expansions. In this investigation, we assume that, by definition, the high-frequency-wide-tube approximation pertains to the reduced frequency domain $\frac{1}{R_\nu} \ll k \ll R_\nu^{1/3}$. The above results are therefore valid, not only in the high-frequency-wide-tube range, but also in the very-high-frequency-very-wide-tube range which will be studied in detail in Section 4.5.

The coefficients α_{0N}^{S} and α_{2N}^{S} are strikingly similar in form to the coefficients α_{1N}^{P} and α_{2N}^{P} defined in the previous subsection. Correspondingly, we will show in Section 4.6 that this mathematical feature is linked with a diffusive behavior of pressure and vorticity

fluctuations in acoustic boundary layers close to the walls of the tube. Expressions for the thickness of these layers may also be derived as in Subsection 4.3.1, and they may be shown to be of the same small order of magnitude $(1/kR_\nu)^{\frac{1}{2}}$, as the viscous and thermal boundary layers associated with the P-modes.

The complex wave numbers all have large real and imaginary parts. In contrast with the P-modes which have distinct phase velocities and attenuation rates, the S-modes have almost identical propagation characteristics, and are highly attenuated at all frequencies. Nevertheless, to each value of the index N, corresponds a specific S-mode shape as shown from (4.56).

Although researchers have been aware of the existence of entropy-dominated modes since the earlier work of Chu and Kovasznay, we do not know of any previous investigation of their properties for a given boundary value problem. In the next subsection, we proceed to determine the vorticity-dominated solutions of the dispersion relations (4.15a,b).

4.3.3 Vorticity-Dominated Modes. The dispersion relations (4.15a,b) are to be solved for the unknown α_2 to order $1/R_\nu$ included. From (4.16) - (4.18) we may write:

$$\beta_z^2 = -ikR_\nu\left[1 - \frac{i\alpha_2^2}{kR_\nu}\right] \tag{4.61}$$

$$\alpha_0 = (1+i)\sqrt{\frac{kR_\nu}{2}}\left[1 - \frac{i}{2}\,\frac{k^2+\alpha_2^2}{kR_\nu}\right] \tag{4.62}$$

$$\alpha_1 = (1+i)\sqrt{\frac{k(1-P_r)R_\nu}{2}}\left[1 - \frac{i\alpha_2^2}{2k(1-P_r)R_\nu}\right.$$

$$\left. -i\,\frac{\nu_0-1}{2}\,\frac{P_r}{1-P_r}\left(\frac{1}{P_r} - \frac{R_\nu}{R_\eta}\right)\frac{k}{R_\nu}\right] \tag{4.63}$$

so that the trigonometric tangents in α_0 and α_1 are approximated by the following expression:

$$\tan \frac{\alpha_0}{2} = \tan \frac{\alpha_1}{2} = i \tag{4.64}$$

Substitution of the above relations into the dispersion relations (4.15a,b) leads to the two following equations in α_2 :

$$\left\{ \begin{matrix} \tan \\ \text{cotan} \end{matrix} \right\} \frac{\alpha_2}{2} = \pm \frac{1+i}{\sqrt{2kR_\nu}} \alpha_2 \tag{4.65a,b}$$

where the upper (respectively, lower) expression corresponds to the symmetric (respectively, antisymmetric) vorticity-dominated modes. By making use of the same procedure as in the previous two subsections, we arrive at the final results:

$$\alpha_{2N}^{V} = N\pi \left[1 + (1+i)\sqrt{\frac{2}{kR_\nu}} + \frac{4i}{kR_\nu} \right] \tag{4.66}$$

where the integer N is of the form,

$$N = 2n \qquad\qquad n = 1 , 2 , 3 , \ldots$$

for the symmetric mode of order n , $SV(n)$, and of the form

$$N = 2n+1 \qquad\qquad n = 0 , 1 , 2 , \ldots$$

for the antisymmetric mode of order n , $AV(n)$.

Expressions for α_0 , α_1 , and β_z are then obtained from (4.61) - (4.63) as follows:

$$\alpha_{0N}^{V} = (1+i)\sqrt{\frac{kR_\nu}{2}} \left[1 - \frac{i}{2} \frac{k^2+(N\pi)^2}{kR_\nu} \right] \tag{4.67}$$

$$\alpha_{1N}^{V} = (1+i)\sqrt{\frac{k(1-P_r)R_\nu}{2}}\left[1 - i\,\frac{(N\pi)^2}{2k(1-P_r)R_\nu}\right.$$

$$\left. -i\,\frac{\gamma_0-1}{2}\,\frac{P_r}{1-P_r}\left(\frac{1}{P_r} - \frac{R_\nu}{R_\eta}\right)\frac{k}{R_\nu}\right] \qquad (4.68)$$

$$\beta_{zN}^{V} = (1-i)\sqrt{\frac{kR_\nu}{2}}\left[1 - i\,\frac{(N\pi)^2}{2kR_\nu}\right] \qquad (4.69)$$

The above expansions have the same domain of validity as those describing the S-modes, i.e., the reduced frequency k is such that:

$$\frac{1}{R_\nu} \ll k \ll R_\nu$$

Consequently, these results characterize the vorticity-dominated modes in both the high-frequency-wide-tube-, and very-high-frequency-very-wide-tube ranges.

The large real and imaginary parts of the coefficients α_{0N}^{V} and α_{1N}^{V} correspond to "diffusion" of pressure and entropy fluctuations in thin layers close to the duct walls, the thickness of these layers being of the order of $(1/kR_\nu)^{\frac{1}{2}}$. As seen from a comparison of (4.69) and (4.59), the propagation characteristics of entropy- and vorticity-dominated modes are strictly analogous, and the reader is referred to the preceding subsection for further details.

Scarton and Rouleau (1973) were the first to conduct a numerical study of the V-modes (in their terminology, the "B band" of eigenvalues) in the case of a circular tube and a non-heat-conducting fluid, and, as we shall see in our final discussion, found very similar results. They noted that $\alpha_2 = 0$ is an exact solution of the axisymmetric dispersion relation, just as it is an exact solution of the symmetric inplane

dispersion relation (3.70) and numerically derived a corresponding non-zero mode shape. However, if α_2 is assumed to be zero in the analysis beginning in Section 3.3, one immediately reaches the conclusion that the only possible mode shape is zero. Hence, $\alpha_2 = 0$ cannot be considered as a relevant symmetric eigenvalue, and the index N cannot be zero in (4.66).*

We have now completed the determination of the symmetric and antisymmetric solutions of the inplane dispersion relations in the high-frequency-wide-tube approximation. At this point, two additional assumptions which have been implicitly made in the previous derivations need to be carefully stated. In order for expressions of the form $\sqrt{kP_r R_\nu}$ to be large quantities, the Prandtl number is taken to be larger than $1/kR_\nu$. Such a restriction is unimportant since most fluids of interest have a Prandtl number of the order of one or larger. Furthermore, if the S- and V-expressions are to be valid, terms of the form $\sqrt{k(1-P_r)R_\nu}$ must also be large. Consequently, in these last two families, the Prandtl number is in addition assumed to differ from unity by a quantity larger than $1/kR_\nu$. This latter restriction could easily be removed by examining the particular case where P_r is unity.

We may now clearly appreciate the advantage of taking α_0, α_1, and α_2 as respective unknowns for the P-, S-, and V-eigenvalues, instead of the complex wave number. If β_z had been chosen as unknown of order $(1/R_\nu)^0$ or of higher order in the dispersion relations, we would have obtained the P-eigenvalues only, since they are the only ones

*A similar situation prevailed in the study of the antisymmetric antiplane modes and antisymmetric S-modes studied in Sections 3.4 and 4.3.2, respectively.

to be characterized by a wave number of order one. The other two families would have been completely ignored, their wave number being of order $R_\nu^{\frac{1}{2}}$ as can be seen from (4.59) and (4.69).

We still have not justified the terminology used to designate the different families of eigenfunctions. A definite explanation will be given when we examine the characteristics of the mode shapes in Section 4.6.

4.4 Low-Frequency-Narrow-Tube Range.

The solutions in the high-frequency-wide-tube approximation were shown to be valid as long as the frequency parameter k is much larger than $1/R_\nu$. For values of k or the order of $1/R_\nu$, the expansions break down. In this section, we seek solutions of the dispersion relation (4.15a,d) for values of the reduced frequency much smaller than $1/R_\nu$. The unknown and the dispersion relations are formally expanded in powers of k and the range of validity of the results is determined a posteriori.

4.4.1. Pressure and Vorticity-Dominated Modes. In the high-frequency-wide-tube approximation, we generally assumed one of the coefficients α_0, α_1, or α_2, to be of order unity which implied that the other coefficients were very large quantities. In contrast with such a situation, we expect in the low-frequency-narrow-tube region all the coefficients α_0, α_1, and α_2 to be of the same order of magnitude, since terms of the form kR_ν are now very small. Hence, no real advantage is gained by following the general procedure described in Section 4.2. In this subsection, we therefore solve the normalized dispersion relations (4.15a,b) for the unknown complex wave number β_z and assume

β_z to be of order unity. Such a procedure will yield both pressure- and vorticity-dominated eigenvalues. The dispersion relations have to be expanded to order k^2 inclusive in order to derive accurate solutions to order k inclusive. From (4.16) - (4.18), α_0 , α_1 , and α_2 may be written in the form:

$$\alpha_0 = i\beta_z \left[1 - \frac{k^2}{2\beta_z^2}\right] \tag{4.70}$$

$$\alpha_1 = i\beta_z \left[1 + \frac{ikP_r R_\nu}{2\beta_z^2}\right] \tag{4.71}$$

$$\alpha_2 = i\beta_z \left[1 + \frac{ikR_\nu}{2\beta_z^2} + \frac{(kR_\nu)^2}{8\beta_z^4}\right] \tag{4.72}$$

When these expansions are substituted into (4.15a,b) and the resulting expressions are expanded to order k^2 , terms of zeroth order cancel out and the final equations, after division by kR_ν , and reordering, are given by:

$$\sin i\beta_z \mp i\beta_z + \frac{i}{4}\left\{\begin{matrix}\tan\\ \text{cotan}\end{matrix}\right\} \frac{i\beta_z}{2} kR_\nu$$

$$+ i\gamma_0 (\sin i\beta_z \pm i\beta_z) \frac{k}{R_\nu} - \frac{3i}{4} \frac{\sin i\beta_z \mp i\beta_z}{\beta_z^2} kR_\nu$$

$$+ i\left(\frac{\gamma_0^{-2}}{P_r} + \frac{P_\nu}{R_\eta}\right)(\sin i\beta_z \mp i\beta_z) \frac{k}{R_\nu} = 0 \tag{4.73a,b}$$

where the upper (respectively, lower) trigonometric function and sign correspond to the symmetric (respectively, antisymmetric) dispersion relation. From (4.73a,b), we immediately deduce zeroth-order estimates

of the eigenvalues of the form

$$\beta_z = -iz \tag{4.74}$$

where z satisfies one of the following transcendental equations

$$\sin z = \pm z \tag{4.75a,b}$$

and the + and - signs correspond to symmetric and antisymmetric eigenvalues. The solutions of the above equations are investigated in detail in Appendix D. They both admit an infinity of non-zero complex solutions. Furthermore, if z is a solution of (4.75a or b), so is $-z$ and the complex conjugate z^*. Consequently, if numerical solutions of these equations are available in the fourth quadrant ($\mathrm{Re}\, z > 0$, $\mathrm{Im}\, z < 0$) of the complex z-plane, the solutions in the three other quadrants may immediately be obtained by elementary symmetry considerations.

Let us introduce the following notations: the complex root of (4.75a) lying in the fourth quadrant of the complex plane and such that

$$2n\pi < \mathrm{Re}\, z < (2n+\tfrac{1}{2})\pi \qquad n = 1, 2, 3, \ldots \tag{4.76}$$

will be designated z_n^+. Correspondingly, the complex root of (4.75b) which lies in the same quadrant and such that

$$(2n+1)\pi < \mathrm{Re}\, z < (2n+\tfrac{3}{2})\pi \qquad n = 0, 1, 2, \ldots \tag{4.77}$$

will be designated z_n^-. The first five roots of each equation have been computed numerically, and are displayed in Table III and IV. For large values of n, they have the following asymptotic forms:

$$z_n^+ = (2n+\tfrac{1}{2})\pi - i \cosh^{-1}(2n+\tfrac{1}{2})\pi \quad \text{as} \quad n \to +\infty \tag{4.78}$$

$$z_n^- = (2n+\tfrac{3}{2})\pi - i \cosh^{-1}(2n+\tfrac{3}{2})\pi \quad \text{as} \quad n \to +\infty \tag{4.79}$$

In agreement with the "radiation condition" stated in Section 3.4, we restrict our attention to complex numbers of negative imaginary part, i.e., to solutions of (4.75a,b) lying in the half plane $\mathrm{Re}\, z > 0$. Hence, the only solutions of interest are $\{z_1^+, \ldots z_n^+, \ldots\}$ and $\{z_0^-, \ldots z_n^-, \ldots\}$ and their complex conjugates. The two families, $\{z_1^+, \ldots z_n^+, \ldots\}$ and $\{z_0^-, \ldots z_n^-, \ldots\}$ have negative imaginary parts and therefore correspond to complex wave numbers of negative real parts. Since higher-order P-modes were shown to have negative phase velocities below their cut-off frequency, in the high-frequency-wide-tube range, we naturally associate these two families of roots to symmetric (excluding $n = 0$) and antisymmetric P-eigenvalues respectively. Similarly, since vorticity modes were shown to have positive real parts, we associate the conjugate families $\{z_1^{+*}, \ldots z_n^{+*}, \ldots\}$ and $\{z_0^{-*}, \ldots z_n^{-*} \ldots\}$ lying in the first quadrant to symmetric and antisymmetric V-eigenvalues respectively.*

We do not consider the above reasoning as a rigorous proof of the correspondence between high-frequency and low-frequency eigenvalues. Such a proof can only be given when the expansions derived in this study are compared with known numerical solutions of the dispersion relations, which allow each eigenvalue to be followed throughout the entire frequency domain, without any interruption. More specifically, the previous identifications will be fully justified when we compare our solutions with the numerical investigation of Scarton and Rouleau.

When the zeroth-order or zero-frequency estimates have been determined as stated above, it is a straightforward procedure to derive a

*The possibility of identifying these roots with the S-eigenvalues may at once be discarded, since such roots still exist when there is no heat conduction, whereas the S-modes do not.

n	α_n^+	β_n^+
1	7.497676	2.768678
2	13.899960	3.352210
3	20.238518	3.716768
4	26.554547	3.983142
5	32.859741	4.193251

TABLE III:

Solutions $z_n^+ = \alpha_n^+ - i\beta_n^+$ of $\sin z = z$

n	α_n^-	β_n^-
0	4.212392	2.250729
1	10.712537	3.103149
2	17.073365	3.551087
3	23.398355	3.858809
4	29.708120	4.093705

TABLE IV:

Solutions $z_n^- = \alpha_n^- - i\beta_n^-$ of $\sin z = -z$

more accurate representation of the complex wave number by assuming that it may be expanded as:

$$\beta_z = -iz(1+ak) \tag{4.80}$$

where a is determined by substituting (4.80) into (4.73a,b), expanding the resulting equations to order k, and setting the coefficient of k equal to zero. The symmetric and antisymmetric pressure-dominated wave numbers are then respectively given by:

$$\beta_{zn}^{SP} = -iz_n^{+}\left[1+\frac{ikR_\nu}{4z_n^{+2}}+\frac{i\gamma_0}{\sin^2\frac{z_n^{+}}{2}}\frac{k}{R_\nu}\right] \tag{4.81}$$

and

$$\beta_{zn}^{AP} = -iz_n^{-}\left[1+\frac{ikR_\nu}{4z_n^{-2}}+\frac{i\gamma_0}{\cos^2\frac{z_n^{-}}{2}}\frac{k}{R_\nu}\right] \tag{4.82}$$

where z_n^{+} and z_n^{-} are the non-zero complex solutions of

$$\sin z = \pm z$$

which lie in the fourth quadrant of the complex z-plane.

The symmetric and antisymmetric vorticity-dominated modes are also given by the above expansions, where z_n^{+} and z_n^{-} have been replaced by their complex conjugates. Substitution of the results for β_z into expressions (4.70) - (4.72) yields the following expansions for α_0, α_1, and α_2:

$$\alpha_{0n}^{SP} = z_n^{+}\left[1+\frac{ikR_\nu}{4z_n^{+2}}+\frac{i\gamma_0}{\sin^2\frac{z_n^{+}}{2}}\frac{k}{R_\nu}\right] \tag{4.83}$$

$$\alpha_{1n}^{SP} = z_n^+ \left[1 + \frac{ik(1-2P_r)R_\nu}{4z_n^{+2}} + \frac{i\gamma_0}{\sin^2 \frac{z_n^+}{2}} \frac{k}{R_\nu}\right] \tag{4.84}$$

$$\alpha_{2n}^{SP} = z_n^+ \left[1 - \frac{ikR_\nu}{4z_n^{+2}} + \frac{i\gamma_0}{\sin^2 \frac{z_n^+}{2}} \frac{k}{R_\nu}\right] \tag{4.85}$$

and

$$\alpha_{0n}^{AP} = z_n^- \left[1 + \frac{ikR_\nu}{4z_n^{-2}} + \frac{i\gamma_0}{\cos^2 \frac{z_n^-}{2}} \frac{k}{R_\nu}\right] \tag{4.86}$$

$$\alpha_{1n}^{AP} = z_n^- \left[1 + ik\frac{(1-2P_r)R_\nu}{4z_n^{-2}} + \frac{i\gamma_0}{\cos^2 \frac{z_n^-}{2}} \frac{k}{R_\nu}\right] \tag{4.87}$$

$$\alpha_{2n}^{AP} = z_n^- \left[1 - \frac{ikR_\nu}{4z_n^{-2}} + \frac{i\gamma_0}{\cos^2 \frac{z_n^-}{2}} \frac{k}{R_\nu}\right] \tag{4.88}$$

The corresponding V-expressions are obtained by replacing z_n^+ and z_n^- by their complex conjugates.

To derive expansions for the higher-order P-modes and all the V-modes, we have assumed the complex wave number to be of order unity. In order to determine the characteristics of the only remaining unknown eigenvalue, i.e., the zeroth-order SP-mode, β_z is taken to be of the form

$$\beta_z^2 = B\,k \tag{4.89}$$

where the unknown constant B of order unity is found by expanding the symmetric dispersion relation (4.15a) to order k^2 inclusive. Terms in k cancel out and when the term in k^2 is set equal to zero, we obtain the following equation for B :

$$B = -\frac{12\, i\, \gamma_0}{R_\nu} \tag{4.90}$$

so that the SP(0) mode is given by:

$$\beta_{z0}^{SP} = (1-i)\sqrt{\frac{6\gamma_0 k}{R_\nu}} \quad (4.91) \; ; \quad \alpha_{00}^{SP} = (1+i)\sqrt{\frac{6\gamma_0 k}{R_\nu}} \tag{4.92}$$

$$\alpha_{10}^{SP} = (1-i)\sqrt{\frac{kP_r R_\nu}{2}\left(1-\frac{12\gamma_0}{P_r R_\nu^2}\right)} \quad (4.93); \quad \alpha_{20}^{SP} = (1-i)\sqrt{\frac{kR_\nu}{2}\left(1-\frac{12\gamma_0}{R_\nu^2}\right)} \quad (4.94)$$

Upon examination of the ratio of successive terms in the previous expansions, one easily determines the range of validity of the low-frequency-narrow-tube approximation:

$$k \ll \frac{1}{R_\nu} \tag{4.95}$$

As mentioned at the beginning of this subsection, the coefficients α_0 , α_1 , and α_2 are now of the same order of magnitude, unity or smaller. The associated mode shapes will therefore present smooth variations in the cross-section of the tube, and will not exhibit a boundary-layer-like character as in the high-frequency-wide-tube regime.

In the limit of zero reduced frequency, i.e., in the case of steady small-amplitude viscous and heat-conducting flow, V-modes and higher-order P-modes are characterized by constant wave numbers. To each higher-order P-eigenvalue of a given attenuation rate and negative phase velocity, one can associate a V-eigenvalue of identical attenuation rate and opposite phase velocity. Scarton and Rouleau have derived similar zero-frequency eigenvalues for the circular geometry and Fitzgerald (1972) used the corresponding eigenfunctions to model the

plasma motions in the gaps between successive red cells in narrow-capillary blood flow. In the present study, additional frequency-dependent terms have been calculated so as to extend the results to a low-frequency-narrow-tube region.

The SP(0)-mode is the well-known unsteady Poiseuille flow analyzed by Rayleigh. In contrast with the high-frequency-wide-tube regime, its phase speed now varies as the square root of frequency. In the limit of zero reduced frequency, this eigenvalue becomes identically zero and is therefore irrelevant. Further remarks on the physical meaning of these results will be given in Section 4.6.

4.4.2 Entropy-Dominated Modes. In the above formulation, the dispersion relations were taken in the form (4.15a,b) and such an approach failed to yield the characteristics of the S-modes. In agreement with the procedure adopted in Subsection 4.3.2, we find it more convenient to solve the dispersion relations in the form (4.15c,d) for the unknown α_1 which is assumed to be of order unity. From (4.16) - (4.18), we may write:

$$\beta_z^2 = -\alpha_1^2\left[1+\frac{ikP_rR_\nu}{\alpha_1^2}-\frac{(\gamma_0-1)}{\alpha_1^2}P_r\left(\frac{1}{P_r}-\frac{R_\nu}{R_\eta}\right)k^2\right] \tag{4.96}$$

$$\alpha_0 = \alpha_1\left[1+\frac{ikP_rR_\nu}{2\alpha_1^2}-\frac{(\gamma_0-1)}{2\alpha_1^2}P_r\left(\frac{1}{P_r}-\frac{R_\nu}{R_\eta}\right)k^2+\frac{k^2}{2\alpha_1^2}+\frac{(kP_rR_\nu)^2}{8\alpha_1^4}\right] \tag{4.97}$$

$$\alpha_2 = \alpha_1\left[1+\frac{ik(P_r-1)}{2\alpha_1^2}-\frac{(\gamma_0-1)P_r}{2\alpha_1^2}\left(\frac{1}{P_r}-\frac{R_\nu}{R_\eta}\right)k^2+\frac{\{k(1-P_r)R_\nu\}^2}{8\alpha_1^4}\right] \tag{4.98}$$

As expected, the coefficients α_0, α_1, and α_2 are seen to be of identical order, and values of α_1 such that,

$$\alpha_1 = N\pi \tag{4.99}$$

where

$$N = 2n+1 \qquad n = 0\ ,\ 1\ ,\ 2\ ,\ \ldots \tag{4.100}$$

or

$$N = 2n \qquad n = 1\ ,\ 2\ ,\ 3\ \ldots \tag{4.101}$$

satisfy the dispersion relation (4.15c), or (4.15d) respectively, to zeroth order in k. Accurate expressions to order k^3 inclusive are needed in order to properly calculate the associated eigenfunctions. Consequently, the coefficient α_1 is assumed to be of the form:

$$\alpha_1 = N\pi + ak^2 + bk^3 \tag{4.102}$$

where a and b are determined by substitution of (4.102) into (4.15c) and (4.15d), and expansion of the resulting equations to order k^3. Terms of zeroth order and order k cancel out and coefficients of k^2 and k^3 must be set equal to zero. The final results are the following:

$$\alpha_{1N}^{S} = N\pi \left[1 - \frac{(\gamma_0-1)(P_r-1)k^2}{2(N\pi)^2}\left\{1 - \frac{ikP_rR_\nu}{(N\pi)^2}\right.\right.$$

$$\left.\left. + i\,\frac{(2P_r-1)\gamma_0-1}{P_r-1}\left(\frac{1}{P_r} - \frac{R_\nu}{R_\eta}\right)\frac{k}{R_\nu} + i\,\frac{\gamma_0(P_r-1)k}{P_rR_\nu}\right\}\right] \tag{4.103}$$

where the integer N is an odd number of the form (4.100) for the symmetric mode of order n, SS(n), and an even number of the form (4.101) for the antisymmetric mode of order n, AS(n). Corresponding expressions for α_0, α_2, and β_z are given by:

$$\alpha_{0N}^{S} = N\pi\left[1 + \frac{ikP_rR_\nu}{2(N\pi)^2} - \frac{(\gamma_0-1)P_r}{2(N\pi)^2}\left(1 - \frac{R_\nu}{R_\eta}\right)k^2 + \frac{k^2}{2(N\pi)^2} + \frac{(kP_rR_\nu)^2}{8(N\pi)^4}\right] \tag{4.104}$$

$$\alpha_{2N}^{S} = N\pi\left[1+\frac{ik(P_r-1)R_\nu}{2(N\pi)^2}-\frac{(\gamma_0-1)P_r}{2(N\pi)^2}\left(1-\frac{R_\nu}{R_\eta}\right)k^2+\frac{\{k(1-P_r)R_\nu\}^2}{8(N\pi)^4}\right] \quad (4.105)$$

$$\beta_{zN}^{S} = -iN\pi\left[1+\frac{ikP_rR_\nu}{2(N\pi)^2}-\frac{(\gamma_0-1)P_r}{2(N\pi)^2}\left(1-\frac{R_\nu}{R_\eta}\right)k^2+\frac{(kP_rR_\nu)^2}{8(N\pi)^4}\right] \quad (4.106)$$

The range of validity of these expansions is the same as for the pressure- and vorticity-dominated modes of the preceding subsection, i.e., the reduced frequency k is such that

$$k \ll \frac{1}{R_\nu} \quad (4.107)$$

In the limit of steady motions, the entropy-dominated eigenvalues are purely imaginary and correspond to non-propagating modes of attenuation rate $N\pi$. We do not know of any previous study of these modes, with which our present results could be compared.

We now proceed to an investigation of the dispersion relations in the very-high-frequency-very-wide-tube approximation.

4.5 Very-High-Frequency-Very-Wide-Tube Range.

In Section 4.3 we pointed out that the expansions pertaining to the P modes were valid for values of the frequency parameter k, lower than $R_\nu^{1/3}$. Such a requirement is particularly evident if we examine relations (4.29a,b) where the right-hand side has been assumed smaller than unity. For values of k of the order of $R_\nu^{1/3}$, the high-frequency-wide-tube results break down. Physically, dilatational attenuation in the bulk of the fluid, and proportional to k^2, becomes of the same order of magnitude as acoustic boundary layer attenuation proportional to $\sqrt{k}$. We now reexamine the pressure-dominated modes in the domain:

$$R_\nu^{1/3} \ll k \ll R_\nu \tag{4.108}$$

where the upper bound on k is a consequence of the continuum hypothesis stated in Section 4.2. As mentioned earlier, high-frequency-wide-tube results associated with the S- and V-modes are still valid in the present approximation. Consequently, we do not need to consider these modes in this section.

Following a well-established procedure, we solve the dispersion relations (4.15a,b) for the unknown α_0 which is assumed to be of order unity. Equations (4.16) - (4.18) yield expansions of β_z^2, α_1, and α_2 given by:

$$\beta_z^2 = k^2\left[1 - i\left(\frac{\gamma_0 - 1}{P_r} + \frac{R_\nu}{R_\eta}\right)\frac{k}{R_\nu} - \frac{\alpha_0^2}{k^2}\right] \tag{4.109}$$

$$\alpha_1 = (1-i)\sqrt{\frac{kP_rR_\nu}{2}}\left[1 + \frac{i}{2}\left(\frac{\gamma_0^{-2}}{P_r} - (\gamma_0 - 1)\frac{R_\nu}{R_\eta}\right)\frac{k}{R_\nu}\right] \tag{4.110}$$

$$\alpha_2 = (1-i)\sqrt{\frac{kR_\nu}{2}}\left[1 - \frac{ik}{2R_\nu}\right] \tag{4.111}$$

The above expressions are all accurate up to order k/R_ν. In (4.109), we have included a higher order term in $1/k^2$ so as to establish a one-to-one relationship between each P-mode and its complex wave number β_z. However, such a term is negligible in the current determination of the equations for α_0. After substitution into the dispersion relations (4.15a,b) and appropriate expansion, one obtains the following relations:

$$\left\{\begin{matrix}\text{cotan}\\ \tan\end{matrix}\right\}\frac{\alpha_0}{2} = \mp\frac{1+i}{1+\dfrac{\gamma_0-1}{\sqrt{P_r}}}\left(\frac{R_\nu}{2k^3}\right)^{\frac{1}{2}}\alpha_0 \qquad (4.112a,b)$$

Note that the corresponding high-frequency-wide-tube equations (4.29a,b) reduce to (4.112a,b) when the term in $1/\sqrt{kR_\nu}$ is neglected in comparison with the term in $(k^3/R_\nu)^{\frac{1}{2}}$ on the right-hand side of (4.29a,b). From (4.112a,b), it is straightforward to solve for α_0. The final results are given by:

$$\alpha_{0N}^{P} = N\pi\left[1+\frac{1+i}{1+\dfrac{\gamma_0-1}{\sqrt{P_r}}}\left(\frac{2R_\nu}{k^3}\right)^{\frac{1}{2}}\right] \qquad (4.113)$$

where the integer N is an odd number

$$N = 2n-1 \qquad n = 1, 2, 3, \ldots \qquad (4.114)$$

for the symmetric higher order mode $SP(n)$, and an even number

$$N = 2n \qquad n = 1, 2, 3, \ldots \qquad (4.115)$$

for the antisymmetric higher order mode $AP(n)$. Equations (4.109) - (4.111) then yield the expansions of α_1, α_2, and β_z:

$$\alpha_{1N}^{P} = (1-i)\sqrt{\frac{kP_r R_\nu}{2}}\left[1+\frac{i}{2}\left\{\frac{\gamma_0-2}{P_r}-(\gamma_0-1)\frac{R_\nu}{R_\eta}\right\}\frac{k}{R_\nu}\right] \qquad (4.116)$$

$$\alpha_{2N}^{P} = (1-i)\sqrt{\frac{kR_\nu}{2}}\left[1-\frac{ik}{2R_\nu}\right] \qquad (4.117)$$

$$\beta_{zN}^{P} = k\left[1-\frac{i}{2}\left(\frac{\gamma_0-1}{P_r}+\frac{R_\nu}{R_\eta}\right)\frac{k}{R_\nu}-\frac{(N\pi)^2}{2k^2}-(1+i)\frac{(N\pi)^2}{1+\dfrac{\gamma_0-1}{\sqrt{P_r}}}\frac{1}{k^2}\left(\frac{2R_\nu}{k^3}\right)^{\frac{1}{2}}\right] \qquad (4.118)$$

In order to derive the expansions pertaining to the SP(0) and AP(0) modes, the coefficient α_0 is assumed to be large of o der $(k^3/R_\nu)^{\frac{1}{2}}$, and such that:

$$\alpha_0 = (1+i)a\left(\frac{k^3}{2R_\nu}\right)^{\frac{1}{2}} \tag{4.119}$$

In this case, equations (4.112a,b) are shown to still be valid. Furthermore, since α_0 is of the form (4.119), its trigonometric tangent is:

$$\tan\frac{\alpha_0}{2} = i \tag{4.120}$$

and equations (4.112a,b) immediately yield the following expressions for α_0 :

$$\alpha_{00}^{SP} = \alpha_{00}^{AP} = (1+i)\left(1+\frac{\gamma_0-1}{\sqrt{P_r}}\right)\left(\frac{k^3}{2R_\nu}\right)^{\frac{1}{2}} \tag{4.121}$$

Corresponding expansions for α_1 and α_2 are given by (4.116) and (4.117), and the complex wave number is

$$\beta_{z0}^{SP} = \beta_{z0}^{AP} = k\left[1-\frac{i}{2}\left(1+\frac{\gamma_0-1}{\sqrt{P_r}}\right)^2\frac{k}{R_\nu}-\frac{i}{2}\left(\frac{\gamma_0-1}{P_r}+\frac{R_\nu}{R_\eta}\right)\frac{k}{R_\nu}\right] \tag{4.122}$$

As seen from the second term in (4.118) and the second and third term in (4.122), all P-modes are characterized by an attenuation rate proportional to the square of the reduced frequency, and Kirchhoff's free space attenuation term is seen to be a significant part of the total attenuation rate. The three coefficients α_0, α_1, and α_2 attached to the SP(0) and AP(0) modes are all complex numbers of very large imaginary part. Hence, one may consider, in addition to viscous

and thermal boundary layer thicknesses associated with α_1 and α_2 and defined in equations (4.44) - (4.45), a new layer of thickness of order $(R_\nu/k^3)^{\frac{1}{2}}$ associated with α_0, and where pressure fluctuations are significant. Such a behavior will be clearly exhibited when we examine the mode shapes in the next section. Zeroth order terms similar to those of (4.113) were derived by Elco and Hughes (1962) for the higher-order P-modes in a viscous fluid contained in a cylindrical duct. Weston (1953a) in his investigation of the characteristics of the zeroth axisymmetric sound mode, also finds expressions which are analogous to the present SP(0)-mode results.

4.6 Mode Shapes.

In the last three sections, the eigenvalues, solutions of the in-plane dispersion relations, were analyzed in detail in the low, high, and very-high frequency ranges. To each eigenvalue corresponds a given mode shape, i.e., given variations of the physical variables with distance x from the duct middle plane. Since the symmetric inplane eigenfunctions are closely related to the axisymmetric eigenfunctions of a cylindrical duct, we will restrict the study to the determination of the symmetric inplane mode shapes. Furthermore, symmetric and antisymmetric eigenvalues were shown to exhibit similar characteristics and a discussion of the antisymmetric eigenfunctions would not reveal any new physical features.

The symmetric mode shapes of Table I will be normalized by requiring that

$$p'(x=0) = 1 \tag{4.123}$$

for the SP-modes,

$$S'(x=0) = 1 \tag{4.124}$$

for the SS-modes, and

$$\frac{d\Omega_y'}{dx}(x=0) = 1 \tag{4.125}$$

for the SV-modes.

Upon enforcement of these conditions in the relations in Table I, the unknown constant A' takes the following forms:

$$A' = \frac{id}{\rho_0 a_0 k} \frac{1}{(1-\frac{i\beta_0^2}{kP_r R_\nu})\frac{1}{\cos\alpha_0/2} - (1-\frac{i\beta_1^2}{kP_r R_\nu})\frac{1}{\cos\alpha_1/2}} \tag{4.126}$$

in the case of SP-modes,

$$A' = d\sqrt{\frac{T_0}{(\gamma_0-1)c_{p_0}}}\frac{P_r R_\nu}{\beta_1^2}\frac{1}{\frac{\beta_0^2}{\beta_1^2}\frac{1}{\cos\alpha_0/2} - \frac{1}{\cos\alpha_1/2}} \tag{4.127}$$

in the case of SS-modes, and

$$A' = \frac{d^2}{kR_\nu}\frac{1}{\frac{k^2}{\beta_0^2} - \frac{k^2}{\beta_1^2}}\frac{\cos\alpha_2/2}{\beta_z} \tag{4.128}$$

in the case of SV-modes.

As mentioned in Section 4.1, the SP-, SS-, and SV-mode shapes are then obtained in the three frequency and duct-width regimes by substituting the expressions for α_0, α_1, α_2, and β_z derived in the preceding sections into the relations of Table I.

In order to exhibit in a relatively simple mathematical form the main features of each family in each reduced frequency domain, all the

terms in the resulting equations can be expanded in powers of the small parameter characterizing the frequency range under consideration, so as to yield first approximations of the physical variables which are uniformly valid throughout the entire cross-section $-\frac{1}{2} \leq x \leq \frac{1}{2}$. Even though we restrict our efforts to the derivation of first-order approximations, the procedure is long and tedious. Since no mathematical difficulties are involved in the derivation, only the final results are presented as shown in the next few pages. Tables V, VI, and VII refer to the SP-, SS-, and SV-mode shapes in the high-frequency-wide-tube range; Tables VIII, IX, and X to the same mode shapes in the low-frequency-narrow-tube range; and, Tables XI and XII to the SP(0) and higher-order SP-mode shapes in the very-high-frequency-very-wide-tube range.

Alternatively, the complete expansions of α_0, α_1, α_2 and β_z can be inserted into the relations of Table I. The resulting expressions are very complicated and do not need to be expanded. The mode shapes are evaluated directly by computing numerically their variations with distance x from the duct axis for given values of the non-dimensional parameters, γ_0, P_r, R_ν, R_η, and k. The complex amplitudes of pressure, entropy, vorticity, axial and transversal velocity, and temperature can then be plotted for the first two modes of each family as shown in Figures 5-10. In any figure, each row of rectangular plots is attached to a given mode indicated at the left end of the row, and each column to a specific physical variable indicated at the bottom of the column. On any individual plot, the variations of the real and imaginary parts of the corresponding physical variable are represented versus transversal distance x (vertical axis on the plot) from $x = 0$ to $x = \frac{1}{2}$, i.e., in the upper half of the duct cross-section only. The

$$p'^{SP}_n(x) = \cos 2n\pi x$$

$$S'^{SP}_n(x) = -\frac{1}{\rho_0 a_0}\sqrt{\frac{(\gamma_0-)c_{p0}}{T_0}}(-1)^n\left[e^{-(1+i)\sqrt{\frac{kP_rR_\nu}{2}}(\frac{1}{2}-x)} + e^{-(1+i)\sqrt{\frac{kP_rR_\nu}{2}}(\frac{1}{2}+x)}\right]$$

$$\Omega'^{SP}_{yn}(x) = \frac{1+i}{\rho_0 a_0 d}\sqrt{\frac{R_\nu}{2k}}\,\beta^{SP}_{zn}(-1)^n\left[e^{-(1+i)\sqrt{\frac{kR_\nu}{2}}(\frac{1}{2}-x)} - e^{-(1+i)\sqrt{\frac{kR_\nu}{2}}(\frac{1}{2}+x)}\right]$$

$$T'^{SP}_n(x) = \frac{1}{\rho_0 a_0}\sqrt{\frac{(\gamma_0-1)T_0}{c_{p_0}}}\left[\cos 2n\pi x - (-1)^n\{e^{-(1+i)\sqrt{\frac{kP_rR_\nu}{2}}(\frac{1}{2}-x)} + e^{-(1+i)\sqrt{\frac{kP_rR_\nu}{2}}(\frac{1}{2}+x)}\}\right]$$

$$\rho'^{SP}_n(x) = \frac{1}{a_0^2}\left[\cos 2n\pi x + (-1)^n(\gamma_0-1)\{e^{-(1+i)\sqrt{\frac{kP_rR_\nu}{2}}(\frac{1}{2}-x)} + e^{-(1+i)\sqrt{\frac{kP_rR_\nu}{2}}(\frac{1}{2}+x)}\}\right]$$

$$V'^{SP}_{zn}(x) = \frac{\beta^{SP}_{zn}}{\rho_0 a_0 k}\left[\cos 2n\pi x - (-1)^n\{e^{-(1+i)\sqrt{\frac{kR_\nu}{2}}(\frac{1}{2}-x)} + e^{-(1+i)\sqrt{\frac{kR_\nu}{2}}(\frac{1}{2}+x)}\}\right]$$

$$V'^{SP}_{xn}(x) = -\frac{2n\pi i}{\rho_0 a_0 k}\sin 2n\pi x$$

$$V'^{SP}_{x0}(x) = \frac{1+i}{\rho_0 a_0 k}\left(\frac{1}{2kR_\nu}\right)^{\frac{1}{2}}\left[2k^{*2}x - \frac{\gamma_0-1}{\sqrt{P_r}}k^2\{e^{-(1+i)\sqrt{\frac{kP_rR_\nu}{2}}(\frac{1}{2}-x)} - e^{-(1+i)\sqrt{\frac{kP_rR_\nu}{2}}(\frac{1}{2}+x)}\} - k^2\{e^{-(1+i)\sqrt{\frac{kR_\nu}{2}}(\frac{1}{2}-x)} - e^{-(1+i)\sqrt{\frac{kR_\nu}{2}}(\frac{1}{2}+x)}\}\right]$$

Table V. High-frequency wide-tube range. SP-mode shapes $n \geq 0$.

$$p'_{SS,n}(x) = -i\rho_0 a_0 \sqrt{\frac{(\gamma_0-1)T_0}{c_{p_0}}} \left(\frac{1}{P_r} - \frac{R_\nu}{R_\eta}\right) \frac{k}{R_\nu} \cos(2n+1)\pi x$$

$$S'_{SS,n}(x) = \cos(2n+1)\pi x$$

$$\Omega'_{SS,yn}(x) = \frac{1-i}{\sqrt{2}} \frac{1}{d} \sqrt{\frac{(\gamma_0-1)T_0}{c_{p_0}}} \sqrt{\frac{P_r}{1-P_r}} \frac{(-1)^n(2n+1)\pi}{1+i\sqrt{\frac{P_r}{1-P_r}}} \frac{1}{P_r} \left(\frac{k}{P_r R_\nu}\right)^{\frac{1}{2}} \left[e^{-(1-i)\sqrt{\frac{k(1-P_r)R_\nu}{2}}\left(\frac{1}{2}-x\right)} - e^{-(1-i)\sqrt{\frac{k(1-P_r)R_\nu}{2}}\left(\frac{1}{2}+x\right)} \right]$$

$$T'_{SS,n}(x) = \frac{T_0}{c_{p_0}} \cos(2n+1)\pi x$$

$$\rho'_{SS,n}(x) = -\frac{\rho_0}{a_0} \sqrt{\frac{(\gamma_0-1)T_0}{c_{p_0}}} \cos(2n+1)\pi x$$

$$V'_{SS,zn}(x) = -\frac{1+i}{\sqrt{2}} \sqrt{\frac{(\gamma_0-1)T_0}{c_{p_0}}} \left(\frac{k}{P_r R_\nu}\right)^{\frac{1}{2}} \cos(2n+1)\pi x$$

$$V'_{SS,xn}(x) = -\frac{(2n+1)\pi}{P_r R_\nu} \sqrt{\frac{(\gamma_0-1)T_0}{c_{p_0}}} \left[\sin(2n+1)\pi x - \frac{(-1)^n}{1+i\sqrt{\frac{P_r}{1-P_r}}} \left\{ e^{-(1-i)\sqrt{\frac{kP_rR_\nu}{2}}\left(\frac{1}{2}-x\right)} - e^{-(1-i)\sqrt{\frac{kP_rR_\nu}{2}}\left(\frac{1}{2}+x\right)} \right\} \right.$$

$$\left. -(-1)^n i \sqrt{\frac{P_r}{1-P_r}} \frac{1}{1+i\sqrt{\frac{P_r}{1-P_r}}} \left\{ e^{-(1+i)\sqrt{\frac{k(1-P_r)R_\nu}{2}}\left(\frac{1}{2}-x\right)} - e^{-(1+i)\sqrt{\frac{k(1-P_r)R_\nu}{2}}\left(\frac{1}{2}+x\right)} \right\} \right]$$

Table VI. High-frequency wide-tube range. SS-mode shapes $n \geq 0$.

$p'^{SV}_{n}(x) = \frac{1-i}{\sqrt{2}} u_0 \frac{(-1)^n}{(kR_\nu)^{\frac{1}{2}}} \left[e^{-(1-i)\sqrt{\frac{kR_\nu}{2}}(\frac{1}{2}-x)} + e^{-(1-i)\sqrt{\frac{kR_\nu}{2}}(\frac{1}{2}+x)} \right]$
$S'^{SV}_{n}(x) = -\frac{1-i}{\sqrt{2}} \sqrt{\frac{(\gamma_0-1)c_{p0}}{T_0}} d \frac{k}{(kR_\nu)^{3/2}} (-1)^n \left[e^{-(1-i)\sqrt{\frac{k(1-P_r)R_\nu}{2}}(\frac{1}{2}-x)} - e^{-(1-i)\sqrt{\frac{k(1-P_r)R_\nu}{2}}(\frac{1}{2}+x)} \right]$
$\Omega'^{SV}_{yn}(x) = \frac{\sin 2n\pi x}{2n\pi}$
$T'^{SV}_{n}(x) = \frac{1-i}{\sqrt{2}} \sqrt{\frac{(\gamma_0-1)T_0}{c_{p_0}}} d \frac{k}{(kR_\nu)^{3/2}} (-1)^n \left[e^{-(1-i)\sqrt{\frac{kR_\nu}{2}}(\frac{1}{2}-x)} + e^{-(1-i)\sqrt{\frac{kR_\nu}{2}}(\frac{1}{2}+x)} - e^{-(1-i)\sqrt{\frac{k(1-P_r)R_\nu}{2}}(\frac{1}{2}-x)} - e^{-(1-i)\sqrt{\frac{k(1-P_r)R_\nu}{2}}(\frac{1}{2}+x)} \right]$
$\rho'^{SV}_{n}(x) = \frac{1-i}{\sqrt{2}} \frac{\rho_0 d}{a_0} \frac{k}{(kR_\nu)^{3/2}} (-1)^n \left[e^{-(1-i)\sqrt{\frac{kR_\nu}{2}}(\frac{1}{2}-x)} + e^{-(1-i)\sqrt{\frac{kR_\nu}{2}}(\frac{1}{2}+x)} + (\gamma_0-1)\left\{ e^{-(1-i)\sqrt{\frac{k(1-P_r)R_\nu}{2}}(\frac{1}{2}-x)} + e^{-(1-i)\sqrt{\frac{k(1-P_r)R_\nu}{2}}(\frac{1}{2}+x)} \right\} \right]$
$V'^{SV}_{zn}(x) = \frac{id}{kR_\nu} \left[\cos 2n\pi x - (-1)^n \left\{ e^{-(1-i)\sqrt{\frac{kR_\nu}{2}}(\frac{1}{2}-x)} + e^{-(1-i)\sqrt{\frac{kR_\nu}{2}}(\frac{1}{2}+x)} \right\} \right]$
$V'^{SV}_{xn}(x) = -\frac{1-i}{\sqrt{2}} \frac{d}{\sqrt{kR_\nu}} \frac{\sin 2n\pi x}{2n\pi}$

Table VII. High-frequency-wide-tube range. SV-mode shapes, $n > 0$.

$n \neq 0$	$n = 0$
$p'^{SP}_{n}(x) = \cos z_n^+ x$	$p'^{SP}_{0}(x) = 1$
$S'^{SP}_{n}(x) = -\frac{1}{\rho_0 a_0}\sqrt{\frac{(\gamma_0-1)c_{p_0}}{T_0}}\cos z_n^+ x$	$S'^{SP}_{0}(x) = -\frac{1}{\rho_0 a_0}\sqrt{\frac{(\gamma_0-1)c_{p_0}}{T_0}}$
$\Omega'^{SP}_{yn}(x) = \frac{1}{\mu_0}\sin z_n^+ x$	$\Omega'^{SP}_{y0}(x) = \frac{1+i}{\rho_0 a_0 d}\sqrt{6\gamma_0 kR_\nu}\, x$
$T'^{SP}_{n}(x) = -\frac{i}{\rho_0 a_0}\sqrt{\frac{(\gamma_0-1)T_0}{c_{p_0}}}\frac{kP_r R_\nu}{2z_n^+}(x\sin z_n^+ x - \frac{1}{2}\tan\frac{z_n^+}{2}\cos z_n^+ x)$	$T'^{SP}_{0}(x) = \frac{i}{2\rho_0 a_0}\sqrt{\frac{(\gamma_0-1)T_0}{c_{p_0}}}\, k P_r R_\nu(\frac{1}{4}-x^2)$
$\rho'^{SP}_{n}(x) = \frac{\gamma_0}{a_0^2}\cos z_n^+ x$	$\rho'^{SP}_{0}(x) = \frac{\gamma_0}{a_0^2}$
$V'^{SP}_{zn}(x) = -\frac{d}{2\mu_0}(x\sin z_n^+ x - \frac{1}{2}\tan\frac{z_n^+}{2}\cos z_n^+ x)$	$V'^{SP}_{z0}(x) = \frac{1+i}{2\rho_0 a_0}\sqrt{6\gamma_0 kR_\nu}\,(\frac{1}{4}-x^2)$
$V'^{SP}_{xn}(x) = \frac{d}{2\mu_0}(x\cos z_n^+ x - \frac{1}{2}\cot\tan\frac{z_n^+}{2}\sin z_n^+ x)$	$V'^{SP}_{x0}(x) = \frac{2i\gamma_0 k}{\rho_0 a_0}x(\frac{1}{4}-x^2)$

Table VIII. Low-frequency narrow-tube range. SP-mode shapes $n \geq 0$.

$p'^{SS}_{n}(x) = i\rho_0 a_0 \sqrt{\frac{(\gamma_0-1)T_0}{c_{p_0}}} \left(\frac{R_\nu}{R_\eta} - 1\right) \frac{k}{R_\nu} \cos(2n+1)\pi x$
$S'^{SS}_{n}(x) = \cos(2n+1)\pi x$
$\Omega'^{SS}_{yn}(x) = -\frac{i}{d} \sqrt{\frac{(\gamma_0-1)T_0}{c_{p_0}}}\, k \sin(2n+1)\pi x$
$T'^{SS}_{n}(x) = \frac{T_0}{c_{p_0}} \cos(2n+1)\pi x$
$\rho'^{SS}_{n}(x) = -\frac{\rho_0}{a_0} \sqrt{\frac{(\gamma_0-1)T_0}{c_{p_0}}} \cos(2n+1)\pi x$
$V'^{SS}_{zn}(x) = -i \sqrt{\frac{(\gamma_0-1)T_0}{c_{p_0}}}\, \frac{k}{(2n+1)\pi} \cos(2n+1)\pi x$
$V'^{SS}_{xn}(x) = 0(k^2)$

Table IX. Low-frequency narrow tube range. SS-mode shapes $n \geq 0$.

$p'^{SV}_n(x) = \mu_0 \frac{\cos z_n^{+*} x}{z_n^{+*}}$
$S'^{SV}_n(x) = -d \sqrt{\frac{(\gamma_0 - 1) c_{p_0}}{T_0}} \frac{1}{R_\nu} \frac{\cos z_n^{+*} x}{z_n^{+*}}$
$\Omega'^{SV}_{yn}(x) = \frac{\sin z_n^{+*} x}{z_n^{+*}}$
$T'^{SV}_n(x) = -id \sqrt{\frac{(\gamma_0 - 1) T_0}{c_{p_0}}} \frac{P_r k}{2 z_n^{+*2}} \left(x \sin z_n^{+*} x - \frac{1}{2} \tan \frac{z_n^{+*}}{2} \cos z_n^{+*} x\right)$
$\rho'^{SV}_n(x) = \frac{\gamma_0 \mu_0}{a_0^2} \frac{\cos z_n^{+*} x}{z_n^{+*}}$
$V'^{SV}_{zn}(x) = -\frac{d}{2 z_n^{+*}} \left(x \sin z_n^{+*} x - \frac{1}{2} \tan \frac{z_n^{+*}}{2} \cos z_n^{+*} x\right)$
$V'^{SV}_{xn}(x) = \frac{d}{2 z_n^{+*}} \left(x \cos z_n^{+*} x - \frac{1}{2} \operatorname{cotan} \frac{z_n^{+*}}{2} \sin z_n^{+*} x\right)$

Table X. Low-frequency narrow-tube range. SV-mode shapes, $n > 0$.

$$p'_{0}(x) = \frac{1}{2}\left[e^{(1-i)\left(1+\frac{\gamma_0-1}{\sqrt{P_r}}\right)\left(\frac{k^3}{2R_\nu}\right)^{1/2} x} + e^{-(1-i)\left(1+\frac{\gamma_0-1}{\sqrt{P_r}}\right)\left(\frac{k^3}{2R_\nu}\right)^{1/2} x} \right]$$

$$S'_{0}(x) = -\frac{1}{2\rho_0 a_0}\sqrt{\frac{(\gamma_0-1)c_{p_0}}{T_0}}\, e^{\frac{1-i}{2}\left(1+\frac{\gamma_0-1}{\sqrt{P_r}}\right)\left(\frac{k^3}{2R_\nu}\right)^{1/2}} \left[e^{-(1+i)\sqrt{\frac{kP_rR_\nu}{2}}\left(\frac{1}{2}-x\right)} + e^{-(1+i)\sqrt{\frac{kP_rR_\nu}{2}}\left(\frac{1}{2}+x\right)} \right]$$

$$\Omega'_{y0}(x) = \frac{1+i}{2\sqrt{2}}\frac{\sqrt{kR_\nu}}{\rho_0 a_0 d}\, e^{\frac{1-i}{2}\left(1+\frac{\gamma_0-1}{\sqrt{P_r}}\right)\left(\frac{k^3}{2R_\nu}\right)^{1/2}} \left[e^{-(1+i)\sqrt{\frac{kR_\nu}{2}}\left(\frac{1}{2}-x\right)} + e^{-(1+i)\sqrt{\frac{kR_\nu}{2}}\left(\frac{1}{2}+x\right)} \right]$$

$$T'_{0}(x) = \frac{1}{2\rho_0 a_0}\sqrt{\frac{(\gamma_0-1)T_0}{c_{p_0}}}\, e^{\frac{1-i}{2}\left(1+\frac{\gamma_0-1}{\sqrt{P_r}}\right)\left(\frac{k^3}{2R_\nu}\right)^{1/2}} \left[e^{-(1-i)\left(1+\frac{\gamma_0-1}{\sqrt{P_r}}\right)\left(\frac{k^3}{2R_\nu}\right)^{1/2}\left(\frac{1}{2}-x\right)} + e^{-(1-i)\left(1+\frac{\gamma_0-1}{\sqrt{P_r}}\right)\left(\frac{k^3}{2R_\nu}\right)^{1/2}\left(\frac{1}{2}+x\right)} - \left\{ e^{-(1+i)\sqrt{\frac{kP_rR_\nu}{2}}\left(\frac{1}{2}-x\right)} + e^{-(1+i)\sqrt{\frac{kP_rR_\nu}{2}}\left(\frac{1}{2}+x\right)} \right\} \right]$$

$$\rho'_{0}(x) = \frac{1}{2a_0^2}\, e^{\frac{1-i}{2}\left(1+\frac{\gamma_0-1}{\sqrt{P_r}}\right)\left(\frac{k^3}{2R_\nu}\right)^{1/2}} \left[e^{-(1-i)\left(1+\frac{\gamma_0-1}{\sqrt{P_r}}\right)\left(\frac{k^3}{2R_\nu}\right)^{1/2}\left(\frac{1}{2}-x\right)} + e^{-(1-i)\left(1+\frac{\gamma_0-1}{\sqrt{P_r}}\right)\left(\frac{k^3}{2R_\nu}\right)^{1/2}\left(\frac{1}{2}+x\right)} + (\gamma_0-1)\left\{ e^{-(1+i)\sqrt{\frac{kP_rR_\nu}{2}}\left(\frac{1}{2}-x\right)} + e^{-(1+i)\sqrt{\frac{kP_rR_\nu}{2}}\left(\frac{1}{2}+x\right)} \right\} \right]$$

$$V'_{z0}(x) = \frac{1}{2\rho_0 a_0}\, e^{\frac{1-i}{2}\left(1+\frac{\gamma_0-1}{\sqrt{P_r}}\right)\left(\frac{k^3}{2R_\nu}\right)^{1/2}} \left[e^{-(1-i)\left(1+\frac{\gamma_0-1}{\sqrt{P_r}}\right)\left(\frac{k^3}{2R_\nu}\right)^{1/2}\left(\frac{1}{2}-x\right)} + e^{-(1-i)\left(1+\frac{\gamma_0-1}{\sqrt{P_r}}\right)\left(\frac{k^3}{2R_\nu}\right)^{1/2}\left(\frac{1}{2}+x\right)} - \left\{ e^{-(1+i)\sqrt{\frac{kR_\nu}{2}}\left(\frac{1}{2}-x\right)} + e^{-(1+i)\sqrt{\frac{kR_\nu}{2}}\left(\frac{1}{2}+x\right)} \right\} \right]$$

$$V'_{x0}(x) = \frac{1+i}{2\rho_0 a_0}\left(\frac{k}{2R_\nu}\right)^{1/2} e^{\frac{1-i}{2}\left(1+\frac{\gamma_0-1}{\sqrt{P_r}}\right)\left(\frac{k^3}{2R_\nu}\right)^{1/2}} \left[\left(1+\frac{\gamma_0-1}{\sqrt{P_r}}\right)\left\{ e^{(1-i)\left(1+\frac{\gamma_0-1}{\sqrt{P_r}}\right)\left(\frac{k^3}{2R_\nu}\right)^{1/2}\left(\frac{1}{2}-x\right)} - e^{-(1-i)\left(1+\frac{\gamma_0-1}{\sqrt{P_r}}\right)\left(\frac{k^3}{2R_\nu}\right)^{1/2}\left(\frac{1}{2}+x\right)} \right\} - \frac{\gamma_0-1}{\sqrt{P_r}}\left\{ e^{-(1+i)\sqrt{\frac{kP_rR_\nu}{2}}\left(\frac{1}{2}-x\right)} - e^{-(1+i)\sqrt{\frac{kP_rR_\nu}{2}}\left(\frac{1}{2}+x\right)} \right\} - \left\{ e^{-(1+i)\sqrt{\frac{kR_\nu}{2}}\left(\frac{1}{2}-x\right)} - e^{-(1+i)\sqrt{\frac{kR_\nu}{2}}\left(\frac{1}{2}+x\right)} \right\} \right]$$

Table XI. Very-high-frequency very-wide-tube range. SP(0)-mode shape.

$$p'_{SP,n}(x) = \cos(2n-1)\pi x$$

$$S'_{SP,n} = \frac{1}{\rho_0 a_0}\sqrt{\frac{(\gamma_0-1)c_{p_0}}{T_0}}\left[\frac{1k}{P_r R_\nu}\cos(2n-1)\pi x - (-1)^n(2n-1)\frac{\pi}{2}\frac{1+i}{1+\frac{\gamma_0-1}{\sqrt{P_r}}}\left(\frac{2R_\nu}{k^3}\right)^{\frac{1}{2}}\left\{e^{-(1+i)\sqrt{\frac{kP_rR_\nu}{2}}(\frac{1}{2}-x)} + e^{-(1+i)\sqrt{\frac{kP_rR_\nu}{2}}(\frac{1}{2}+x)}\right\}\right]$$

$$\Omega'_{SP,yn} = \frac{i}{\rho_0 a_0 d}(-1)^n\frac{(2n-1)\pi}{1+\frac{\gamma_0-1}{\sqrt{P_r}}}\frac{R_\nu}{k}\left[e^{-(1+i)\sqrt{\frac{kR_\nu}{2}}(\frac{1}{2}-x)} - e^{-(1+i)\sqrt{\frac{kR_\nu}{2}}(\frac{1}{2}+x)}\right]$$

$$T'_{SP,n} = \frac{1}{\rho_0 a_0}\sqrt{\frac{(\gamma_0-1)T_0}{c_{p_0}}}\cos(2n-1)\pi x$$

$$\rho'_{SP,n} = \frac{1}{a_0^2}\cos(2n-1)\pi x$$

$$V'_{SP,zn} = \frac{1}{\rho_0 a_0}\cos(2n-1)\pi x$$

$$V'_{SP,xn} = -\frac{i(2n-1)\pi}{\rho_0 a_0 k(1+\frac{\gamma_0-1}{\sqrt{P_r}})}\left[(1+\frac{\gamma_0-1}{\sqrt{P_r}})\sin(2n-1)\pi x + (-1)^n\frac{\gamma_0-1}{\sqrt{P_r}}\left\{e^{-(1+i)\sqrt{\frac{kP_rR_\nu}{2}}(\frac{1}{2}-x)} - e^{-(1+i)\sqrt{\frac{kP_rR_\nu}{2}}(\frac{1}{2}+x)}\right\}\right.$$

$$\left. + (-1)^n\left\{e^{-(1+i)\sqrt{\frac{kR_\nu}{2}}(\frac{1}{2}-x)} - e^{-(1+i)\sqrt{\frac{kR_\nu}{2}}(\frac{1}{2}+x)}\right\}\right]$$

Table XII. Very high frequency very wide tube range.
SP(n) mode shapes, $n > 0$.

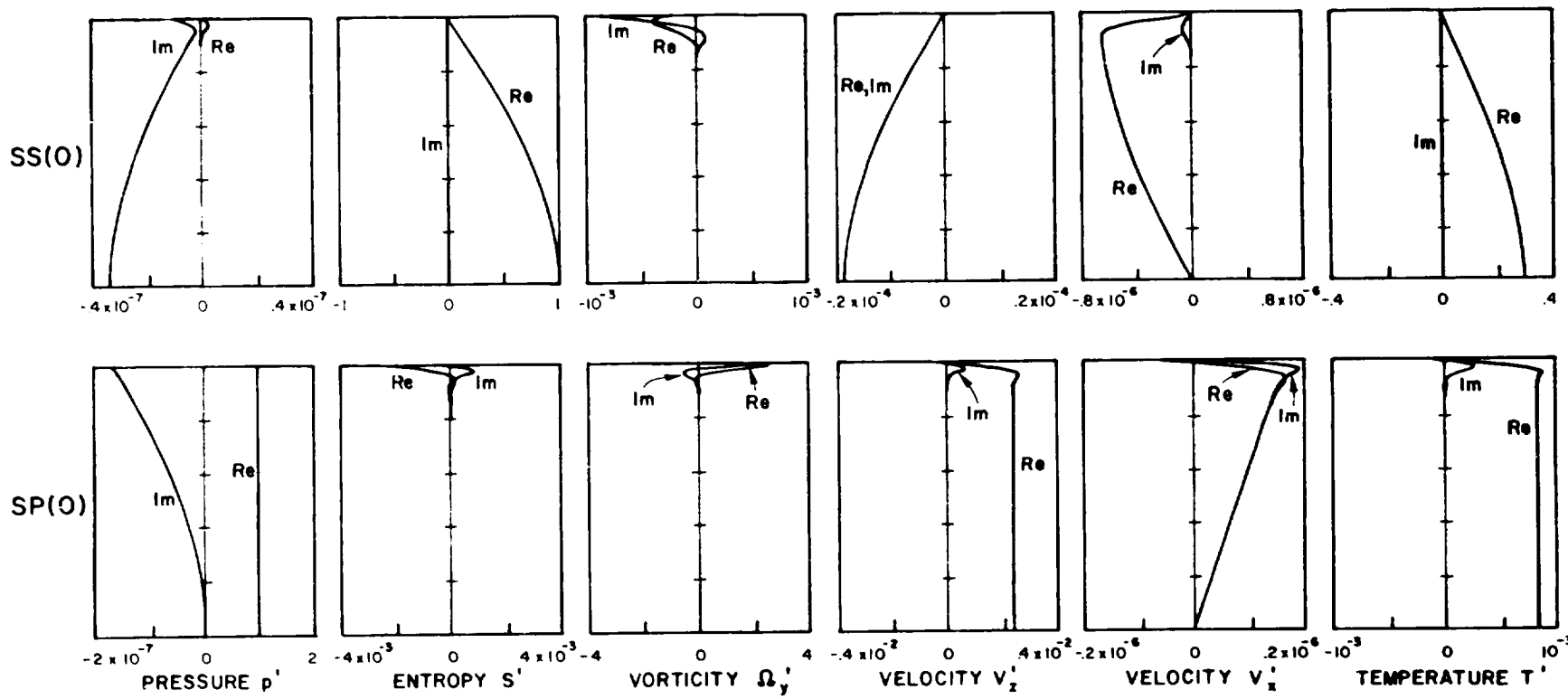

Figure 5. High-Frequency Wide-Tube Range. Zeroth-order symmetric inplane mode shapes for $k = 10^{-2}$, $R_\nu = 2.35\times10^6$, $R_\eta = 1.76\times10^6$, $P_r = .72$, $\gamma_0 = 1.4$, $d = 10^{-1}$m, medium is air at 15°C, 1 atm, $K_0 = 0$.

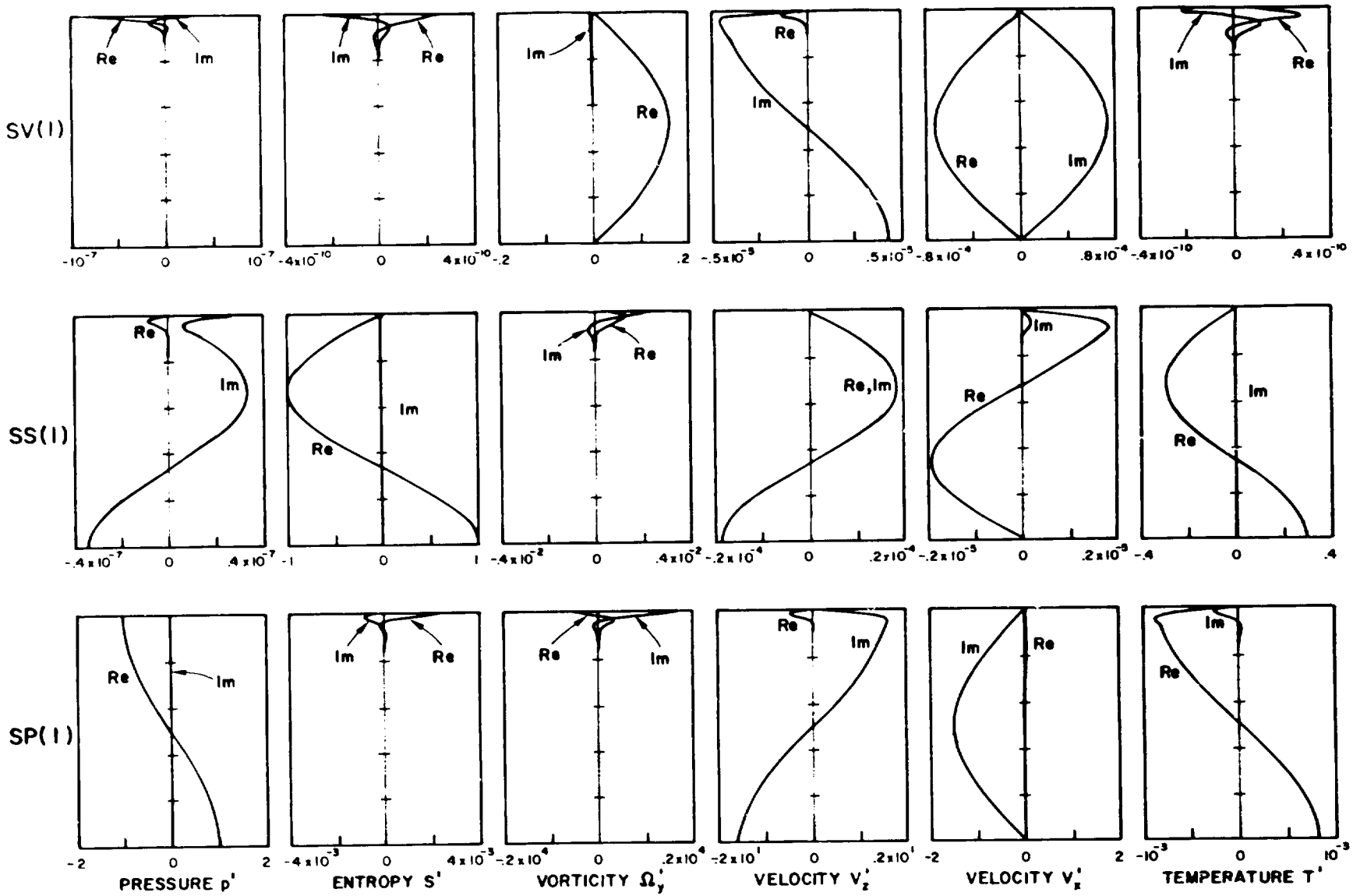

Figure 6. High-Frequency Wide-Tube Range. First-order symmetric inplane mode shapes. Same values of the parameters as in Figure 5.

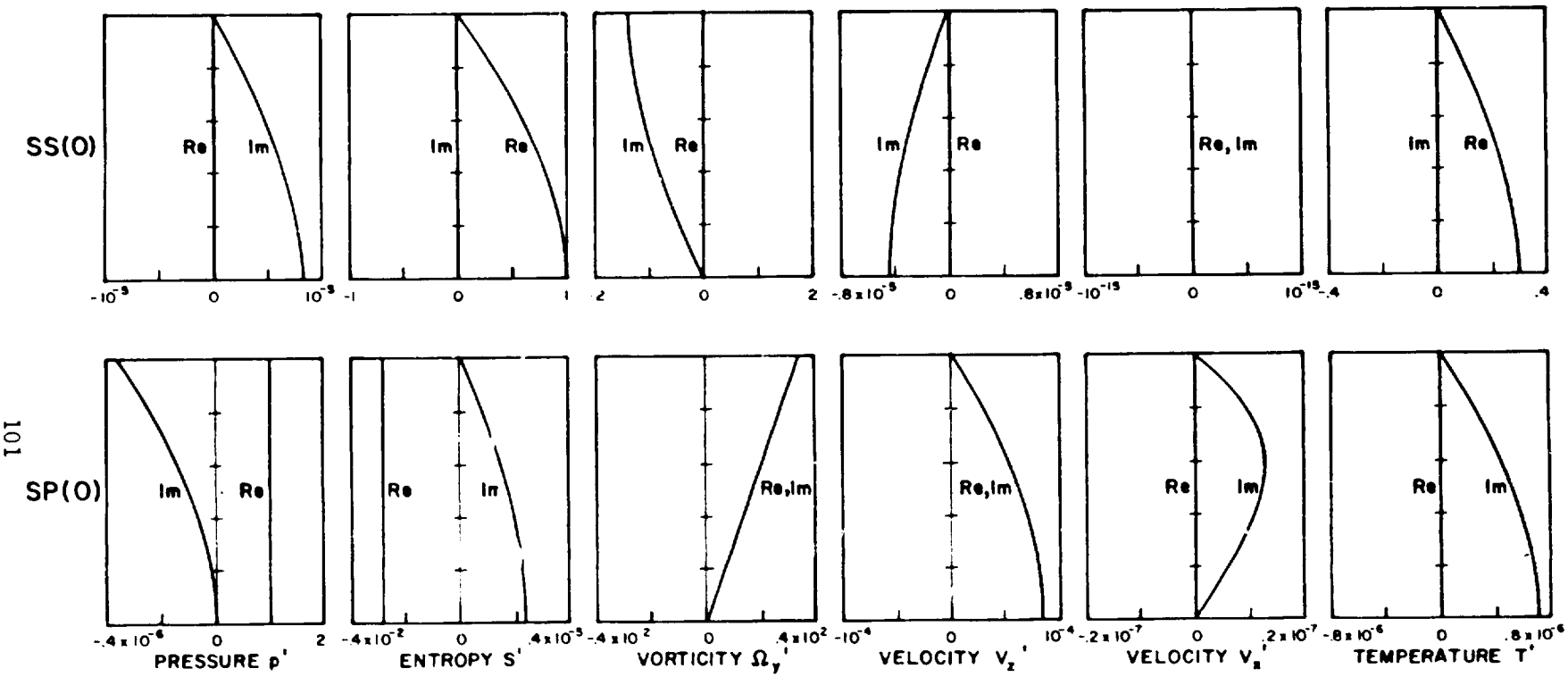

Figure 7. Low-Frequency Narrow-Tube Range. Zeroth-order symmetric inplane mode shapes for $k = 4\times10^{-5}$, $R_\nu = 2.35\times10^{2}$, $R_\eta = 1.76\times10^{2}$, $P_r = .72$, $\gamma_0 = 1.4$, $d = 10^{-5}$m, medium is air at 15^{o}, 1 atm, $K_C = 0$.

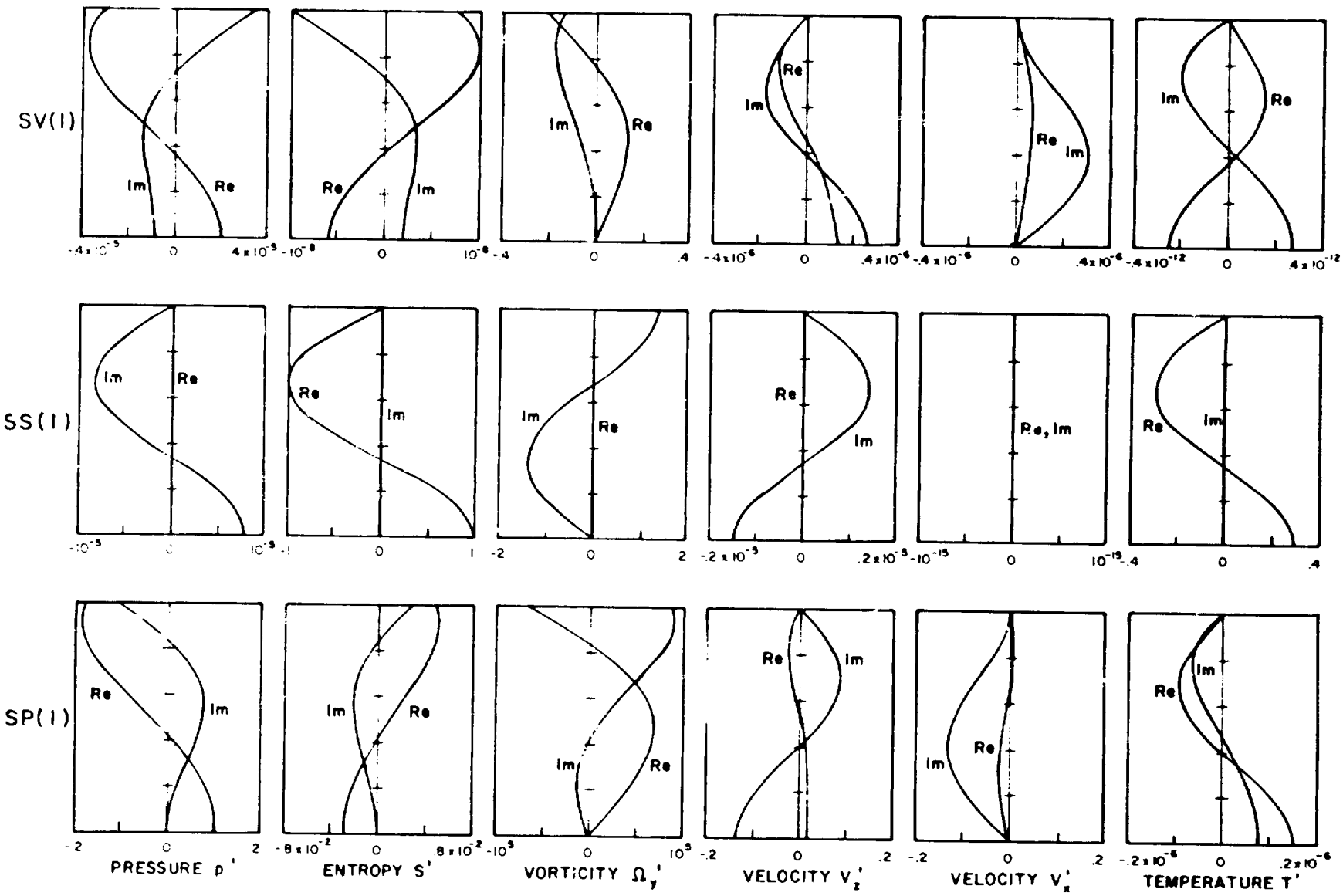

Figure 8. Low-Frequency Narrow-Tube Range. First-order symmetric inplane mode shapes. Same values of the parameters as in Figure 7.

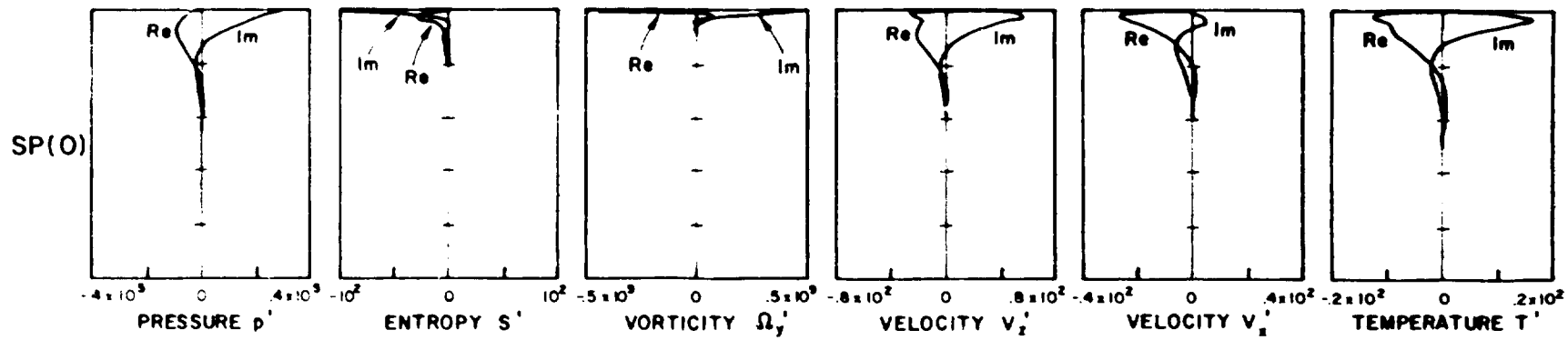

Figure 9. Very-High-Frequency Very-Wide-Tube Range. Zeroth-order SP-mode shapes for $k = 6.65\times10^{1}$, $R_\nu = 6.58\times10^{2}$, $R_\eta = 4.94\times10^{2}$, $P_r = .72$, $\gamma_0 = 1.4$, $d = 2.8\times10^{-5}$ m, medium is air at 15°C, 1 atm, $K_C = 0$.

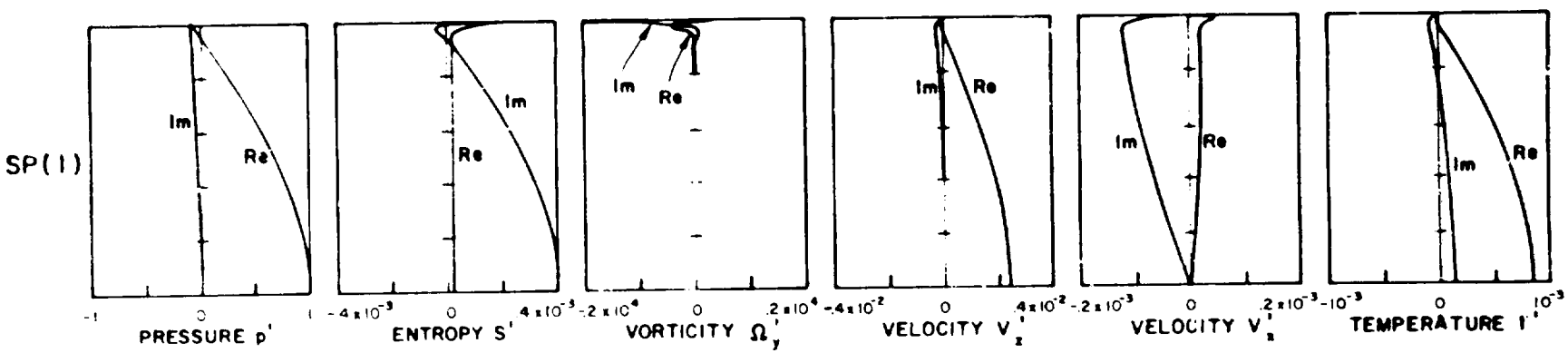

Figure 10. Very-High-Frequency Very-Wide-Tube Range. First-order SP-mode shapes. Same values of the parameters as in Figure 9.

lower half of the mode shape would be obtained by symmetry with respect to the duct middle plane for all physical variables except vorticity and transversal velocity which are antisymmetric. In the following subsections, we successively discuss the main results concerning the SP-, SS-, and SV-mode shapes in the low, high, and very-high frequency regimes as they are summarized in the aforementioned tables and graphs.

4.6.1 High-Frequency-Wide-Tube Mode Shapes. As it is clear from Table V, the SP-mode shapes in the central region of the duct are, to a first approximation, the same as the corresponding inviscid ones. Enforcement of the boundary conditions at the walls is responsible for the presence of diffusive terms in the form of decaying complex exponentials. Such terms are negligible outside thin viscous and thermal boundary layers of respective thickness $(2/kR_\nu)^{\frac{1}{2}}$ and $(2/kP_rR_\nu)^{\frac{1}{2}}$, but they play a critical role inside these layers as exemplified in Figures 5 and 6. The viscous boundary layer is associated with diffusion of vorticity of order $(k/R_\nu)^{-\frac{1}{2}}$ whereas the thermal boundary layer is characterized by diffusion of entropy fluctuations of order unity. We remarked in Section 3.4 that a standing wave form, $\cos 2n\pi x$ travelling along the positive z-direction, could be viewed as the superposition of two travelling plane waves propagating in symmetric directions with respect to the duct axis and reflecting against the boundaries. Let us isolate in the expression for $p_n'^{SP}(x)$, the plane pressure wave

$$p' \simeq e^{i(t-n\pi x-\beta_z z)} \tag{4.129}$$

As seen from Table V, this wave, upon reflection at the upper wall, will give rise to two secondary waves: a highly attenuated "vorticity wave"

of the form

$$\Omega'_y \simeq e^{-\sqrt{\frac{kR_\nu}{2}}\left(\frac{1}{2}-x\right)} \cdot e^{i\left[t+\sqrt{\frac{kR_\nu}{2}}\,x-\beta_z z\right]} \tag{4.130}$$

propagating in a direction almost perpendicular to the plane of the boundary, and associated with axial velocity fluctuations of the same form, and a highly attenuated "entropy wave" given by

$$S' \simeq e^{-\sqrt{\frac{kP_rR_\nu}{2}}\left(\frac{1}{2}-x\right)} \cdot e^{i\left[t+\sqrt{\frac{kP_rR_\nu}{2}}\,x-\beta_z z\right]} \tag{4.131}$$

also propagating in a direction nearly perpendicular to the wall, and associated with temperature and density fluctuations of the form (4.131). The same interpretation may be given for the plane wave propagating towards the lower boundary. Hence, we may conclude that an SP-mode is nothing but the superposition of two plane pressure waves which propagate in symmetric directions with respect to the middle plane, and upon reflection at the duct walls, give rise to very attenuated secondary vorticity and entropy waves.

We also note that SP(0) has a non-zero transversal velocity V'_x of order $(k/R_\nu)^{\frac{1}{2}}$ which varies linearly with x in the central region of the duct and rapidly drops to zero in the boundary layers under the cancelling effect of viscous and thermal diffusive terms. In contrast with this situation, the transversal velocity of the higher-order SP-modes is, to a first approximation, the same as in the inviscid case.

As mentioned in the introduction to this section, the graphs constitute a more accurate representation of the eigenfunctions since the contributions of higher order terms in α_0, α_1, α_2, and β_z are taken into account. In order to illustrate this feature, we have

displayed in Figure 5, the non-zero imaginary part of the SP(0) pressure amplitude which, according to Table V, is to a first approximation identically zero. From a comparison of Figures 5 and 6, and Table V, we infer that higher-order terms only bring about slight changes to the mode shapes.

If we now turn our attention to the results of Table VI and the graphs of Figures 5 and 6 pertaining to the SS-modes, we clearly see that the perturbations in the central core of the duct are composed of entropy waves of order unity associated with temperature and density fluctuations of the same order, pressure fluctuations of order k/R_ν, and velocity fluctuations V'_z and V'_x of order $(k/R_\nu)^{\frac{1}{2}}$ and $1/R_\nu$, respectively. As in the case of the SP modes, enforcement of the boundary conditions leads to the diffusion of vorticity fluctuations of order $(k/P_r R_\nu)^{\frac{1}{2}}$ in layers of thickness $(\frac{2}{k(1-P_r)R_\nu})^{\frac{1}{2}}$ close to the duct walls. In addition, these entropy waves give rise to diffusion of pressure fluctuations in layers of thickness $(2/kP_r R_\nu)^{\frac{1}{2}}$. Such a phenomenon is not directly apparent in Table VI, except through the associated transversal velocity fluctuations, because it is of higher order than the term shown in the expression relative to p'^{SS}_n on Table VI. However, it definitely occurs, as seen from the more accurate variations of pressure amplitude displayed in Figures 5 and 6. The results may be interpreted in exactly the same manner as those pertaining to the pressure-dominated eigenfunctions: An SS-mode can be considered as the superposition of two plane entropy waves which propagate in symmetric directions with respect to the duct middle plane, and upon reflection at the walls of the tube, give rise to secondary pressure and vorticity waves.

The vorticity-dominated mode shapes described in Figures 5 and 6 and Table VII, can be analyzed in a strictly analogous fashion. In this case, a vorticity wave associated with axial and transversal velocity fluctuations of order $1/kR_\nu$ and $(1/kR_\nu)^{\frac{1}{2}}$, respectively, propagates along the axis, in the central region of the tube. In order to satisfy the boundary conditions, such a wave has to be supplemented by two types of boundary layers. On the one hand, entropy fluctuations of order $(1/kR_\nu)^{3/2}$ associated with density and temperature fluctuations of the same order of magnitude, are diffused away from the walls in layers of thickness $(2/k(1-P_r)R_\nu)^{\frac{1}{2}}$. On the other hand, diffusion of pressure fluctuations of order $(1/kR_\nu)^{\frac{1}{2}}$ occurs in layers of thickness $(2/kR_\nu)^{\frac{1}{2}}$. These fluctuations are also associated with temperature, density, and velocity perturbations as seen in Table VII. The SV-modes can also be interpreted in terms of two primary vorticity waves and secondary pressure and entropy waves.

As seen from this detailed discussion, there is ample evidence that the high-frequency-wide-tube range is nothing but the so-called acoustic boundary layer approximation. The peak of the SP(0) axial velocity in the boundary layers, or so-called "Richardson annular effect,"* is seen to be the particular manifestation of a much more general phenomenon caused by the secondary decaying waves generated at the walls of the tube. Such a peak occurs for all higher-order SP-modes as well as for the SV- and SS-modes. The amplitude of the SP- and SV-temperature fluctuations also presents a maximum near the walls. Furthermore, in light of the interpretation of the results given above, we have fully justi-

*cf Richardson and Tyler (1929).

fied the terminology used in designating the three families of modes.

4.6.2 Low-Frequency-Narrow-Tube Mode Shapes. It is clear from the expressions of Tables VIII-X and the graphs of Figures 7 and 8, that the low-frequency-narrow-tube mode shapes are drastically different from their high-frequency-wide-tube counterparts. The amplitude variations of the physical variables are now smooth throughout the cross-section and no boundary layers can be isolated near the duct walls. The vorticity and entropy fluctuations of the SP-modes, for instance, can no longer be restricted to thin diffusive layers. They are spread throughout the tube and are of the same order of magnitude as the pressure fluctuations. Similar remarks can be made about the vorticity-dominated eigenfunctions. This feature would seem to invalidate the argument developed in the preceding subsection regarding the terminology used in this study. However, since most practical cases fall into the high-frequency-wide-tube range, where the three families assume clearly distinct features, we find it convenient to stay with the present convention.

The SP- and SV-mode shapes are seen to be closely related, since their shape factors $z_n^{\pm}$ are complex conjugates of each other. Furthermore, on account of the close proximity of the walls, both families are characterized by weak temperature fluctuations of order k, so that they may be considered as propagating almost isothermally. The parabolic axial velocity profile of the SP(0)-mode is easily identified as pertaining to the classical unsteady Poiseuille flow situation.

The SS-mode shapes are characterized by entropy, temperature, and density fluctuations of order unity. The variations of entropy, in particular, are unchanged when compared with the corresponding high-frequency-

wide-tube results. The transversal velocity of order k^2 has not been determined, as it would require the knowledge of terms of order k^4 in the expansion of α_1 .

We may therefore conclude that, in the low-frequency-narrow-tube range, viscous and thermal effects are dominant in the entire cross-section of the tube.

4.6.3 Very-High-Frequency-Very-Wide-Tube Mode Shapes. As shown in Table XI and XII and in Figures 9 and 10, the SP-mode shapes give rise to entropy and vorticity diffusion in viscous and thermal layers of the same thickness $(2/kR_\nu)^{\frac{1}{2}}$ as in the high-frequency approximation. However, the SP(0)-mode is no longer a plane pressure wave, as it was in the other frequency regimes. More specifically, pressure fluctuations as well as all other physical quantities are exponentially large in layers of approximate thickness $(2R_\nu/k^3)^{\frac{1}{2}}$ close to the boundaries of the tube. Outside these layers, a more precise evaluation would indicate that the pressure amplitude is of order unity. We also note that such layers are thicker than their viscous and thermal counterparts. At very high reduced frequencies, all fluctuations of significant magnitude are concentrated near the walls, resulting in an "annular" SP(0) eigenfunction.

The higher-order SP-mode shapes are pressure released, i.e., the pressure amplitude is to a first approximation, equal to zero at the walls, as seen from Table XII. Consequently, in contrast with the high-frequency case, fluctuations in temperature and axial velocity naturally decrease to zero at the boundaries whereas transversal velocities reach a maximum close to the walls, and require the generation of secondary-entropy and vorticity waves. The pressure waves are associated with

entropy fluctuations of order k/R_ν in the core of the tube, which may be interpreted as increased dissipation in the bulk of the fluid, due to the very high frequencies under consideration. The SS- and SV-mode shapes do not have to be discussed since their characteristics are the same as in the high-frequency-wide-tube regime.

4.7 Dispersion and Attenuation Characteristics.

The expansions of the complex wave number pertaining to the SP-, SS-, and SV-modes were discussed in detail in Sections 4.3, 4.4, and 4.5 for high, low, and very-high values of the frequency parameter k. From these expressions, one can determine the dimensionless attenuation rate, i.e., the attenuation rate per unit diameter along the duct axis, $|\mathrm{Im}\,\beta_z|$, as well as the phase velocity non-dimensionalized with respect to the speed of sound:

$$V_{ph} = \frac{k}{\mathrm{Re}\beta_z} \tag{4.132}$$

Both of these parameters are characteristic of the dispersion and attenuation properties of each mode, and have been plotted versus reduced frequency k in Figures 11 and 12 for given values of the parameters γ_0, P_r, R_ν, and R_η. The first three symmetric modes of each family have been represented.

All curves break down around $k \simeq \frac{1}{R_\nu}$, on account of the limited range of validity of the low and high frequency expansions. The SP-results present an additional breakdown around the value $k \sim R_\nu^{1/3}$ which separates the high-frequency region from the very-high-frequency region.

In the low-frequency-narrow-tube range, all modes with the exception

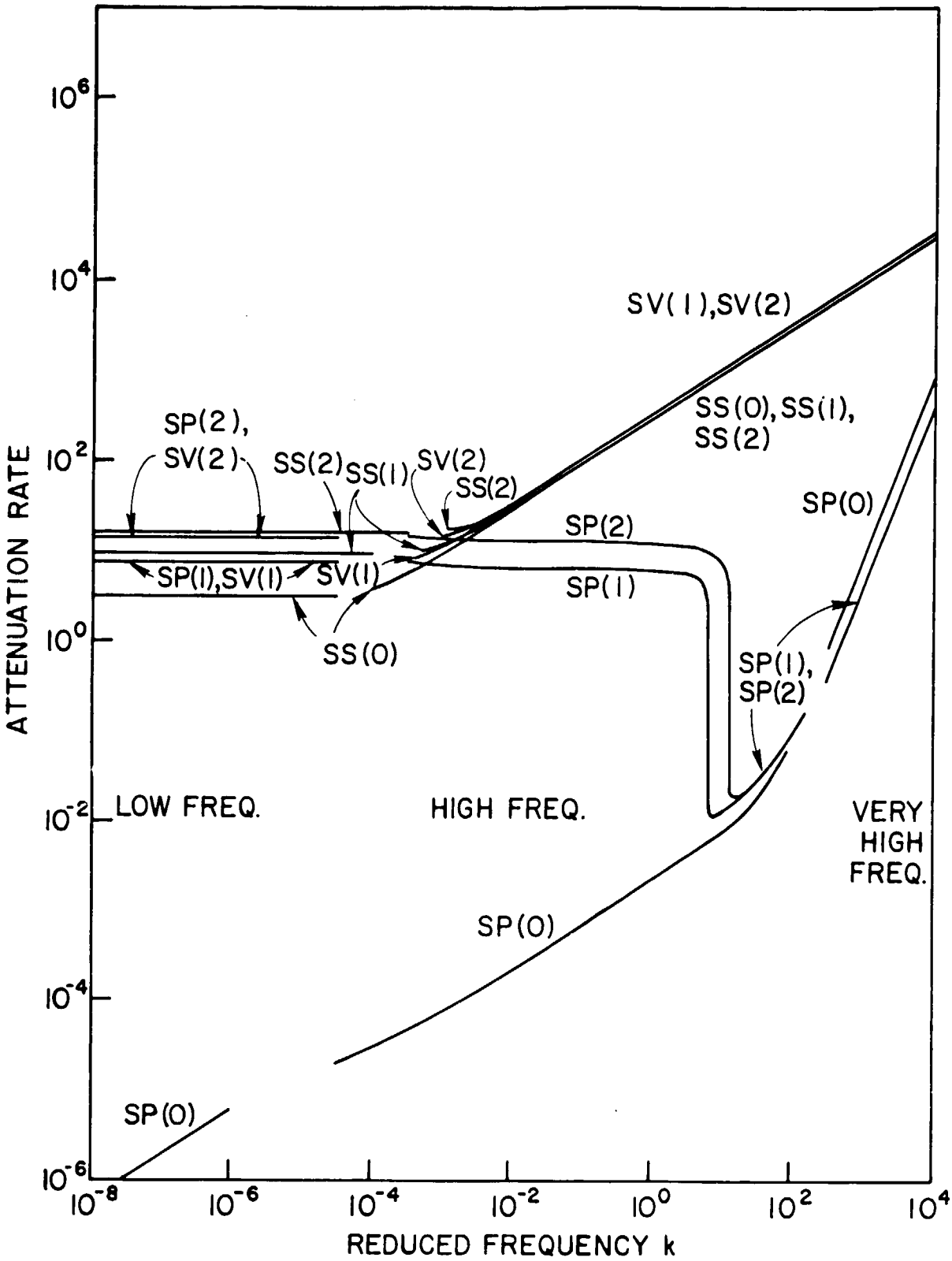

Figure 11. Symmetric Inplane Modes. Attenuation rate $-\mathrm{Im}\beta_z$ versus reduced frequency k for $R_\nu = 2.35\times10^5$, $R_\eta = 1.76\times10^5$, $P_r = .72$, $\gamma_0 = 1.4$, $d = 10^{-2}$m, medium is air at 15°C, 1 atm, $K_0 = 0$.

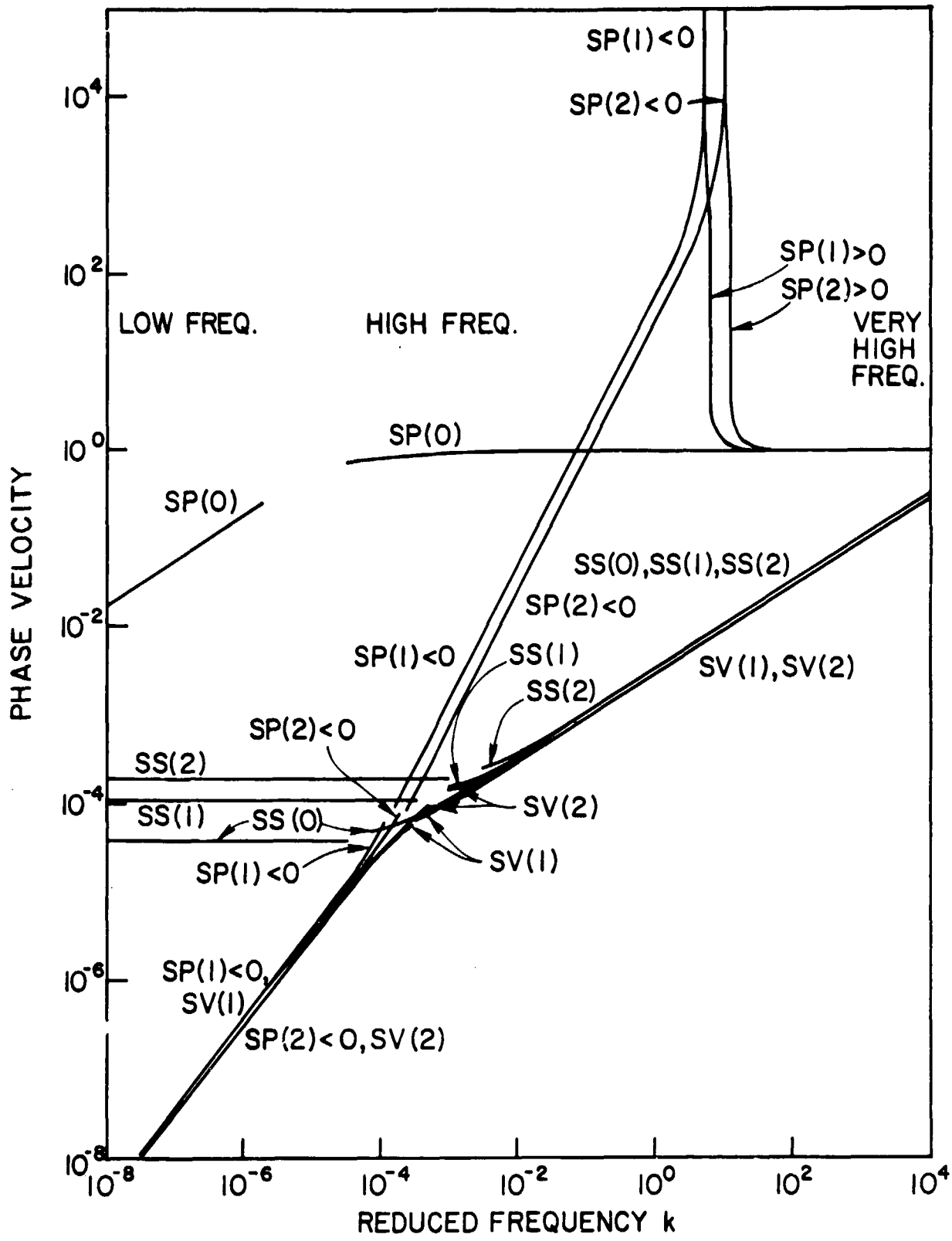

Figure 12. Symmetric Inplane Modes. Phase velocity versus reduced frequency k . Same values of the parameters as in Figure 11.

of the unsteady Poiseuille mode SP(0) , have high attenuation rates independent of reduced frequency. As mentioned in Subsection 4.4.1, higher order SP- and SV-modes are characterized by almost equal attenuation rates and opposite phase velocities.* Entropy-dominated eigenfunctions are non-dispersive as their decay rate and phase velocity is independent of k . The SP(0)-mode, on the contrary, is highly dispersive, both its attenuation and phase velocity varying as $\sqrt{k}$.

Basic changes in the frequency dependence of these two parameters take place as we examine the high-frequency-wide-tube range. The attenuation rate of all SV- and SS-modes increases with $\sqrt{k}$, instead of being constant, and merges asymptotically into the SS(0) and SV(1) attenuation rates respectively. The same behavior holds for their phase velocities. As expected, SP(0) wave fronts propagate with a velocity approaching the isentropic speed of sound a_0 , and decay at a rate proportional to $\sqrt{k}$. The most interesting features that occur in this frequency range are associated with the higher-order SP-modes. They are highly attenuated waves of negative phase velocity** below their cut-off frequency and weakly attenuated waves of positive phase velocity above cut-off. As the reduced frequency k increases through the value $R_\nu^{1/3}$, the decay rate changes from a $\sqrt{k}$ frequency dependence due to dissipation in the acoustic boundary layers, to a k^2 dependence due to dissipation in the bulk of the fluid. Finally, we note that the phase velocity is infinite at cut-off, as a standing wave pattern is formed in the transversal x-direction.

It is interesting to compare the results of the present investiga-

---

*Note that the absolute value of the phase velocity is plotted in Figure 12.

**This phenomenon was investigated in detail in Subsection 4.3.1 and in Appendix C.

tion with those pertaining to the propagation of sound in an invsicid fluid contained in a two-dimensional duct. As we let the parameters R_ν , R_η , and P_r go to infinity, the SP- and SV-families vanish altogether, as their attenuation rate becomes infinite. The SP-modes then coincide with the symmetric sound modes encountered in classical duct acoustics, their mode shape being given by

$$p_n'^{SP}(x) = \cos 2n\pi x \tag{4.133}$$

The zeroth mode propagates unattenuated with the isentropic speed of sound a_0 . Higher-order modes are non-propagating below their cut-off frequency $2n\pi$ and their decay rate is

$$|\operatorname{Im} \beta_{zn}^{SP}| = \sqrt{4(n\pi)^2 - k^2} \tag{4.134}$$

Above cut-off they propagate with no attenuation and their phase velocity is

$$V_{ph} = \frac{k}{\sqrt{k^2 - 4(n\pi)^2}} \tag{4.135}$$

As we have seen in the high-frequency-wide-tube regime, the presence of viscosity and heat conduction results in a finite negative phase velocity below cut-off and a small but non-zero attenuation rate above cut-off. It also leads to a dispersive SP(0)-mode with a finite decay rate. Furthermore, the SP-characteristics were shown to be drastically altered as we investigated the low- and very-high-frequency regimes. In these two ranges, the inviscid results do not lead to meaningful predictions.

4.8 Comparison With a Numerical Study.

It is of interest to compare the analytical results derived in this

chapter with those obtained by the numerical approach of Scarton and Rouleau (1973). These investigators assume that the fluid is viscous but non-heat-conducting, and that it is contained in a rigid cylindrical duct of circular cross-section. Their work is concerned with the determination of the characteristics of the axisymmetric modes by the method of eigenvalleys. Since it was pointed out in Section 4.2 that the dispersion relations pertaining to the axisymmetric and inplane symmetric eigenvalues respectively, could be written in analogous mathematical form, it is legitimate to seek the common features between the numerical solutions of the first relation and the analytical solutions of the second relation.

For convenience, we discuss Scarton and Rouleau's results in terms of the three non-dimensional parameters k, R_ν, and R_η introduced in Section 3.2, where the duct width d is replaced by the radius R*. As we let the Prandtl number go to infinity, the attenuation rate of the entropy-dominated modes becomes infinite in both geometries so that the SS-modes and their axisymmetric counterparts are identically zero. Hence, this section is concerned with a comparative evaluation of only two families, namely, the pressure- and vorticity-dominated modes. These two families are referred to by Scarton and Rouleau as the A- and B-bands, respectively. In Figures 13 and 14, we have reproduced typical plots of their dimensionless attenuation rate, i.e., attenuation rate per unit radius, and dimensionless phase velocity versus reduced frequency k, for a given set of values of the parameters R_ν and R_η.

*In their formulation, Scarton and Rouleau prefer to use the equivalent set k, $1/R_\nu$, and $K_0/\rho_0 a_0 R$.

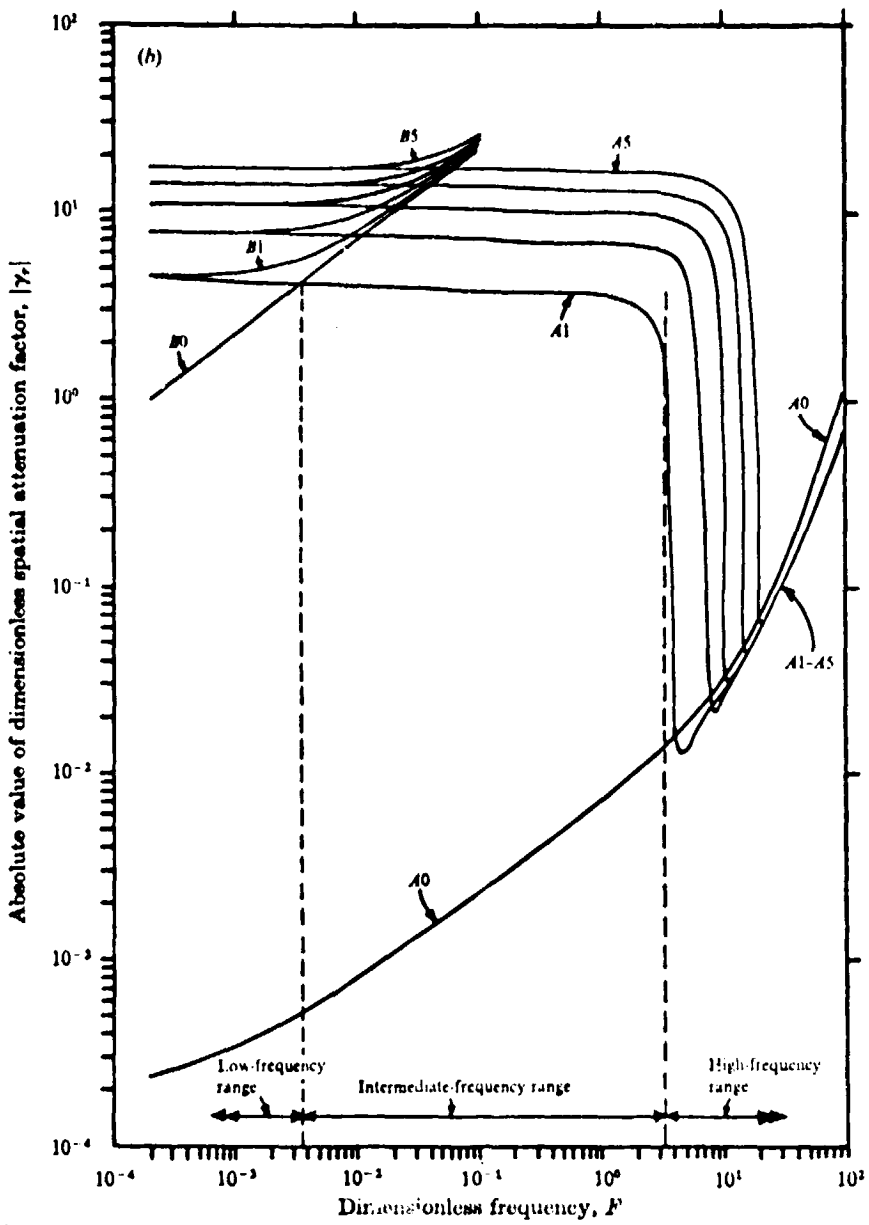

Figure 13. (From Scarton and Rouleau, Fig. 4(b), p. 604) Dimensionless attenuation rate versus reduced frequency $k = \omega R/a_0$. Non-heat-conducting viscous fluid; rigid circular duct. $R_\nu = a_0 R/\nu_0 = 10^4$, $K_0 = 0$.

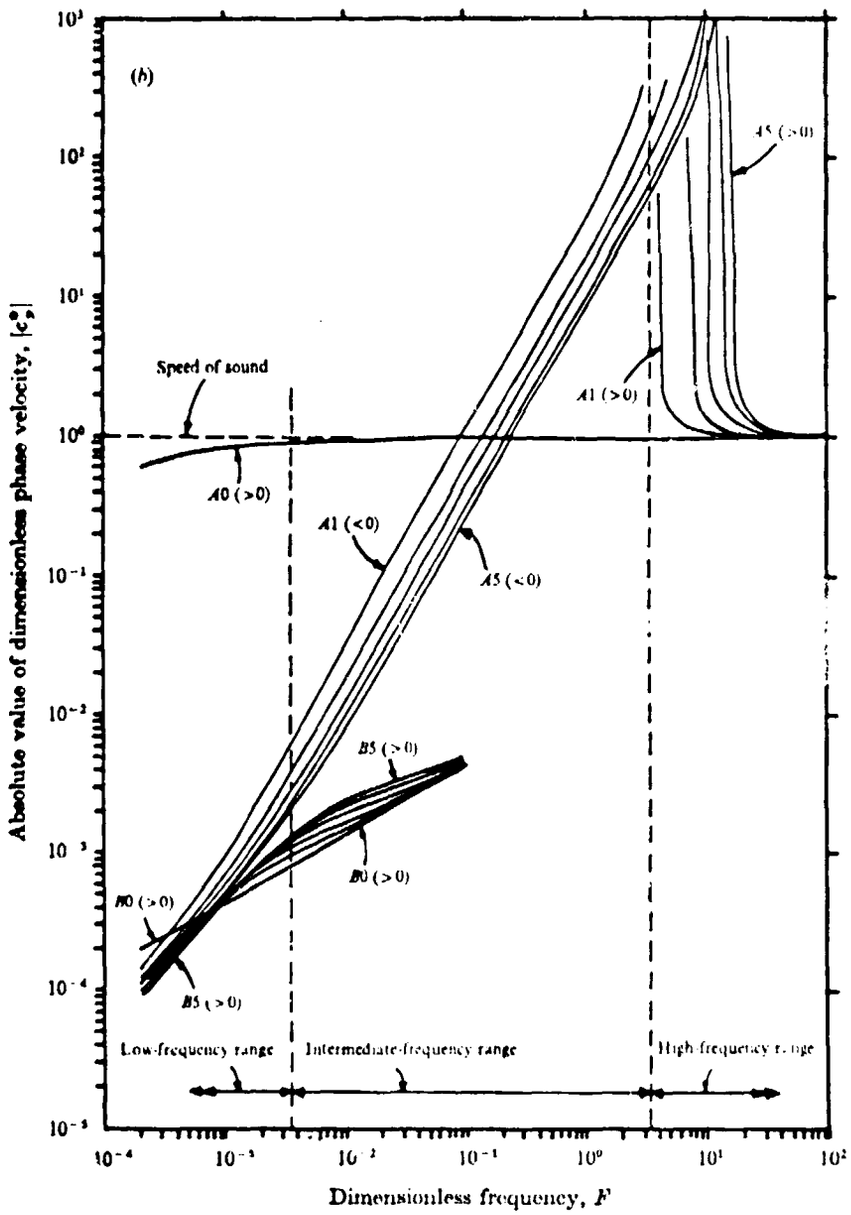

Figure 14. (From Scarton and Rouleau, Fig. 5(b), p. 608). Dimensionless phase velocity versus reduced frequency k . Same values of the parameters as in Figure 13.

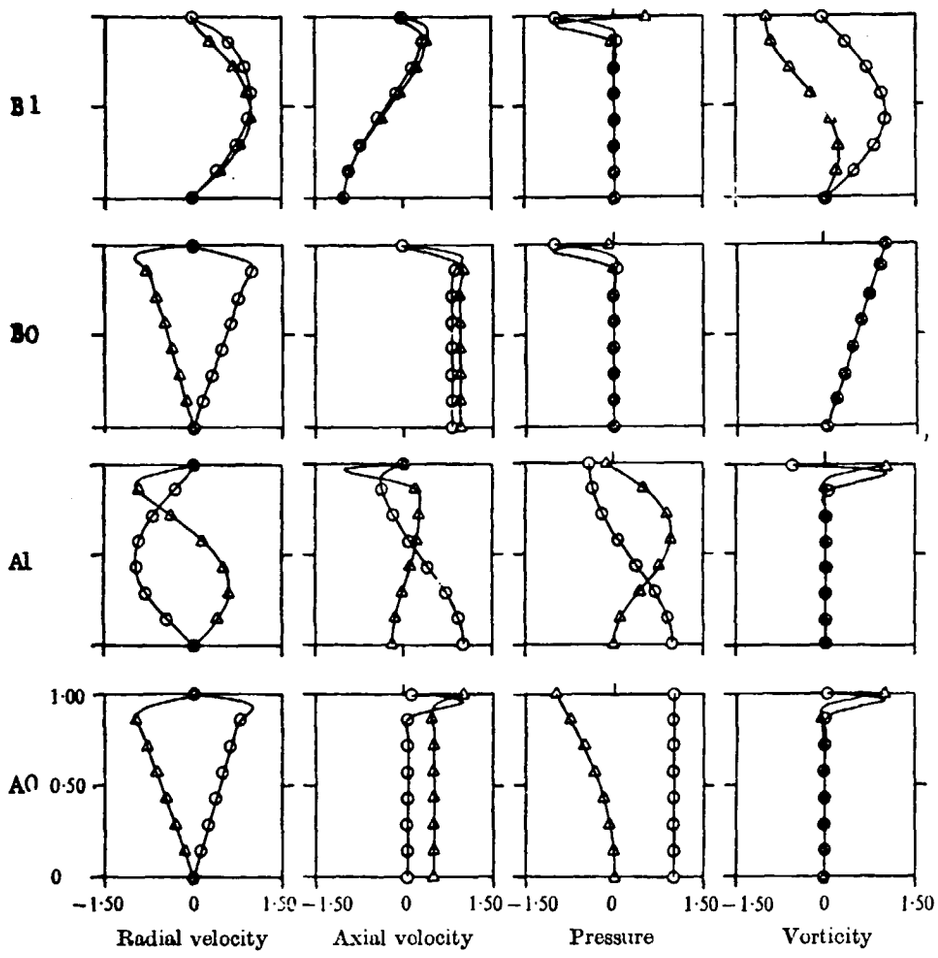

Figure 15. (From Scarton and Rouleau, Fig. 7, p. 613). Zeroth and first order mode shapes for $k = 10^{-1}$, $R_\nu = 10^4$. O, real part; Δ imaginary part.

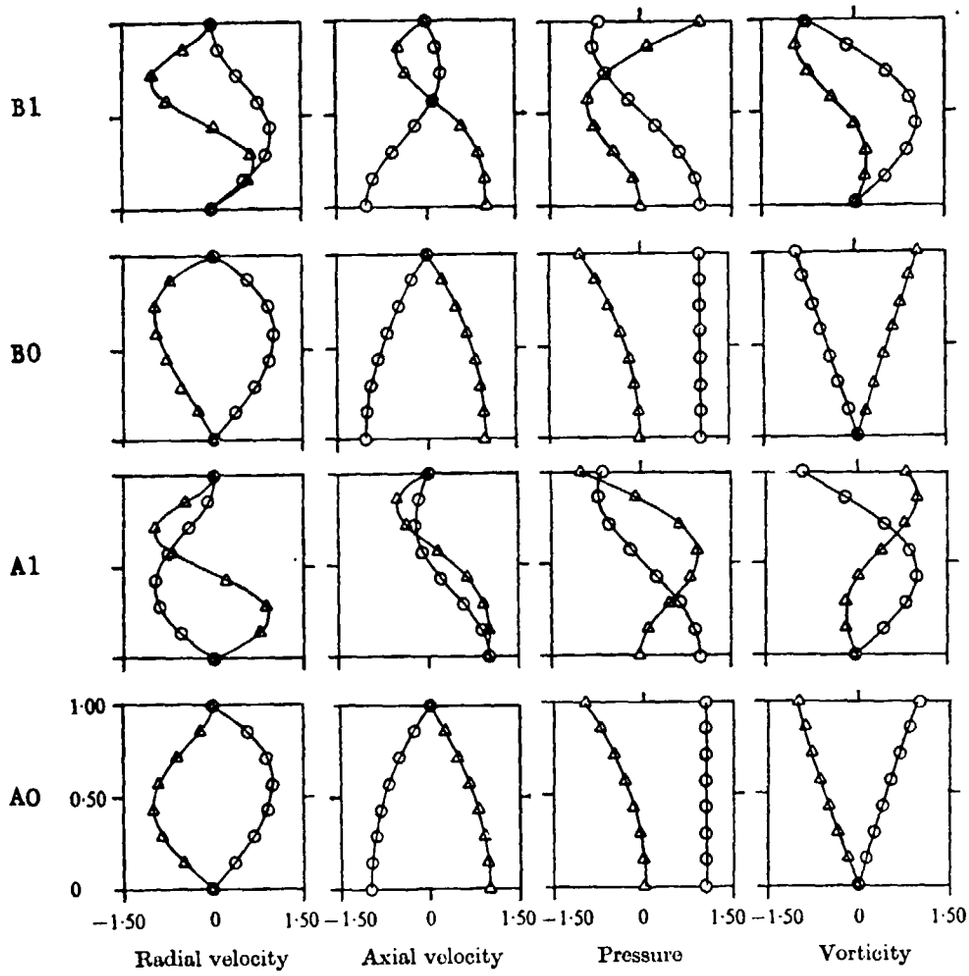

Figure 16. (From Scarton and Rouleau, Fig. 6, p. 612). Zeroth and first order mode shapes for $k = 10^{-2}$, $R_\nu = 10^2$. 0 real part; Δ imaginary part.

The reduced frequencies considered in these graphs span the entire high-frequency range and the edges of the low- and very-high-frequency regions. The overall similarity between Figures 13-14 and Figures 11-12 is striking. In the low-frequency regime, the higher order A- and B-modes have identical attenuation rates and opposite phase velocities, in complete agreement with the observations of Section 4.7. As the reduced frequency k is increased through the transition region, the propagation characteristics of the A- and B-band closely approach those of the SP- and SV-modes in the high frequency range. This observation confirms that in the low-frequency region, the solutions of equation (4.75a) located in the first and fourth quadrant of the complex plane do correspond to the SV- and SP-eigenvalues, respectively. As mentioned in Section 4.4, such a choice could not have been fully justified without a knowledge of the behavior of the SP- and SV-complex wave numbers in the transition region between low and high frequencies. In the high-frequency region, higher-order A-modes experience in the same manner as higher order SP-modes, a sharp decrease in decay rate and a change of sign in phase velocity, as k crosses their cut-off frequency. Since Scarton and Rouleau consider a purely viscous fluid, the cut-off frequencies are the same as in the case of an inviscid medium, and no downward shift is observed. As the reduced frequency is further increased, the $\sqrt{k}$ dependence of the SP-attenuation rates gradually shifts to a k^2 dependence. However, there seems to be an apparent discrepancy between the respective magnitudes of the A0- and SP(0)-decay rates above the cut-off frequency of the first-order pressure-dominated mode. Whereas the axisymmetric A0-mode is more attenuated than the higher-order A-modes in this frequency domain, the two-dimen-

sional SP(0)-mode is less attenuated than the higher-order SP-modes. Beatty (1950) used an equivalent impedance model to show that the higher-order pressure modes were indeed the least attenuated of all axisymmetric modes, and that the opposite situation prevailed in the two-dimensional case. A study of the cylindrical configuration on the same lines as the present investigation would confirm this particular point.

In Figure 15, we have reproduced plots of the modal amplitudes pertaining to the zeroth and first modes in the A- and B-band, as obtained numerically by Scarton and Rouleau. The values of k and R_ν correspond to a typical high-frequency-wide-tube situation. Since the real and imaginary parts have been normalized by their maximum in the interval $0 \leq R \leq 1$, a detailed comparison is impossible. However, we note the general similarity between Figure 15 and Figures 5 and 6 of the present study. In both instances, pressure- and vorticity-dominated modes are characterized by the diffusion of vorticity and pressure, respectively, in thin boundary layers close to the walls. Scarton and Rouleau note that the thickness of these layers increases as the mode index increases and the frequency parameter decreases. This trend is clearly demonstrated by the analytical expressions (4.44) and (4.45).

Even though the value of the reduced frequency associated with the mode shapes of Figure 16 is located at the edge of the low-frequency-narrow-tube region, we note in these plots the absence of boundary layers. Pressure and vorticity fluctuations diffuse in the entire cross-section, a situation which is very reminiscent of the low-frequency mode shapes displayed in Figures 7 and 8.

As is clear from the examination of Figures 13-16, Scarton and

Rouleau claim that there exists a B0-eigenvalue associated to an eigenfunction which is not identically zero. If this were to be true, we would have to admit that the corresponding exact solution $\alpha_2 = 0$ of the inplane symmetric dispersion relation (3.70) is a relevant eigenvalue with a non-zero SV(0)-eigenfunction. As mentioned in Section 4.3.3, if α_2 is assumed to be zero in the basic equation (3.42), one is naturally led to conclude that the only possible mode shape is identically zero. Hence, the solution $\alpha_2 = 0$ and its axisymmetric counterpart B0 are not genuine eigenvalues.

4.9 Concluding Remarks.

The discussion of the last three sections was restricted to the symmetric modes. The propagation characteristics and shapes of the antisymmetric modes could be analyzed in an identical fashion, in light of the solutions of the antisymmetric dispersion relation derived in Sections 4.3 - 4.5.

The determination of the inplane modes, in view of the complexity of the basic relations describing their motion, required the implementation of perturbation procedures. We were therefore unable to obtain analytical results in the transition regions where no small parameter could be defined. No such difficulties were encountered in the case of the antiplane modes and their characteristics were determined exactly in the entire reduced frequency domain. A simple explanation of this difference between the two types of motion can now be given: the antiplane modes are solely composed of vorticity waves, whereas the inplane modes are the result of the coupling of primary waves and secondary waves generated at the boundaries. In particular, the inplane vorticity-

dominated modes, in sharp contrast with their antiplane counterparts, give rise to pressure and entropy fluctuations.

The following question remains to be answered: given a source distribution located inside the duct, in the cross-sectional plane $z = 0$, what is the nature of the disturbances propagating along the duct axis. Their character will naturally depend on the modal content of the source amplitude for each reduced frequency k. A generator of pressure fluctuations, such as a piston oscillating in the axial direction, or a pulsating sphere, will give rise to a wave pattern composed of pressure-dominated modes. Similarly, if a heat source or a distribution of heat sources is situated inside the tube, the wave will consist of entropy-dominated modes. Finally, a piston oscillating in its own plane in the x- or y-direction will give rise to a wave pattern made up of inplane vorticity-dominated modes or antiplane vortical modes. The number of eigenfunctions to be considered and their respective weight will be determined by the modal structure of the source.

We noted in Chapter II that pressure and entropy waves are inherently coupled as they propagate in an unbounded medium, whereas vortical waves are not. From the results of this chapter, we may conclude that the presence of solid boundaries has led to additional coupling between vortical fluctuations and the two other types of fluctuations. For instance, the presence of turbulence at some station along the duct will generate vorticity-dominated modes which include pressure and entropy fluctuations. In the absence of boundaries, the radiation field would solely be composed of purely vortical waves. It is important to remark that this conclusion is not in contradiction with Lighthill's theory of aerodynamic noise generation. The present formulation does not include

the pressure waves generated by the non-linear fluctuating Reynolds stresses. Hence, turbulence does not give rise to pressure disturbances in the linear approximation, when the medium is unbounded. However, when there are solid walls, we have shown that even in the linear approximation, pressure fluctuations are induced at the walls and propagate along the axis at a very high attenuation rate.

In Figure 17, we have summarized on a $k - R_\nu$ diagram the ranges of the parameters k and R_ν in which inplane solutions have been obtained. As explained in Section 4.2, regions of the $k - R_\nu$ plane located on the left of the straight lines $R_\nu = 1$ and $k = R_\nu$ have to be excluded on account of the continuum hypothesis. The lines $k = 1/R_\nu$ and $k = R_\nu^{1/3}$ separate the low- and high-, the high- and very-high-frequency ranges, respectively. In fact, our results are not valid for points located near these lines, and a more accurate representation would have to separate the different domains by transition bands around the lines $k = 1/R_\nu$ and $k = R_\nu^{1/3}$.

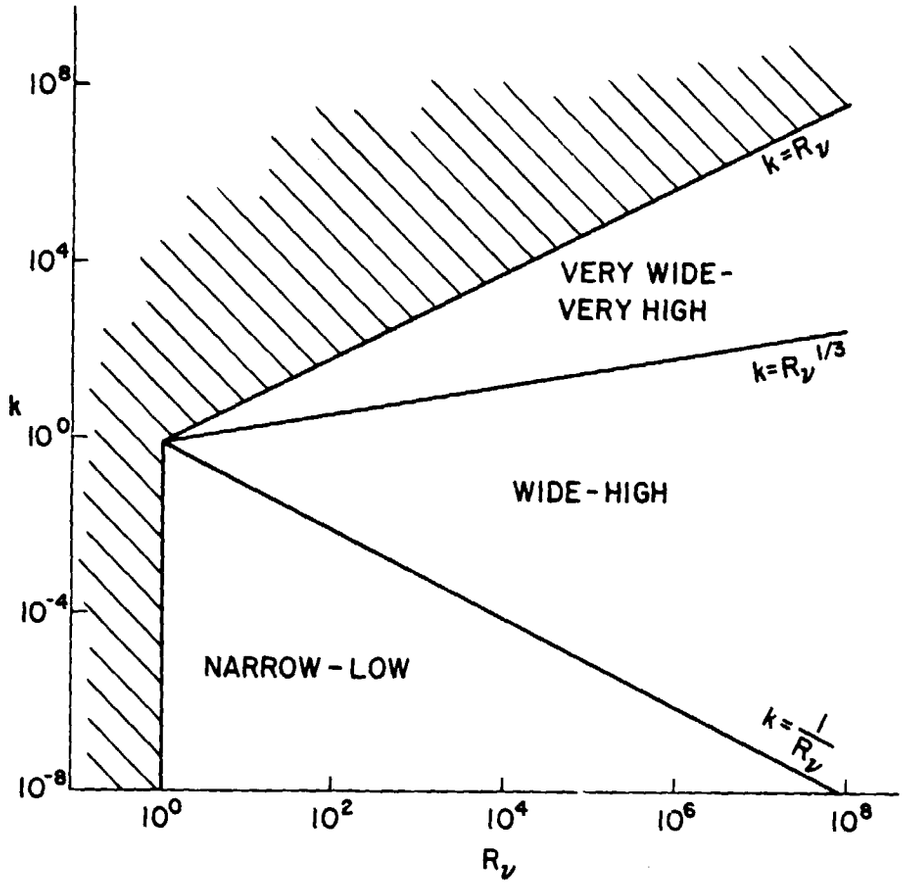

Figure 17. Domain of validity of the low-, high-, and very-high-frequency approximations in the R_ν-k plane.

V. CONCLUSIONS AND RECOMMENDATIONS

5.1 Conclusions.

The important achievements of this study are outlined below.

1. A new mathematical formulation of the small fluctuating motions of a viscous, heat-conducting and compressible fluid has been developed, which reduces such problems to the determination of three unknown functions, namely, the acoustic, thermal, and viscous potentials, satisfying three linear partial differential equations. As a consequence, the total number of unknown functions has decreased from five "physical" variables, i.e., p', ρ', S', T', and $\vec{V}'$, to three "auxiliary" variables, Φ_a, Φ_{th}, and $\vec{A}$.

2. This model has been applied to a detailed investigation of the propagation of sound in a two-dimensional infinite duct with rigid and isothermal walls. It has been shown that four distinct types of wave motions, i.e., inplane and antiplane waves of symmetric or antisymmetric amplitude with respect to the duct middle plane, can be considered independently.

3. The characteristics of the symmetric and antisymmetric antiplane modes have been obtained exactly for arbitrary values of the parameters. They consist of purely vortical velocity fluctuations.

4. In the case of symmetric or antisymmetric inplane motions, three families, namely, pressure-, entropy-, and vorticity-dominated modes, respectively, have been distinguished and their characteristics have been determined in the low-frequency-narrow-tube, high-frequency-wide-tube, and very-high-frequency-very-wide-tube approximations.

5. The analytical results pertaining to the symmetric inplane modes have been found to be in good agreement with those obtained in a numerical

study of the axisymmetric modes of a cylindrical duct in the limit of zero heat-conduction.

5.2 Recommendations.

The general features of the fluctuating field generated by an arbitrary source distribution were discussed qualitatively in the last section of the preceding chapter. A mathematical treatment of this problem will require a detailed investigation of the completeness of the modes and their orthogonality properties. A proof of their completeness will ensure that any arbitrary disturbance may always be regarded as a linear combination of the eigenfunctions. When the scalar product of two modes is defined as the integral of their product over the cross-section, it is immediately verified that the modes are not orthogonal. However, a systematic inquiry might reveal the existence of more complicated orthogonality relationships. Such properties would greatly simplify the calculation of the coefficients multiplying each eigenfunction in the linear combination mentioned above.

It would also be of interest to compare the analytical results of the present investigation with those obtained by a numerical study of the inplane dispersion relations. The analytical results themselves provide excellent first guesses of the roots in a wide range of values of the parameters, and the implementation of a standard Newton-Raphson procedure would enable us to determine numerically the eigenvalues in these ranges as well as in the transition regions which have been excluded in the course of the perturbation analysis.

The methodology developed in the present work and the aforementioned suggested extensions then could be applied in a straightforward manner,

to the determination of the characteristics of the axisymmetric and spinning modes in a circular duct. The main difference would reside in the introduction of Bessel functions instead of trigonometric functions.

In many practical cases, such as the propagation of sound in the atmosphere or through aircraft engine-ducts, velocity and temperature gradients are present in the medium. It would be worthwhile to examine possible extensions of the mathematical formulation of Chapter II to include complex mean flow situations. Such a theory would encompass a broad range of problems and provide a general framework to analyze the propagation of sound in a viscous and heat-conducting fluid which is inhomogeneous and non-uniformly moving.

APPENDIX A

CALCULATION OF $(\frac{\partial p}{\partial S})_\rho$, $(\frac{\partial T}{\partial \rho})_S$, $(\frac{\partial T}{\partial S})_\rho$

In this Appendix we will omit the subscript 0 with the understanding that we are considering the state of the medium at rest. The characteristics of the fluid are assumed to be specified in terms of:

- the temperature T
- the density ρ
- the isentropic speed of sound $a_0 = \sqrt{(\frac{\partial p}{\partial \rho})_S}$
- the specific heat at constant pressure c_p
- the ratio of specific heats γ

The partial derivatives $(\frac{\partial p}{\partial S})_\rho$, $(\frac{\partial T}{\partial \rho})_S$, $(\frac{\partial T}{\partial S})_\rho$ are to be expressed as a function of the five properties of the fluid mentioned above. In the following derivation we make use of the First and Second Laws of Thermodynamics without introducing any additional assumption such as a particular equation of state.

From the definition of partial derivatives, we may write:

$$dp = a^2 d\rho + (\frac{\partial p}{\partial S})_\rho \, dS \qquad \text{(A-1)}$$

$$dT = (\frac{\partial T}{\partial \rho})_S \, d\rho + (\frac{\partial T}{\partial S})_\rho \, dS \qquad \text{(A-2)}$$

Equation (A-2) is then used to express dS as follows:

$$dS = \frac{1}{(\frac{\partial T}{\partial S})_\rho} \left[dT - (\frac{\partial T}{\partial \rho})_S \, d\rho \right] \qquad \text{(A-3)}$$

The First and Second Laws of Thermodynamics reduce to the differential form:

$$de = TdS + \frac{p}{\rho^2} d\rho \qquad (A-4)$$

and when (A-3) is substituted into (A-4) we obtain the following relation:

$$de = \frac{T}{(\frac{\partial T}{\partial S})_\rho} dT + [\frac{p}{\rho^2} - T \frac{(\frac{\partial T}{\partial \rho})_S}{(\frac{\partial T}{\partial S})_\rho}] d\rho \qquad (A-5)$$

The coefficient of dT in (A-5) is nothing else but the specific heat at constant volume so that

$$c_v = \frac{T}{(\frac{\partial T}{\partial S})_\rho} \qquad (A-6)$$

or

$$(\frac{\partial T}{\partial S})_\rho = \frac{T}{c_v} \qquad (A-7)$$

which provides an expression for $(\frac{\partial T}{\partial S})_\rho$ as a function of T and c_v. In view of this result, equations (A-3) and (A-5) may be rewritten as:

$$dS = \frac{c_v}{T} [dT - (\frac{\partial T}{\partial \rho})_S d\rho] \qquad (A-8)$$

$$de = c_v dT + [\frac{p}{\rho^2} - c_v (\frac{\partial T}{\partial \rho})_S] d\rho \qquad (A-9)$$

Since both de and dS are exact differentials, we have from (A-8) and (A-9):

$$\frac{1}{T}(\frac{\partial c_v}{\partial \rho})_T = \frac{c_v}{T^2} (\frac{\partial T}{\partial \rho})_S - \frac{1}{T} [\frac{\partial}{\partial T}(c_v (\frac{\partial T}{\partial \rho})_S)]_\rho \qquad (A-10)$$

$$(\frac{\partial c_v}{\partial \rho})_T = \frac{1}{\rho^2} (\frac{\partial p}{\partial T})_\rho - [\frac{\partial}{\partial T}(c_v (\frac{\partial T}{\partial \rho})_S)]_\rho \qquad (A-11)$$

Substitution of (A-11) into (A-10) then results into the following simple relation:

$$c_v \left(\frac{\partial T}{\partial \rho}\right)_S = \frac{T}{\rho^2} \left(\frac{\partial p}{\partial T}\right)_\rho \tag{A-12}$$

where $\left(\frac{\partial p}{\partial T}\right)_\rho$ is to be expressed in terms of $\left(\frac{\partial p}{\partial S}\right)_\rho$. When (A-8) is used in (A-1), dp is related to dT and $d\rho$ through the equation

$$dp = \frac{c_v}{T} \left(\frac{\partial p}{\partial S}\right)_\rho dT + \text{const.}\, d\rho \tag{A-13}$$

so that

$$\left(\frac{\partial p}{\partial T}\right)_\rho = \frac{c_v}{T} \left(\frac{\partial p}{\partial S}\right)_\rho \tag{A-14}$$

and, with the help of (A-14), (A-12) becomes:

$$\left(\frac{\partial T}{\partial \rho}\right)_S = \frac{1}{\rho^2} \left(\frac{\partial p}{\partial S}\right)_\rho \tag{A-15}$$

The above result provides a first equation between the unknowns $\left(\frac{\partial T}{\partial \rho}\right)_S$ and $\left(\frac{\partial p}{\partial S}\right)_\rho$. The second equation is obtained by expressing the First and Second Laws of Thermodynamics in terms of the enthalpy h :

$$dh = T\,dS + \frac{dp}{\rho} \tag{A-16}$$

Equations (A-1) and (A-2), together with the result (A-7), then lead to the following relation between dS, and dp and dT :

$$dS = \frac{a^2 dT - \left(\frac{\partial T}{\partial \rho}\right)_S dp}{\frac{a^2 T}{c_v} - \left(\frac{\partial p}{\partial S}\right)_\rho \left(\frac{\partial T}{\partial \rho}\right)_S} \tag{A-17}$$

which, after substitution into (A-16) results in:

$$dh = \frac{a^2 T}{\frac{a^2 T}{c_v} - \left(\frac{\partial p}{\partial S}\right)_\rho \left(\frac{\partial T}{\partial \rho}\right)_S} dT + \text{const.}\, dp \qquad \text{(A-18)}$$

The coefficient of dT in (A-18) is the specific heat at constant pressure so that

$$c_p = \frac{a^2 T}{\frac{a^2 T}{v} - \left(\frac{\partial p}{\partial S}\right)_\rho \left(\frac{\partial T}{\partial \rho}\right)_S} \qquad \text{(A-19)}$$

which provides a second equation between the unknowns $\left(\frac{\partial T}{\partial \rho}\right)_S$ and $\left(\frac{\partial p}{\partial S}\right)_\rho$:

$$c_p \left(\frac{\partial p}{\partial S}\right)_\rho \left(\frac{\partial T}{\partial \rho}\right)_S = (\gamma - 1) a^2 T \qquad \text{(A-20)}$$

Equations (A-15) and (A-20) are immediately solved for $\left(\frac{\partial T}{\partial \rho}\right)_S$ and $\left(\frac{\partial p}{\partial S}\right)_\rho$, and the final results are shown below:

$$\left(\frac{\partial p}{\partial S}\right)_\rho = \rho a \sqrt{\frac{(\gamma - 1) T}{c_p}} \qquad \text{(A-21)}$$

$$\left(\frac{\partial T}{\partial \rho}\right)_S = \frac{a}{\rho} \sqrt{\frac{(\gamma - 1) T}{c_p}} \qquad \text{(A-22)}$$

$$\left(\frac{\partial T}{\partial S}\right)_\rho = \frac{\gamma T}{c_p} \qquad \text{(A-23)}$$

APPENDIX B

DERIVATION OF SPLITTING THEOREM

Let us first introduce the following notations:

$$L_1(\Phi_a + \Phi_{th}) = \frac{\partial}{\partial t}(\Phi_a + \Phi_{th}) - \frac{\eta_0}{\rho_0}\nabla^2(\Phi_a + \Phi_{th}) + \frac{p'}{\rho_0} \tag{B-1}$$

$$L_2(\vec{A}) = \frac{\partial \vec{A}}{\partial t} - \nu_0 \nabla^2 \vec{A} \tag{B-2}$$

$$L_3(\Phi_{th}) = \Phi_{th} - \frac{1}{\rho_0 a_0}\sqrt{\frac{\gamma_0 - 1}{c_{p_0} T_0}}\, k_0 T' \tag{B-3}$$

The problem considered in this Appendix may then be stated in the following manner:

Assumptions: Let the set $\{ \Phi_a^*, \Phi_{th}^*, \vec{A}^* \}$ satisfy the following system:

$$\text{grad}\,[L_1(\Phi_a^* + \Phi_{th}^*)] + \text{curl}\,[L_2(\vec{A}^*)] = 0 \tag{B-4}$$

$$\nabla^2 L_3(\Phi_{th}^*) = 0 \tag{B-5}$$

and $\vec{V}'$, p', and S' be given by the relations:

$$\vec{V}' = \text{grad}\,(\Phi_a^* + \Phi_{th}^*) + \text{curl}\,\vec{A}^* \tag{B-6}$$

$$\frac{\partial p'}{\partial t} = -\rho_0 a_0^2 \nabla^2 \Phi_a^* \tag{B-7}$$

$$\frac{\partial S'}{\partial t} = a_0 \sqrt{\frac{c_{p_0}}{(\gamma_0 - 1)T_0}}\, \nabla^2 \Phi_{th}^* \tag{B-8}$$

with

$$\text{div}\,\vec{A}^* = 0 \tag{B-9}$$

Question: Is it possible to find a new set $\{ \Phi_a , \Phi_{th} , \vec{A} \}$ which will yield the same values of the physical variables through the relations

$$\vec{V}' = \text{grad}\,(\Phi_a + \Phi_{th}) + \text{curl}\,\vec{A} \tag{B-10}$$

$$\frac{\partial p'}{\partial t} = -\rho_0 a_0^2 \nabla^2 \Phi_a \tag{B-11}$$

$$\frac{\partial S'}{\partial t} = a_0 \sqrt{\frac{c_{p_0}}{(\gamma_0 - 1)T_0}}\, \nabla^2 \Phi_{th} \tag{B-12}$$

with

$$\text{div}\,\vec{A} = 0 \tag{B-13}$$

and which will satisfy the simpler system of governing equations:

$$L_1(\Phi_a + \Phi_{th}) = 0 \tag{B-14}$$

$$L_2(\vec{A}) = 0 \tag{B-15}$$

$$L_3(\Phi_{th}) = 0 \tag{B-16}$$

Proof: Let us examine the following new set $\{ \Phi_a , \Phi_{th} , \vec{A} \}$:

$$\Phi_a = \Phi_a^* + \Phi_{th}^* - \int_0^t L_1(\Phi_a^* + \Phi_{th}^*)\,d\tau - \frac{1}{\rho_0 a_0} \sqrt{\frac{\gamma_0 - 1}{c_{p_0} T_0}}\, k_0 T' \tag{B-17}$$

$$\Phi_{th} = \frac{1}{\rho_0 a_0} \sqrt{\frac{\gamma_0 - 1}{c_{p_0} T_0}}\, k_0 T' \tag{B-18}$$

$$\vec{A} = \vec{A}^* - \int_0^t L_2(\vec{A}^*)\,d\tau \tag{B-19}$$

and verify that it complies with the requirements (B-10) - (B-16).

(a) From (B-19) we have:

$$\operatorname{div}\vec{A} = \operatorname{div}\vec{A}^{*} - \int_0^t \operatorname{div} L_2(\vec{A}^{*})\,d\tau \tag{B-20}$$

and

$$\operatorname{div} L_2(\vec{A}^{*}) = \frac{\partial}{\partial t}\operatorname{div}\vec{A}^{*} - \nu_0 \operatorname{div}\nabla^2\vec{A}^{*} = \frac{\partial}{\partial t}\operatorname{div}\vec{A}^{*} - \nu_0\nabla^2\operatorname{div}\vec{A}^{*} \tag{B-21}$$

Since (B-9) is satisfied, (B-20) and (B-21) require that

$$\operatorname{div}\vec{A} = 0 \tag{B-22}$$

which proves (B-13).

(b) Let us now consider

$$\operatorname{grad}(\Phi_a + \Phi_{th}) + \operatorname{curl}\vec{A} = \operatorname{grad}(\Phi_a^{*} + \Phi_{th}^{*}) + \operatorname{curl}\vec{A}^{*} \tag{B-23}$$

$$-\int_0^t \{\operatorname{grad} L_1(\Phi_a^{*} + \Phi_{th}^{*}) + \operatorname{curl} L_2(\vec{A}^{*})\}\,d\tau$$

and therefore, from (B-6) and (B-4)

$$\operatorname{grad}(\Phi_a + \Phi_{th}) + \operatorname{curl}\vec{A} = \vec{V}' \tag{B-24}$$

which proves (B-10).

(c) Let us calculate

$$\nabla^2\Phi_a = \nabla^2\Phi_a^{*} + \nabla^2\left[\Phi_{th}^{*} - \frac{1}{\rho_0 a_0}\sqrt{\frac{\gamma_0 - 1}{c_{p_0} T_0}}\, k_0 T'\right]$$

$$-\int_0^t \nabla^2 L_1(\Phi_a^{*} + \Phi_{th}^{*})\,d\tau \tag{B-25}$$

When we take the divergence of (B-4), we have

$$\nabla^2 L_1(\Phi_a^{*} + \Phi_{th}^{*}) = 0 \tag{B-26}$$

so that (B-26) and (B-5) require that

$$\nabla^2 \Phi_a = \nabla^2 \Phi_a^* \tag{B-27}$$

which, together with (B-7) proves (B-11).

(d) Similarly, we may write

$$\nabla^2 \Phi_{th} = \frac{1}{\rho_0 a_0} \sqrt{\frac{\gamma_0 - 1}{c_{p_0} T_0}}\, k_0 \nabla^2 T' \tag{B-28}$$

so that, from (B-5) we have

$$\nabla^2 \Phi_{th} = \nabla^2 \Phi_{th}^* \tag{B-29}$$

which together with (B-8) proves (B-12).

(e) From (B-17) - (B-18) we may write:

$$L_1(\Phi_a + \Phi_{th}) = L_1(\Phi_a^* + \Phi_{th}^*) - \frac{\partial}{\partial t} \int_0^t L_1(\Phi_a^* + \Phi_{th}^*) d\tau$$

$$+ \frac{\eta_0}{\rho_0} \int_0^t \nabla^2 L_1(\Phi_a^* + \Phi_{th}^*) d\tau \tag{B-30}$$

so that with the use of (B-26)

$$L_1(\Phi_a + \Phi_{th}) = 0 \tag{B-31}$$

which proves (B-14).

(f) From (B-19) we have

$$L_2(\vec{A}) = L_2(\vec{A}^*) - \frac{\partial}{\partial t} \int_0^t L_2(\vec{A}^*) d\tau + \nu_0 \int_0^t \nabla^2 L_2(\vec{A}^*) d\tau \tag{B-32}$$

When we take the curl of (B-4) and take into account (B-9), we may write:

$$\nabla^2 L_2(\vec{A}^*) = 0 \tag{B-33}$$

which shows that (B-32) implies:

$$L_2(\vec{A}) = 0 \tag{B-34}$$

(g) Finally, using (B-19), we have

$$L_3(\Phi_{th}) = 0 \tag{B-35}$$

which proves (B-16).

The new set $\{ \Phi_a , \Phi_{th} , \vec{A} \}$ therefore meets the requirements (B-10) - (B-16). In particular, it is governed by the system of partial differential equations (B-14) - (B-16).

APPENDIX C ACOUSTIC POWER AND ENERGY TRANSPORT VELOCITY OF HIGHER-ORDER SP-MODES

The radiation condition used in the present investigation requires that waves be attenuated in the positive z-direction, i.e., that the imaginary part of the complex wave number be negative. We showed in Section 4.3.1 that such a condition results in the existence of pressure-dominated backward-propagating waves of negative phase velocity below cut-off. In this Appendix, we prove that in spite of the change in sign of the phase velocity through cut-off, the acoustic energy of the higher order SP-modes always propagates in the positive z-direction.

Karamcheti (1974) showed that the classical definition of acoustic intensity is not affected by the introduction of viscosity and heat-conduction effects. The acoustic power is therefore taken to be given by

$$P = R_e \{ \frac{d}{2} \int_{-\frac{1}{2}}^{\frac{1}{2}} p' V_z'^* dx \} \qquad (C\text{-}1)$$

where the duct width d has been introduced because x is a non-dimensionalized coordinate. We are interested in deriving a <u>first approximation</u> of the acoustic power radiated by the higher-order SP-modes in the high-frequency range. In this context, the acoustic power needs to be evaluated to order $(1/R_\nu)^{\frac{1}{2}}$ inclusive. The pressure and axial velocity amplitudes are given in Table I. After expansion of the coefficients multiplying the cosine functions, p' and $V_z'^*$ can be written as

$$p'(x,z,t) = -\frac{i\rho_0 a_0 k}{d} A' \left[\frac{\cos \alpha_0 x}{\cos \alpha_0/2} + i(\gamma_0 - 1) \cdot \left(\frac{1}{P_r} - \frac{R_\nu}{R_\eta} \right) \frac{k}{R_\nu} \frac{\cos \alpha_1 x}{\cos \alpha_1/2} \right] e^{i(t - \beta_z z)} \qquad (C\text{-}2)$$

$$V_z'^*(x,z,t) = \frac{iA'^*}{d}\beta_z^*\left[\frac{\cos\alpha_0^* x}{\cos\alpha_0^*/2} - i(\gamma_0-1)\frac{k}{P_r R_\nu}\cdot\frac{\cos\alpha_1^* x}{\cos\alpha_1^*/2} - \frac{\cos\alpha_2^* x}{\cos\alpha_2^*/2}\right]e^{-i(t-\beta_z^* z)} \tag{C-3}$$

where the SP superscript and n subscript have been omitted for convenience. In the preceding expressions, α_0, α_1, α_2, and β_z are given by equations (4.35), (4.36), (4.37), and (4.39), respectively, and A' by equation (4.126). In order to evaluate the power, we need the values of the following elementary integrals

$$\int_{-\frac{1}{2}}^{\frac{1}{2}} \frac{\cos\alpha_0 x \cos\alpha_2^* x}{\cos\alpha_0/2 \cos\alpha_2^*/2}\,dx = \frac{2}{\alpha_0^2 - \alpha_2^{*2}}(\alpha_0 \tan\alpha_0/2 - \alpha_2^* \tan\alpha_2^*/2) \tag{C-4}$$

and

$$\int_{-\frac{1}{2}}^{\frac{1}{2}} \frac{\cos\alpha_0 x \cos\alpha_0^* x}{\cos\alpha_0/2 \cos\alpha_0^*/2}\,dx = \frac{2\mathrm{Im}\{\alpha_0 \tan\alpha_0/2\}}{\mathrm{Im}\,\alpha_0^2} \tag{C-5}$$

After substitution of the expansions of α_0 and α_2, these integrals can be reduced to

$$\int_{-\frac{1}{2}}^{\frac{1}{2}} \frac{\cos\alpha_0 x \cos\alpha_2^* x}{\cos\alpha_0/2 \cos\alpha_2^*/2}\,dx = (1+i)\sqrt{\frac{2}{kR_\nu}} \tag{C-6}$$

and

$$\int_{-\frac{1}{2}}^{\frac{1}{2}} \frac{\cos\alpha_0 x \cos\alpha_0^* x}{\cos\alpha_0/2 \cos\alpha_0^*/2}\,dx = \frac{1}{2}\left[1 - \frac{k^{*2} - 4(n\pi)^2}{4(n\pi)^2}\sqrt{\frac{2}{kR_\nu}}\right] \tag{C-7}$$

where terms of order $1/R_\nu$ have been neglected. Similar expressions can be derived for the other integrals which appear in the acoustic power. Integrals of the same form as (C-6) and corresponding to the pairs (α_0,α_1^*), (α_1,α_0^*), (α_1,α_1^*), and (α_1,α_2^*) are found to be of order $(1/R_\nu)^{\frac{1}{2}}$. When these intermediate results are substituted into (C-1) only two terms need to be retained, so that the power P is given by

$$P = \frac{\rho_0 a_0 k}{2d} A'A'^{*} \operatorname{Re}\left\{ \beta_z^{*}\left[\int_{-\frac{1}{2}}^{\frac{1}{2}} \frac{\cos\alpha_0 x \cos\alpha_0^{*} x}{\cos\alpha_0/2 \cos\alpha_0^{*}/2}\, dx \right.\right.$$

$$\left.\left. - \int_{-\frac{1}{2}}^{\frac{1}{2}} \frac{\cos\alpha_0 x \cos\alpha_2^{*} x}{\cos\alpha_0/2 \cos\alpha_2^{*}/2}\, dx \right]\right\} e^{2\mathrm{Im}\beta_z z} \qquad \text{(C-8)}$$

The first integral represents the contribution to the acoustic power of the irrotational part of the fluctuating motion whereas the second integral involves coupling between the irrotational and rotational fluctuations in the acoustic boundary layers. When the constant A' given by (4.126) is expanded and use is made of (C-6) and (C-7), the power finally equals

$$P = \frac{d}{4\rho_0 a_0 k} \operatorname{Re}\left\{ \beta_z^{*}\left[1 - \frac{k^{*2} - 4(n\pi)^2}{4(n\pi)^2} \sqrt{\frac{2}{kR_\nu}} \right.\right.$$

$$\left.\left. -2(1+i) \sqrt{\frac{2}{kR_\nu}} \right]\right\} e^{2\mathrm{Im}\beta_z z} \qquad \text{(C-9)}$$

Instead of reasoning in terms of acoustic power, it is convenient to normalize P by the acoustic energy per unit length along the duct axis. In other words, we prefer to consider the energy transport velocity non-dimensionalized with respect to a_0 and defined as follows:

$$V_{en} = \frac{P}{a_0 E_s} \qquad \text{(C-10)}$$

where E_s is the acoustic energy per unit length. Note that in the present case of a dissipative medium, the energy transport velocity does not necessarily coincide with the group velocity. The first approximation of E_s in the high-frequency range isidentical to the inviscid acoustic energy. Furthermore, in the case of an inviscid medium,

the acoustic energy is of order unity throughout the entire frequency domain. Consequently, in order to obtain a <u>first approximation</u> of V_{en}, only the inviscid value of E_s is needed. It is given by

$$E_s = \frac{d}{4\rho_0 a_0^2} \int_{-\frac{1}{2}}^{\frac{1}{2}} p' p'^* \, dx + \frac{\rho_0 d}{4} \int_{-\frac{1}{2}}^{\frac{1}{2}} \vec{V}' \cdot \vec{V}'^* \, dx \qquad \text{(C-11)}$$

where p' and $\vec{V}'$ are the pressure and velocity fluctuations associated with the symmetric acoustic modes propagating in the inviscid medium. When we use the results mentioned at the end of Section 4.7, we find that E_s is given by

$$E_s = \frac{d}{4\rho_0 a_0^2} \qquad \text{when} \quad k > 2n\pi \qquad \text{(C-12)}$$

and

$$E_s = d \frac{(n\pi)^2}{\rho_0 a_0^2} e^{2\mathrm{Im}\beta_z z} \qquad \text{when} \quad k \leq 2n\pi \qquad \text{(C-13)}$$

From equations (C-9), (C-10), (C-12), and (C-13), and the expansions for the complex wave number β_z derived in Subsection 4.3.1, one can determine the acoustic power and the energy transport velocity, and follow their variations as the frequency parameter k decreases.

<u>When $k > 2n\pi$</u>, the acoustic power is given by

$$P = \frac{d}{4\rho_0 a_0 k} \sqrt{k^2 - 4(n\pi)^2} \qquad \text{(C-14)}$$

and the energy transport velocity is

$$V_{en} = \frac{\sqrt{k^2 - 4(n\pi)^2}}{k} \qquad \text{(C-15)}$$

These expressions do not exhibit any new features. They are identical to the inviscid results.

When $k = 2n\pi$, the wave number is given by equation (4.48) and the power and energy transport velocity respectively equal

$$P = \frac{d}{2\rho_0 a_0}\left(\frac{\gamma_0-1}{\sqrt{P_r}}\right)^{\frac{1}{2}}\left(\frac{1}{2n\pi R_\nu}\right)^{\frac{1}{4}}\cos\frac{\pi}{8}\cdot e^{-8n\pi\left(\frac{\gamma_0-1}{\sqrt{P_r}}\right)^{\frac{1}{2}}\left(\frac{1}{2n\pi R_\nu}\right)^{\frac{1}{4}}\sin\frac{\pi}{8}z} \tag{C-16}$$

$$V_{en} = 2\left(\frac{\gamma_0-1}{\sqrt{P_r}}\right)^{\frac{1}{2}}\left(\frac{1}{2n\pi R_\nu}\right)^{\frac{1}{4}}\cos\frac{\pi}{8} \tag{C-17}$$

The energy propagates with a velocity and decay rate proportional to $(1/R_\nu)^{\frac{1}{4}}$. In the inviscid case, both these quantities would be zero and remain equal to zero for lower values of k.

When $2n\pi < k < \dfrac{2n\pi}{(1+(\gamma_0-1)/\sqrt{P_r})^{\frac{1}{2}}}$, the wave number is given by equation (4.49) and we have:

$$P = \frac{d}{4\rho_0 a_0 k}\sqrt{\frac{2(4(n\pi)^2-k^2)}{kR_\nu}}\left[\frac{k^{*2}-4(n\pi)^2}{4(n\pi)^2-k^2}+2\right]e^{-2\sqrt{4(n\pi)^2-k^2}\,z} \tag{C-18}$$

$$V_{en} = \frac{k}{4(n\pi)^2}\sqrt{\frac{2(4(n\pi)^2-k^2)}{kR_\nu}}\left[\frac{k^{*2}-4(n\pi)^2}{4(n\pi)^2-k^2}+2\right] \tag{C-19}$$

The first and second terms in the brackets of (C-18) represent the contributions of the irrotational and rotational components of the fluctuations, respectively. They are positive and of the same order of magnitude. The total power is positive. Equation (C-19) can be interpreted in the same manner.

When $k = \dfrac{2n\pi}{(1+(\gamma_0-1)/\sqrt{P_r})^{\frac{1}{2}}}$, the appropriate values of P and V_{en} are obtained by simply replacing the reduced frequency by its value in (C-18) and (C-19). It is easily checked that, to this approximation,

the power is associated with the coupling of rotational and irrotational fluctuations in the boundary layers. The purely irrotational part of the power is of higher order. Hence, at cut-off, the energy propagates at a high attenuation rate in the viscous boundary layers. Below cut-off, the rotational component is still positive and larger in magnitude than the negative irrotational component, as seen from equation (C-18). In this frequency range, the rotational part of the energy propagates in the positive z-direction in the viscous layers, whereas the irrotational part propagates in the opposite direction and is distributed in the entire cross-section. The net power is still positive.

The results of this discussion are summarized in Figure 18. The velocity of energy transport pertaining to the SP(1) mode is plotted versus the reduced frequency. It is clear from the graph that the vortical fluctuations play a crucial role in keeping the velocity of energy transport positive. Identical conclusions would result from an analogous study of the antisymmetric modes.

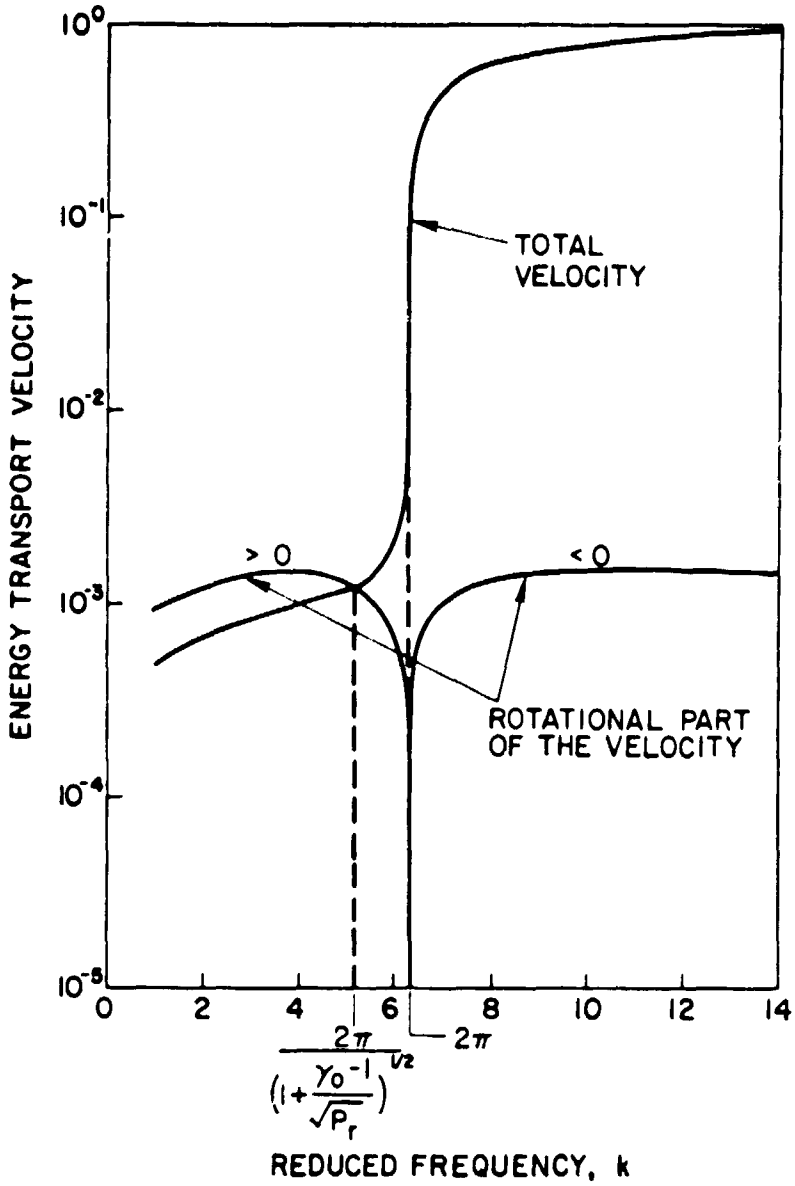

Figure 18. SP(1)-energy transport velocity versus reduced frequency k . Same values of the parameters as in Figure 12.

APPENDIX D

SOLUTIONS OF SIN Z = ± Z

In this Appendix, we discuss the main properties of the roots of the transcendental equations:

$$\sin z = \pm z \qquad \text{(D-1a,b)}$$

and briefly describe a method of solution.

Equations (D-1a,b) both admit the trivial solution zero. They also have an infinite number of complex roots which are symmetrically located in each quadrant of the complex z plane. We will restrict our attention to the roots which lie in the quarter-plane ($\mathrm{Re}\, z > 0$, $\mathrm{Im}\, z < 0$), and all others will be obtained by symmetry with respect to the origin and the coordinate axes. Consequently, let us examine solutions of (D-1a) of the form:

$$z = \alpha - i\beta \qquad \alpha > 0 \; ; \quad \beta > 0 \qquad \text{(D-2)}$$

Substitution of (D-2) into (D-1a) leads to the following system of coupled equations:

$$\sin\alpha \cosh\beta = \alpha \qquad \text{(D-3)}$$

$$\cos\alpha \sinh\beta = \beta \qquad \text{(D-4)}$$

Since $\cosh\beta$ is necessarily positive for any value of β, (D-3) implies that $\sin\alpha$ is also positive. Hence, possible values of α are such that

$$2n\pi \le \alpha \le (2n+1)\pi \qquad n = 0, 1, 2, \ldots \qquad \text{(D-5)}$$

The above system may then equivalently be written in the following form:

$$F(\alpha) = \cos\alpha \sqrt{\left(\frac{\alpha}{\sin\alpha}\right)^2 - 1} - \cosh^{-1}\left(\frac{\alpha}{\sin\alpha}\right) = 0 \qquad \text{(D-6)}$$

$$\beta = \cosh^{-1}\left(\frac{\alpha}{\sin\alpha}\right) \qquad \text{(D-7)}$$

We have therefore reduced the problem to the determination of the zeros of $F(\alpha)$. Such a function is only defined in the intervals given by (D-5). Its derivative is:

$$\frac{dF}{d\alpha} = -\frac{(2\alpha - \sin\alpha)^2}{4\sin^3\alpha \left[\left(\frac{\alpha}{\sin\alpha}\right)^2 - 1\right]^{\frac{1}{2}}} < 0 \qquad \text{(D-8)}$$

Moreover:

when $\alpha \to 2n\pi+$ and $n \neq 0$ $\quad F(\alpha) \to +\infty$

when $\alpha \to 0+$ $\quad F(\alpha) \to 0$

when $\alpha \to (2n+1)\pi-$ $\quad F(\alpha) \to -\infty$

It may be concluded from the resulting variations of $F(\alpha)$ sketched in Figures 19 that $F(\alpha)$ has only one zero α_n^+ in each interval $(2n\pi\ ,\ (2n+1)\pi\ )$. Since $F((2n+\frac{1}{2})\pi) < 0$ each solution of (D-6) can be further bounded as follows:

$$2n\pi \leq \alpha_n^+ \leq (2n+\tfrac{1}{2})\pi \qquad n = 0\ ,\ 1\ ,\ \ldots \qquad \text{(D-9)}$$

and the corresponding value of β is then given by (D-8) as:

$$\beta_n^+ = \cosh^{-1}\left(\frac{\alpha_n^+}{\sin\alpha_n^+}\right) \qquad \text{(D-10)}$$

With this information, one may immediately develop an iterative numerical scheme which will yield the roots

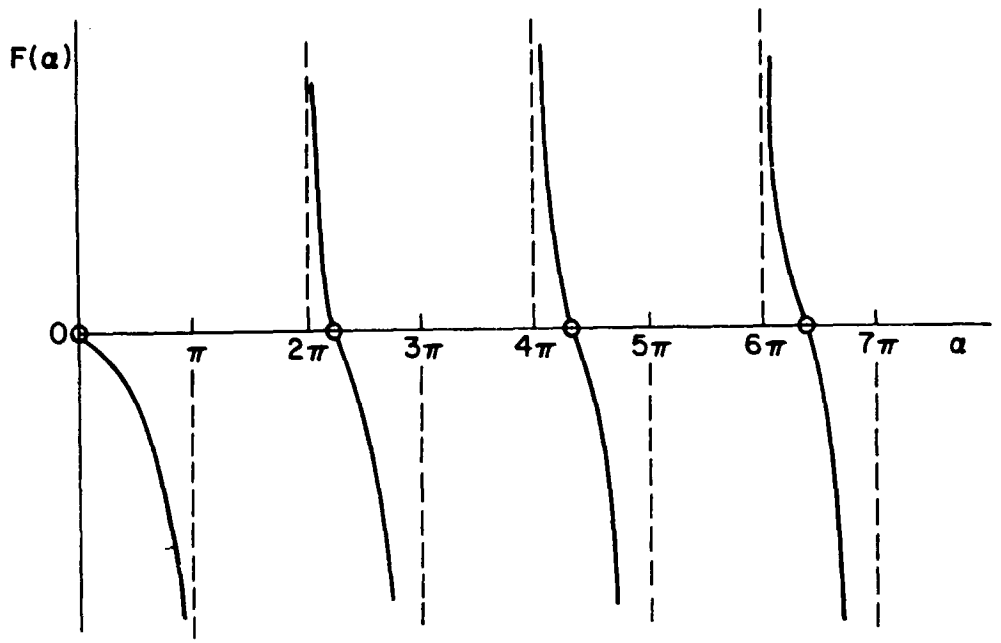

Figure 19. Sketch of function $F(\alpha)$ defined in (D6) .

$$z_n^+ = \alpha_n^+ - i\beta_n^+ \tag{D-11}$$

of the transcendental equation (D-1a). The results are shown in Table III. Finally, as n goes to infinity in (D-9) and (D-10), both real and imaginary parts become infinite. From equations (D-3) and (D-4) we then obtain the following limiting form of z_n^+ :

$$z_n^+ = (2n+\tfrac{1}{2})\pi - i\cosh^{-1}(2n+\tfrac{1}{2})\pi \tag{D-12}$$

The transcendental equation (D-1b) may be studied in exactly the same manner. It is found that the roots are given by

$$z_n^- = \alpha_n^- - i\beta_n^- \tag{D-13}$$

where

$$(2n+1)\pi < \alpha_n^- \leq (2n+\tfrac{3}{2})\pi \qquad n = 0, 1, \ldots \tag{D-14}$$

and

$$\beta_n^- = \cosh^{-1}\left(\frac{-\alpha_n^-}{\sin\alpha_n^-}\right) \tag{D-15}$$

The corresponding numerical results are displayed in Table IV. As the index n goes to infinity, the asymptotic limit of the roots is:

$$z_n^- = (2n+\tfrac{3}{2})\pi - i\cosh^{-1}(2n+\tfrac{3}{2})\pi \tag{D-16}$$

REFERENCES

Achenbach, J.D., (1973), Wave Propagation in Elastic Solids, North Holland Publishing Co., Amsterdam.

Beatty, R.E., (1950a), "Attenuation of (n,0)Transverse Modes in a Rectangular Tube," J. Acoust. Soc. Amer., 22, 5, 639.

Beatty, R.E., (1950b), "Boundary Layer Attenuation of Higher Order Modes in Rectangular and Circular Tubes," J. Acoust. Soc. Amer., 22, 6, 850-854.

Bogert, B.P., (1950), "Classical Viscosity in Tubes and Cavities of Large Dimensions," J. Acoust. Soc. Amer., 22, 4, 432-437.

Brown, F.T., (1962), "The Transient Response of Fluid Lines," J. Basic Eng., Trans. A.S.M.E., Series D, 84, 547-553.

Chu, B.T., and Kovasznay, L.S.G., (1958), "Non-Linear Interaction in a Viscous, Heat-Conducting Compressible Gas," J. Fluid Mech., 3, 494-514.

Cohen, H., and Tu, Y.O., (1962), "Viscosity and Boundary Effects in the Dynamic Behavior of Hydraulic Systems," J. Basic Eng., Trans., A.S.M.E., Series D, 84, 593-601.

Cremer, L., (1948), "Über die akustische Grenzschicht vor starren Wänden," Arch. elektr. Übertragung, 2, 136-139.

Doak, P.E., (1973), "Analysis of Internally Generated Sound In Continuous Materials: 3. The Momentum Potential Field Description of Fluctuating Fluid Motion As a Basis For a Unified Theory of Internally Generated Sound," J. Sound and Vibration, 26(1), 91-120.

Elco, R.A., and Hughes, W.F., (1962), "Acoustic Waveguide Mode Interference and Damping in Viscous Fluids," 4th Int. Congr. Acoustics, Copenhagen, K54.

Fay, R.D., (1940), "Attenuation of Sound In Tubes," J. Acoust. Soc. Amer., 12, 62-67.

Fitz-Gerald, J.M., (1972), "Plasma Motions in Narrow Capillary Flow," J. Fluid Mech., 51, 463-476.

Gerlach, C.R., and Parker, J.D., (1967), "Wave Propagation in Viscous Fluid Lines Including Higher Mode Effects," J. Basic Eng., Trans. A.S.M.E., Series D, 89, 782-788.

Hartig, H.E., and Lambert, R.F., (1950), "Attenuation in a Rectangular Slotted Tube of (1,0) Transverse Acoustic Waves," J. Acoust. Soc. Amer., 22, 1, 42-47.

Huerre, P., and Karamcheti, K., (1975), "Effects of Friction and Heat Conduction on Sound Propagation in Ducts," AIAA 2nd Aero-Acoustics Conf., Paper No. 75-520 to be published in the Proceedings of the 2nd Aero-Acoustics Conference, Vol. II, AIAA Progress Series in Aeronautics and Astronautics.

Iberall, A.S., (1950), "Attenuation of Oscillating Pressures in Instrument Lines," J. Research, National Bureau of Standards, 45, 85-108.

Karamcheti, K., (1974), Lecture Notes, "Fundamentals of Acoustics," Stanford University, Winter 1974.

Kemp, G.T., and Nolle, A.W., (1953), "The Attenuation of Sound in Small Tubes," J. Acoust. Soc. Amer., 25, 6, 1083-1086.

Kirchhoff, G., (1868), "Ueber den Einfluss der Wärmeleitung in einem Gase auf die Schallbewegung," Ann. Phys. Lpz., 134, 177-193.

Lagerstrom, P.A., Cole, J.D., and Trilling, L., (1949), "Problems in the Theory of Viscous Compressible Fluids," Monograph, Calif. Inst. of Tech.

Lighthill, M.J., (1956), "Viscosity Effects in Sound Waves of Finite Amplitude," in Survey in Mechanics, Batchelor, G.K., and Davies, R.M., ed., Cambridge Univ. Press, N.Y.

Lance, G.N., (1956), "Motion of a Viscous Fluid In a Tube Which Is Subjected To a Series of Pulses," Quart. Appl. Math., 14, 312-350.

Meeker, T.R., and Meitzler, A.H., (1964), "Guided Wave Propagation In Elongated Cylinders and Plates," in Physical Acoustics, Vol. 1, Part A, Mason, W.P., (ed.), Academic Press, N.Y.

Meitzler, A.H., (1965), "Backward-Wave Transmission of Stress Pulses in Elastic Cylinders and Plates," J. Acous. Soc. Amer., 38, 835-842.

Meyer, E., and Güth, W., (1953), "Zur Akustischen Zähigkeitsgrenzschicht," Acustica, 3, 185-187.

Nayfeh, A.H., (1973), "Effect of the Acoustic Boundary Layer On the Wave Propagation In Ducts," J. Acoust. Soc. Amer., 54, 6, 1737-1742.

Nerem, R.M., Seed, W.A., and Wood, N.B., (1972), "An Experimental Study of the Velocity Distribution and Transition To Turbulence in the Aorta," J. Fluid Mech., 52, 137-160.

Rayleigh, J.W.S., (1877), The Theory of Sound, Dover, New York, Vol. II, pp. 312-328.

Regnault, V., (1868), "Sur la vitesse de propagation des ondes dans les milieux gazeux," C.R. Acad. Sci. Paris, 66, 209-220.

Richardson, E.G., and Tyler, E., (1929), "The Transverse Velocity Gradient Near the Mouths of Pipes in Which an Alternating or Continuous Flow of Air Is Established," Proc. Phys. Soc., 42, 1, 1-15.

Rott, N., (1969), "Dampened and Thermally Driven Acoustic Oscillations In Wide and Narrow Tubes," ZAMP, 20, 230-243.

Scarton, H.A., and Rouleau, W.T., (1973), "Axisymmetric Waves In Compressible Newtonian Liquids Contained In Rigid Tubes: Steady-Periodic Mode Shapes and Dispersion By the Method of Eigenvalleys," J. Fluid Mech., 58, 595-621.

Sergeev, S.I., (1966), "Fluid Oscillations In Pipes At Moderate Reynolds Numbers," Fluid Dyn., 1, 1, 121-122.

Sexl, T., (1930), "Über den von E.G. Richardson entdeckten "Annulareffekt,"" Z. Physik, 61, 349-362.

Shaw, E.A.G., (1950), "Attenuation of (1,0) "Transverse" Acoustic Waves In a Rectangular Tube," J. Acoust. Soc. Amer., 22, 512-513.

Shaw, E.A.G., (1953), "The Attenuation of the Higher Modes of Acoustic Waves In a Rectangular Tube," Acustica, 3, 87-95.

Shields, F.D., Lee, K.P., and Wiley, W.J., (1965), "Numerical Solution for Sound Velocity and Absorption In Cylindrical Tubes," J. Acoust. Soc. Amer., 37, 4, 724-729.

Tijdeman, H., (1969), "Remarks On the Frequency Response of Pneumatic Lines," J. Basic Eng., Trans. A.S.M.E., Series D, 91, 325-327.

Tijdeman, H.,(1975), "On the Propagation of Sound Waves In Cylindrical Tubes," J. Sound and Vib., 39, (1), 1-33.

Truesdell, C., (1953), "Precise Theory of the Absorption and Dispersion of Forced Plane Infinitesimal Waves According to the Navier-Stokes Equations," J. Rat. Mech. An., 2, 643-741.

Uchida, S., (1956), "The Pulsating Viscous Flow Superposed On the Steady Laminar Motion of Incompressible Fluid In a Circular Pipe," ZAMP, 7, 403-422.

Weston, D.E., (1953a), "The Theory of the Propagation of Plane Sound Waves In Tubes," Proc. Phys. Soc., B66, 695-709.

Weston, D.E., (1953b), "Experiments on the Propagation of Plane Sound Waves In Tubes. I: The Adiabatic Region. II: The Transition Region.," Proc. Phys. Soc., B66, 769-774.

Womersley, J.R., (1955), "Oscillatory Motion Of a Viscous Liquid In a Thin-Walled Elastic Tube. I: The Linear Approximation For Long Waves, Phil. Mag., 7, 46, 199-221.

Wu, T.Y., (1956), "Small Perturbations In the Unsteady Flow Of a Compressible Viscous and Heat-Conducting Fluid," J. Math. Phys., 35, 13-27.